THE ANTIBIOTIC KINOME

UNCOVERING THE ANTIBIOTIC KINOME WITH SMALL MOLECULES

By

TUSHAR SHAKYA, B.Sc.

A Thesis

Submitted to the School of Graduate Studies

in Partial Fulfillment of the Requirements

for the Degree

Doctor of Philosophy

McMaster University

DOCTOR OF PHILOSOPHY (2011) McMaster University

(Biochemistry and Biomedical Sciences) Hamilton, ON

TITLE: Uncovering the Antibiotic Kinome with Small Molecules

AUTHOR: Tushar Shakya, B.Sc. (McMaster University)

SUPERVISOR: Dr. Gerard D. Wright

NUMBER OF PAGES: xi, 127

ABSTRACT

The 20th century introduction of antibiotics made once fatal infectious diseases readily treatable. This taken-for-granted therapy is now threatened by rising antibiotic resistance. The ability of pathogens to acquire numerous simultaneous resistance mechanisms has given rise to an alarming number of increasingly difficult to treat multi-drug resistant infections. When coupled with a sharp decline in development of novel antibiotic therapies, health practitioners today are left with limited therapeutic options. Several alternative methodologies have been employed to find novel therapeutics, including new techniques in natural product isolation and the production of semi-synthetic and synthetic antibiotics; however, there has been limited focus on targeting antibiotic resistance mechanisms directly to create synergistic therapies. We demonstrate the potential in using small molecules to target antibiotic kinases, thereby rescuing the antibiotic action of aminoglycosides and macrolides when used in combination. We conducted a thorough examination of these enzymes including: kinetic analysis; an assessment of phosphate donor specificity; and in-depth structural comparison, including a case study on the structure-function relationship of APH(4)-Ia. This analysis culminated in an intensive screening initiative of fourteen antibiotic kinases against a set of well defined protein kinase inhibitors. From this work, we have identified several inhibitors that have the potential for use in future combination therapeutics. This study illustrates the benefit of a structure-activity based approach to drug discovery, an important tool at a time when novel therapeutic strategies are required.

ACKNOWLEDGEMENTS

Over the past seven years I have had the great fortune of working in an environment which has allowed me to grow as both as scientist and as an individual. This was all due to Dr. Gerard D. Wright, who readily took me under his wing and gave me this unique and prestigious opportunity. My committee members, Dr. Russell Bishop and Dr. Alba Guarné, also need recognition for their part in my scientific development. Although I provided the foundation for the work presented here, the full story was only made possible through the hard work and dedication of the numerous collaborators who contributed their time and effort. I wish to recognize, Dr. Peter Stogios, Elena Evdokimova, Dr. Alexei Savchenko, Nick Todorovic, Dr. Fred Capretta, Jan Blanchard, Peter Spanogiannopolous, Nick Waglechner and Dr. Andrew McArthur, for their invaluable contributions.

In addition to having access to state-of-the-art equipment and facilities, I also had the ability to work along some very talented scientists who have come and gone from the Wright Lab. Namely, I would like to thank Dr. Ishac Nazi, Dr. Tariq Mukhtar, Linda Ejim and Laura Rossi, for taking the time to teach me the intricate workings of the Wright Lab upon my arrival; Kalinka Koteva for assisting me in all things "chemical" and acting as a surrogate mother in the lab; and lastly, Patricia Taylor, whose support, dedication and love made my time as graduate student unforgettable.

Ultimately, this work would not have been possible without love and support from my sister, Amrita Shakya, and my mother, Usha Shakya, both of whom had to deal with my absence from home, as well as my varying temperament. And finally, I dedicate this work to the memory of my late father Ram Prakash Shakya, whose love of science and dedication towards my education led me down this path of discovery, innovation and scholarship.

TABLE OF CONTENTS

LIST OF FIGURES

LIST OF TABLES

LIST OF ABBREVIATIONS

AAC	aminoglycoside acetyltransferase
ADP	adenosine triphosphate
AG	Aminoglycoside
AK	antibiotic kinase
AME	aminoglycoside modify enzyme
AMPPNP	adenosine 5′-(β,γ-imido)triphosphate
Amp^R	ampicillin resistance
ANT	aminoglycoside adenylyltransferase
APH	aminoglycoside phosphotransferase
ATP	adenosine triphosphate
CAK	choline and aminoglycoside kinases
CM	Chloramphenicol
CPT	chloramphenicol phosphotransferase
ELK	eukaryotic-like kinase
ePK	eukaryotic protein kinase
FL-AG	flavonoid-aminoglycoside
GDP	guanosine diphosphate
GMPPNP	guanosine 5′-(β,γ-imido)triphosphate
GTP	guanosine triphosphate
HEPES	4-(2-hydroxyethyl)-1-piperazineethanesulfonic acid
hygB	hygromycin B
IPTG	isopropyl β-D-1-thiogalactopyranoside
Kan^R	kanamycin resistance
KPC	*Klebsiella pneumoniae* carbapenemase
LB	Luria-Bertani
MDR	multi-drug resistant
ML	Macrolide
MPH	macrolide phosphotransferase
MRSA	methicillin-resistant *Staphylococcus aureus*
NADH	nicotinamide adenine dinucleotide
NTP	nucleotide triphosphate
PEP	phosphoenol pyruvate
PK/LDH	pyruvate kinase/lactate dehydrogenase
PKL	protein kinase-like
PP	pyrazolo-pyrimidine
PTK	protein tyrosine kinase

RTK	receptor tyrosine kinase
SFK	Src family of kinases
TBAHS	Tetrabutylammonium hydrogen sulphate
VRE	vancomycin-resistant *Enterococci*

CHAPTER ONE
INTRODUCTION

THE RISE AND FALL OF ANTIBIOTICS

The history of the co-evolution of infectious diseases goes back to ancient times with the earliest record of an epidemic being traced back to Ancient Greece in 430 BC, when a plague of typhoid fever wiped out 1/3 of Athens' population. This created political destabilization in the region resulting in the fall of Athens as the capital city-state of Greece. Since this time the health, political and socio-economic impacts of infectious disease have been well known and feared across the globe. A number of plagues and epidemics would wreak havoc, culminating in the Bubonic plague. Caused by the flea-borne *Yersinia pestis*, this pandemic decimated the population of Europe in a span of over 300 years and focused the efforts of researchers and physicians towards the elimination of these pathogens (Stenseth et al., 2008). Unfortunately, the ability of pathogens to adapt and evolve against our offences has made this mostly an uphill battle that is still being waged today.

Several key discoveries have advanced this ongoing struggle, from the use of aseptic techniques and quarantine, up to the discovery of arsenic-based compound Salvarsan by Paul Ehrlich, which was hailed as a 'magic bullet' against syphilis. The most acclaimed discovery was that of penicillin by Alexander Fleming in 1928 (Fleming, 1944). Penicillin revolutionized the field of antimicrobial discovery, leading to vigorous campaigns of natural product discovery and heralding a 'Golden Era' in the field of infectious disease research. The following 30 years marked the discovery of almost a dozen new classes of antibiotics, with new variants in each class being discovered. Antibiotics quickly flooded the market, with prescriptions being written for every minor infection and in the treatment of viral infections. This overuse, and misuse, of antibiotics led to their diminished clinical efficacy, a phenomenon termed antibiotic resistance. Some antibiotics endured several decades without succumbing to the effects of clinical resistance, whereas others saw resistance in a few short years (Figure 1-1).

There are four major modes of action which can lead to antimicrobial resistance: target modification, antibiotic inactivation, active efflux and altered uptake/permeability (Figure 1-2). The diversity of these mechanisms continues into specific types of each mechanism based upon substrate specificities, chemical reaction and structural class. The most prolific and mobile mode of resistance is antibiotic inactivation. Several modes of inactivation have been classified, including: acetylation, adenylylation, phosphorylation, glycosylation, and hydrolysation. These modes of resistance have been very well characterized and reviewed thoroughly throughout the literature (Wright, 2005).

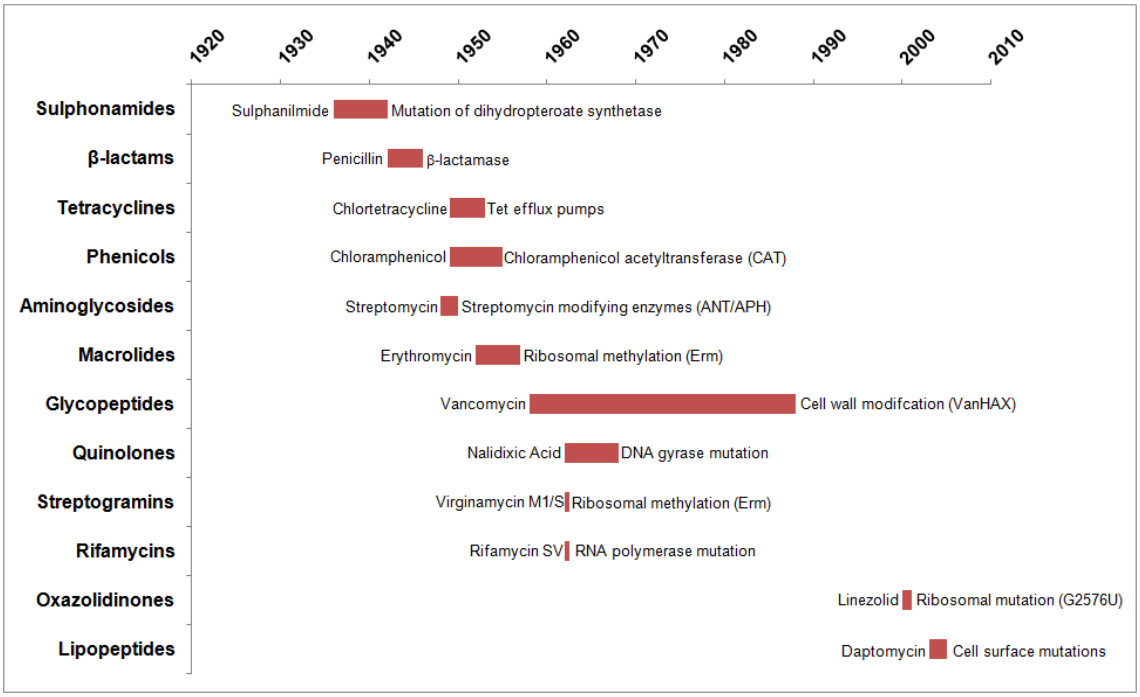

Figure 1-1: Timeline of Antibiotic resistance. A survey of a dozen antibiotic classes showing the first antibiotic in that class to be discovered, the amount of time before resistance was discovered (red bar), and the mechanism of resistance. The data for this table was derived from Walsh, CT. Antibiotics: Actions, Origins and Resistance, in addition to a literature survey of NCBI Pubmed.

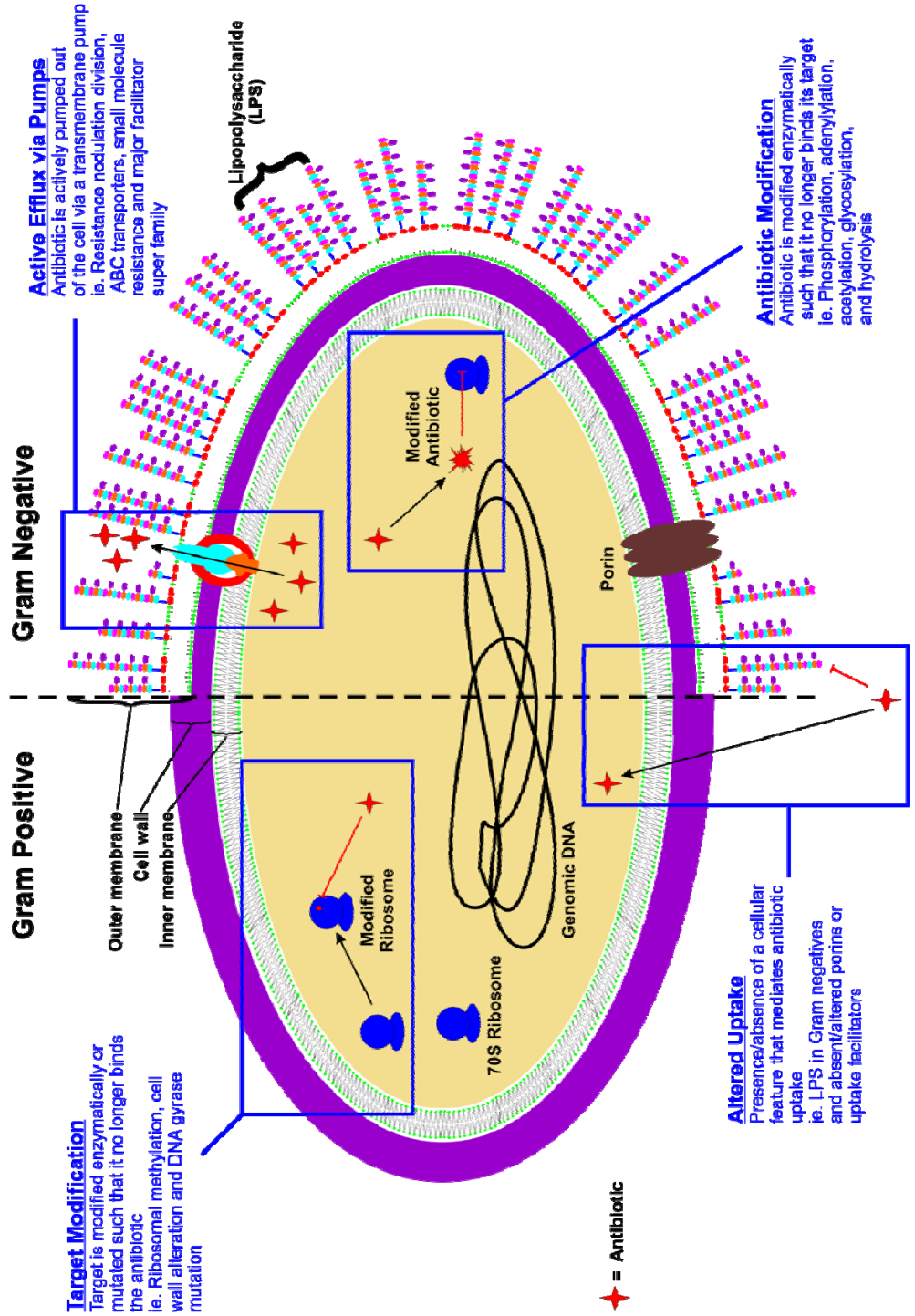

Figure 1-2: Modes of Antibiotic Resistance. The above diagram shows the various modes of antibiotic resistance as seen both Gram positive (G+) and Gram negative (G-) bacteria. There are four types of resistance illustrated here: target modification (G+ and G-), efflux (G- and to a lesser extent G+), altered uptake (G-) and antibiotic modification (G+ and G-). Black arrows show a positive interaction, and red lines show inhibition, with red four sided stars representing antibiotics.

Resistance is an acquired trait among most pathogenic organisms, so where is it acquired from? Antibiotic resistance mechanisms are widely distributed among environmental organisms and function as self-protection mechanisms for bacterial species that produce antibiotics and as a defensive mechanism for species that are proximal to these producing organisms (Cundliffe and Demain, 2010). The idea that these environmental organisms could provide a reservoir of resistance genes for pathogenic organisms was suggested early based on the similarity of aminoglycoside modifying enzymes in producing bacteria and pathogens (Benveniste and Davies, 1973). There now is growing favour to support this claim of an environmental reservoir of resistance (Allen et al., 2010; Canton, 2009; Wright, 2010). Other theories suggest that resistance is adaptive due to the constant exposure of antibiotics to pathogenic organisms. This could occur via 'sleeper genes' in the genome which have been silenced and are turned on due to antibiotic exposure, or genes that have mutated to accept an antibiotic substrate, as seen with efflux pumps in *Pseudomonas* spp. (Fernandez et al., 2011). This body of bona fide and putative resistance genes have been collectively coined the Antibiotic Resistome (D'Costa et al., 2006).

As physicians continue to respond to resistance mechanisms by altering treatments with varied antibiotics, organisms fight back by acquiring multiple resistance mechanisms, making this strategy increasingly difficult. The rise in multi-drug resistant (MDR) pathogens such as methicillin-resistant *Staphylococcus aureus* (MRSA) (Enright, 2003; Eriksen, 1964), vancomycin-resistant *Enterococci* (VRE) (Uttley et al., 1988), carbapenem-resistant *Enterobacteriaceae* (Nordmann et al., 2009) and MDR *Acinetobacter* spp. (Montefour et al., 2008), has renewed interest in novel antibiotic discovery.

It has been quickly learned that the discovery of novel antibiotic scaffolds is not as easy as it once was. The first round of antibiotics were discover from natural products; however, experts now believe that the 'low hanging fruits' have all been picked and that if natural sourced antibiotics are to be a viable reservoir, new methodologies for discovery need to be employed (Baltz, 2006). An alternative strategy has focused on efforts for the creation of small, synthetic molecules as inhibitors of essential bacterial pathways. This has been successful in cases such as the dihydrofolate reductase inhibitor trimethoprim (Bushby and Hitchings, 1968). However, overall progress through these campaigns has been limited, as documented in a recent survey conducted by Glaxo Smith-Kline, leading to a decreased interest in synthetic molecules as antibiotics (Payne et al., 2007).

A less realized strategy is the use of inhibitors of a resistance mechanism paired with the target antibiotic to create a synergistic therapy. This methodology has gained acclaim and has been especially successful in the field of β-lactam antibiotics. The first β-lactam synergistic therapy found was Augmentin ® (Leigh et al., 1981), it is comprised of the natural product clavulanate, a potent β-lactamase inhibitor, paired with the β-lactam antibiotic amoxicillin. Together, these two β-lactams were able to overcome several resistant organisms. In addition to Augmentin, several other combination therapies have been developed including Zozysn® (Piperacillin-tazobactam) (Akova et al., 1990) and Unasyn® (ampicillin-sulbactam) (Labia et al., 1986). If this same methodology is applicable to other antibiotic inactivating enzymes, it can offer a strategic advantage against resistant pathogens. Some good candidates for this type of therapy include several protein synthesis inhibitors such as the aminoglycoside and macrolide antibiotics. These two classes demonstrate either widespread or emerging antibiotic inactivation in bacterial species.

PROTEIN SYNTHESIS INHIBITORS

The Eubacterial Ribosome

The ribosome is the largest macromolecular catalyst which is required for the existence of life. It is the workhorse of the cell responsible for the production of proteins by translating the mRNA transcript of the genetic code. There are several critical sites on the ribosome which are required for its function. The first of these critical centres are the three tRNA binding sites, which are: the aminoacyl site (A-site), where the aminoacyl-tRNA is first recruited; the second site is the peptidyl site (P-site), where peptidyl-tRNA binds; and the exit site (E-site), where the bare tRNA binds prior to dissociation from the ribosome. In order for the ribosome to function correctly, a proof-reading mechanism is required to ensure cognate codon-anticodon. This machinery is embedded deep within the A-site below where the mRNA pairs with the aminoacyl-tRNA. When correct pairing occurs, key residues in helix 44 shift interact with the decoding loop (or accuracy switch), a part of helix 27, which allows for polymerization of the new amino acid. The final critical region is the peptide exit tunnel where the growing nascent peptide chain exits the ribosome (Figure 1-3) (Carter et al., 2000; Poehlsgaard and Douthwaite, 2005).

The essentiality of the ribosome has made it an attractive target for several major classes of antibiotics, some of which include: the phenicols, macrolides, lincosamides, streptogramins, oxazolidinones, tetracyclines and aminoglycosides (Poehlsgaard and Douthwaite, 2005). The precise action of these antibiotics had been previously determined based on early genetic foot-printing and mutational analyses; however, the elucidation of the high resolution three dimensional structure of the eubacterial ribosome

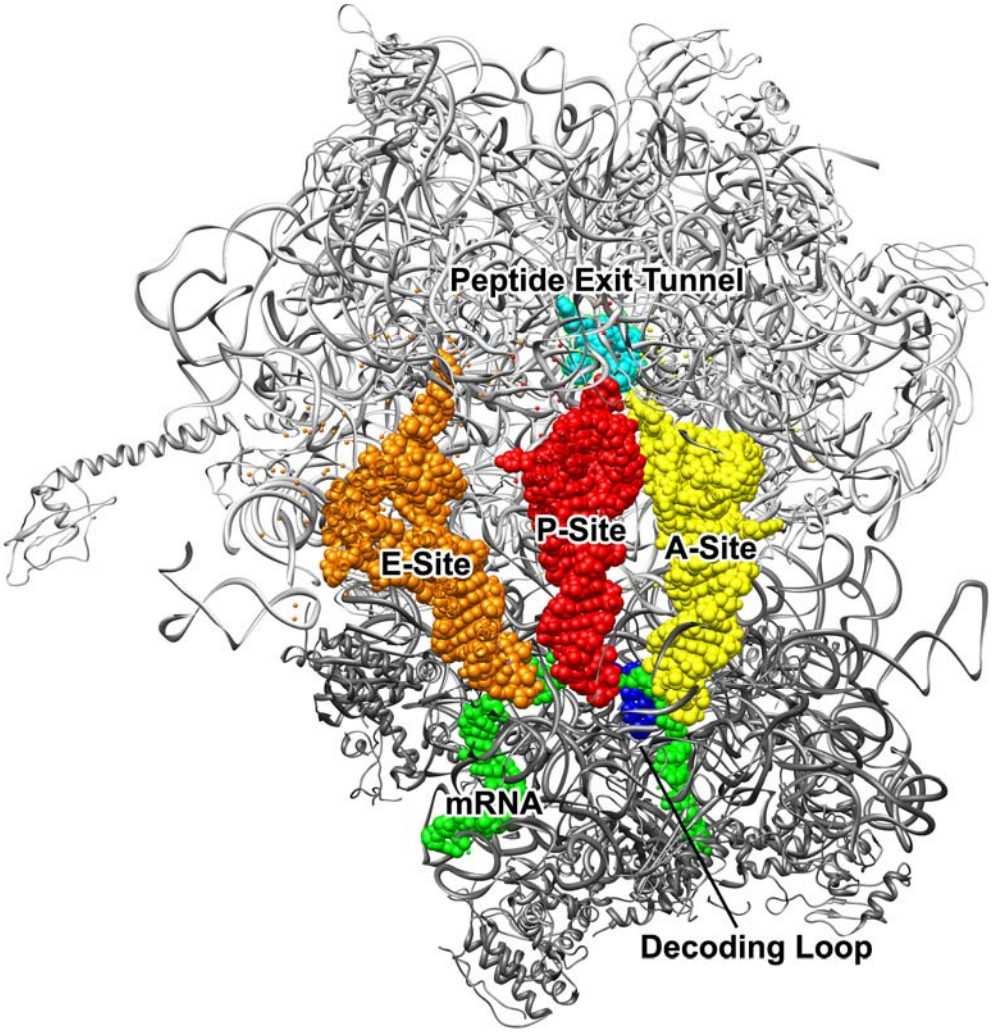

Figure 1-3: Overall structure of the 70S Ribosome. This representation of the 70S ribosome from *Thermus thermophilus* (PDB# 3I8F and 3I8G) with three tRNA molecules bound to the A-site (yellow), the P-site (red) and the E-site (orange) as well as a short mRNA strand (green) (Jenner et al., 2010). This structure also highlights important residues involved in codon-anticodon pairing (blue) (Carter et al., 2000) and peptide exit tunnel (cyan) (Bulkley et al., 2010; Dunkle et al., 2010).

(Clemons et al., 1999; Yusupov et al., 2001) has led to important discoveries in mechanisms of antibiotic action and resistance. To date, ribosomal structures of *Thermus thermophilus* (Clemons et al., 1999; Selmer et al., 2006; Yusupov et al., 2001), *Deinococcus radiodurans* (Harms et al., 2001), *Escherichia coli* (Vila-Sanjurjo et al., 2003) and the archaeon *Haloarcula marismortui* (Ban et al., 2000) have been solved, all of which have been also solved bound to the aforementioned classes of antibiotics. The most striking feature of these antibiotics is their ability to specifically target the aforementioned critical centres on the ribosome, which speaks to their level of co-evolution with the bacterial cell. The sites of action of these antibiotics can be reduced to three of the aforementioned areas: the peptide exit tunnel, the tRNA-mRNA pairing accuracy switch (helix 27) and the aminoacyl-tRNA binding site (helix 44) (Poehlsgaard and Douthwaite, 2005). The importance of these regions can be better understood by observing antibiotic action.

The Aminoglycosides

The discovery of streptomycin in 1944 by Dr. Selman Waksman led to the birth of a new class of antibiotics called the aminoglycosides (AGs) (Schatz et al., 2005). Since the initial discovery of streptomycin, the family of AG antibiotics has grown to over 25 different molecules, of either natural or semi-synthetic origin, and divided into three major sub-divisions; 4,5-disubstituted, 4,6-disubstituted, and atypical (Figure 1-4). The first two classes of AGs are generally made up of a 2-deoxystreptamine (DOS) core bound to amino sugars, whereas the atypical class lacks this DOS core, with the exception of neamine, and maintain unique core elements such as streptidine in streptomycin and its derivatives. Originally used as the only effective treatment against *Mycobacterium tuberculosis*, they gained utility in treating a wide range of nosocomial infections caused by species of *Enterococcus*, *Pseudomonas* and *Staphylococcus* (Vakulenko and Mobashery, 2003). Gaining notoriety as broad spectrum bactericidal agents, their utility began to decline due to ototoxic (deafness) (Hutchin and Cortopassi, 1994) and nephrotoxic (renal malfunction) (Mingeot-Leclercq and Tulkens, 1999) effects, as well as acquired resistance among bacterial species. Although the toxic side effects can be avoided with careful patient monitoring, the effects of resistance require a more chemotherapeutic approach such as novel resistance-proof AGs or inhibitors of resistance.

AGs act on the cell by penetrating the bacterial cell envelope through a series of diffusion and energy-dependant processes (Taber et al., 1987). Once in the cytosol, these small cationic molecules can bind to the several specific sites on anionic rRNA of the 30S subunit at the A-site to disrupt protein synthesis (Figure 1-5a) (Carter et al., 2000; Vicens and Westhof, 2001, 2002). The majority of aminoglycosides, namely the 4,5-

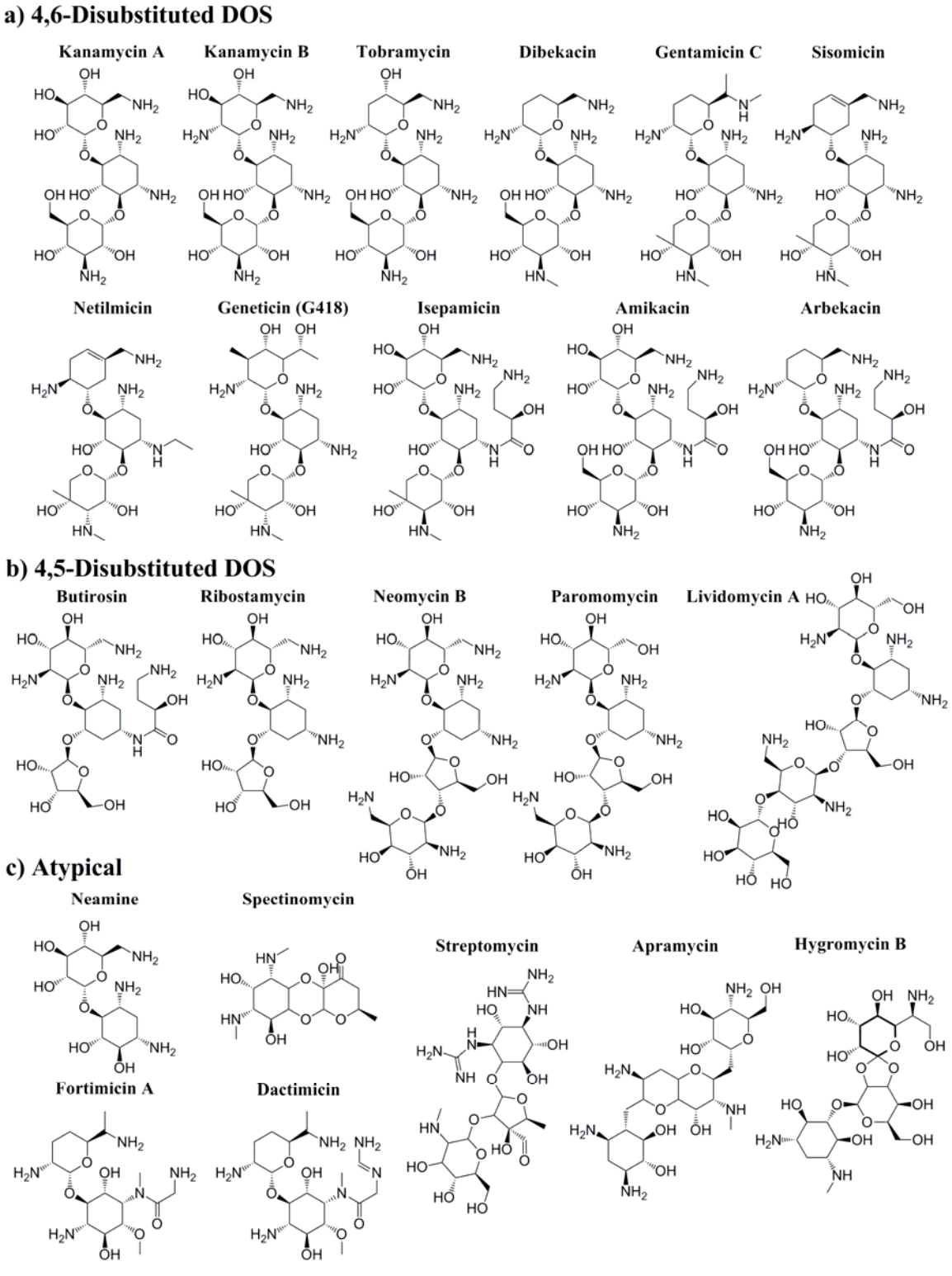

Figure 1-4: Structures of aminoglycoside antibiotics. Aminoglycoside antibiotics are divided into three major classes, a) 4,6-disubsituted DOS, b) 4,5-disubstituted DOS and c) atypical.

disubstituted and the 4,6-disubstituted families, act on the same site within the 30S subunit (Francois et al., 2005). The structure of paramomycin, a 4,5-disubstituted AG, in complex with the 30S subunit reveals that it makes a tight interaction with the major groove of helix 44 in the 16S rRNA (Figure 1-5b) (Carter et al., 2000). This in turn causes the decoding loop in helix 27 to shift from its hyper-accurate conformation (residues 888-890 paired with 910-912) to its error-prone conformation or ribosomal ambiguity (ram) state (residues 885-887 paired with 910-912), this leads residues A1492 and A1493 to move, which mimics the event when the aminoacyl-tRNA correctly pairs with the corresponding mRNA codon. With the ribosome in a constant 'on' state, it prevents proof-reading allowing any tRNA to pair with the mRNA. The atypical aminoglycoside streptomycin functions similarly to other AGs, but instead binds in a unique fashion to create the same end outcome of stabilizing the ram state (Figure 1-5b) (Carter et al., 2000). Preventing cognate codon-anticodon pairing ultimately leads to the production of mistranslated proteins of either null or altered function. These aberrant proteins produced by these interactions disseminate throughout the cell disrupting normal cellular functions and are believed to facilitate a second phase of lethal uptake of AGs, which is ultimately responsible for cell death. If the AG-ribosome binding event does not occur, the second uptake is blocked, and cell death does not ensue (Taber et al., 1987). This second uptake is typically blocked by either ribosomal or antibiotic modification, both of which reduce affinity of the antibiotic to the target site on the ribosome.

The aminocyclitol spectinomycin alternatively binds to the A-site to prevent translocation of the peptidyl-tRNA from the A-site to the P-site, it does so by interacting with only four residues; G1064, C1066, G1068 and C1192 (Figure 1-5b) (Carter et al., 2000). This action is not bacteriocidal and is readily reversed once intracellular concentrations of spectinomycin are reduced. Its action is also perturbed by ribosomal mutation or antibiotic modification, like the other AGs.

Mechanisms of AG Inactivation

Antibiotic modification is the most prevalent cause of aminoglycoside resistance and can be found in microbes both in the clinic and the environment. There are three major modes of inactivation that occur as a result of aminoglycoside modifying enzymes (AMEs): *N*-acetylation via aminoglycoside acetyltransferases (AACs), *O*-adenylylation via aminoglycoside nucleotidyltransferases (ANTs), and *O*-phosphorylation via aminoglycoside phosphotransferases (APHs) (Ramirez and Tolmasky, 2010) (Figure 1-6). Since this family of enzymes is large and diverse, a unified nomenclature system has been developed by *Shaw et al.*, which starts with a three letter identifier to state its chemical activity (AAC, ANT or APH), followed by a number in parenthesis to denote its regiospecific activity on the target drug, a roman numeral to state its drug spectrum

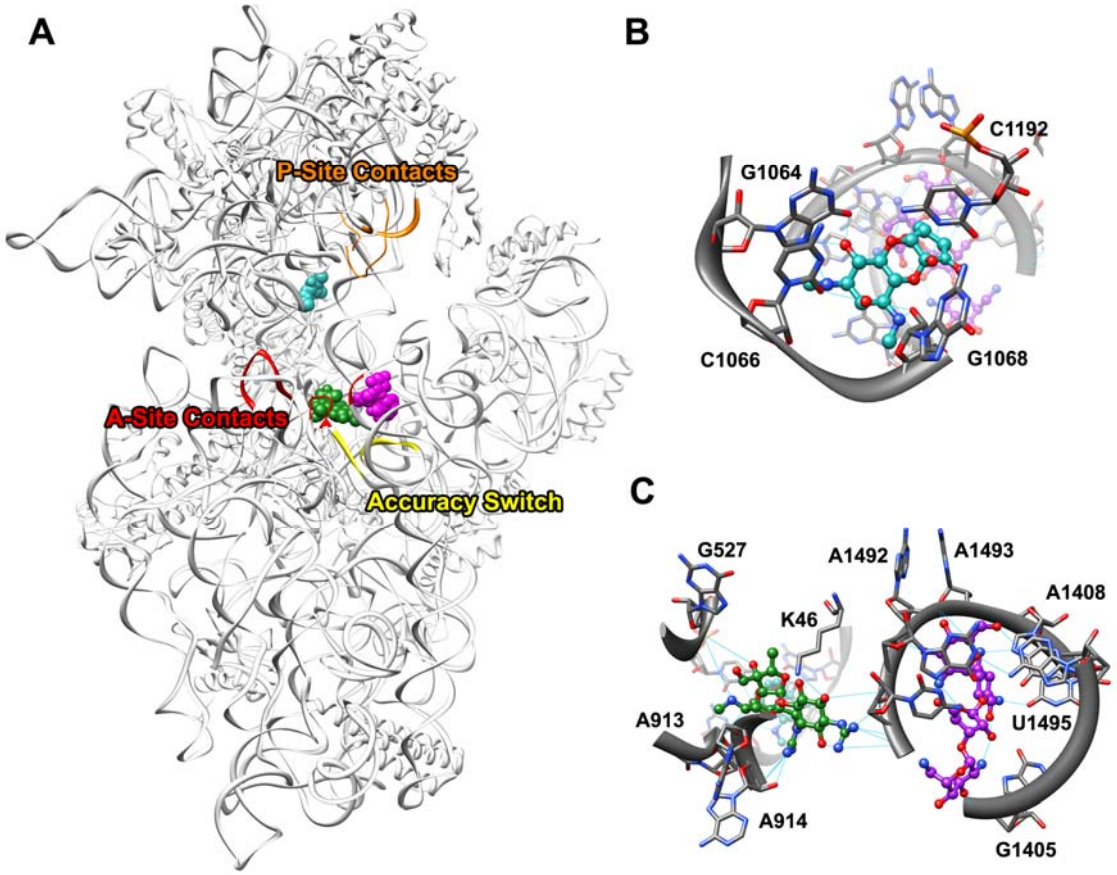

Figure 1-5: Aminoglycoside binding to the 30S ribosome. Aminoglycosides have been shown to bind to three distinct locations on the ribosome. Panel a) shows how paramomycin (purple), streptomycin (green) and spectinomycin (cyan) bind to the 30S subunit of the *Thermus thermophilus* ribosome with respect to the A-site tRNA contacts (red), the P-site tRNA contacts (orange) and the accuracy switch (yellow). b) Specific contacts between spectinomycin and the 16S rRNA with hydrogen bonds (light blue). c) Specific contacts between paramomycin and streptomycin with the 16S rRNA and ribo-proteins with hydrogen bonds (light blue). (PDB# 1FJG) (Carter et al., 2000).

(different for every regiospecific activity) and a lower-case letter to identify every new variant of the enzyme (Shaw et al., 1993). The evolution of these modifications has clearly been selected to disrupt known contacts between the AGs and the bacterial ribosome. Referring to Figure 1-5c, streptomycin is susceptible to phosphorylation and adenylylation at the C6-OH via APH(6) (Distler et al., 1987) and ANT(6) (Ounissi et al., 1990) enzymes and at the C3"-OH via ANT(3")(9) (Hollingshead and Vapnek, 1985) and APH(3") (Heinzel et al., 1988) enzymes respectively. Inspection of the co-structure of streptomycin with the 30S ribosomal subunit reveals that phosphorylation of C6-OH adds a large anionic phosphate group which will block the hydrogen bond formed by the anionic phosphate from G527 with the C6-OH. Similarly, addition of a large AMP moiety also abolishes this interaction. Similar effects can be seen by modification at the C3"-OH site with either an AMP or phosphate interferes with the phosphates of A914 and U14. These small modifications on AGs have major impacts on hydrogen bond formation and add steric hindrance and charge repulsions, which are all detrimental to antibiotic action by reducing affinity for their ribosomal target.

Proliferation of AMEs is also of great concern. They have been found to exist on mobile genetic elements, pathogenicity islands and embedded in chromosomes, either in an AG biosynthetic pathway or on their own in non-AG producing species. It has been desired to discover resistance-proof aminoglycosides or broad spectrum inhibitors capable of counteracting the effects of all AMEs. However, this goal is unlikely due to the diversity in substrate specificities, regiospecific activities and chemical action of AMEs. Efforts have been made to remove sites of modification via synthetic chemistry; however, many of these sites, as demonstrated, are essential for binding to the ribosome and can abolish antibiotic activity, making this approach increasingly difficult. Instead of focusing efforts on designing resistance-proof AGs, we can look at inhibitors for each family of AMEs and target their secondary substrate site (ATP or AcCoA) which donates the inactivating group to the AG.

The Macrolides

The use of macrolide antibiotics began with the discovery of erythromycin in 1952 from *Saccharopolyspora erythreae* by scientists at Eli Lilly (Lund, 1953; McGuire et al., 1952). Acclaimed for their excellent oral availability and efficient bacteriostatic activity against Gram positive pathogens, macrolides antibiotics are still extensively used in clinical settings.

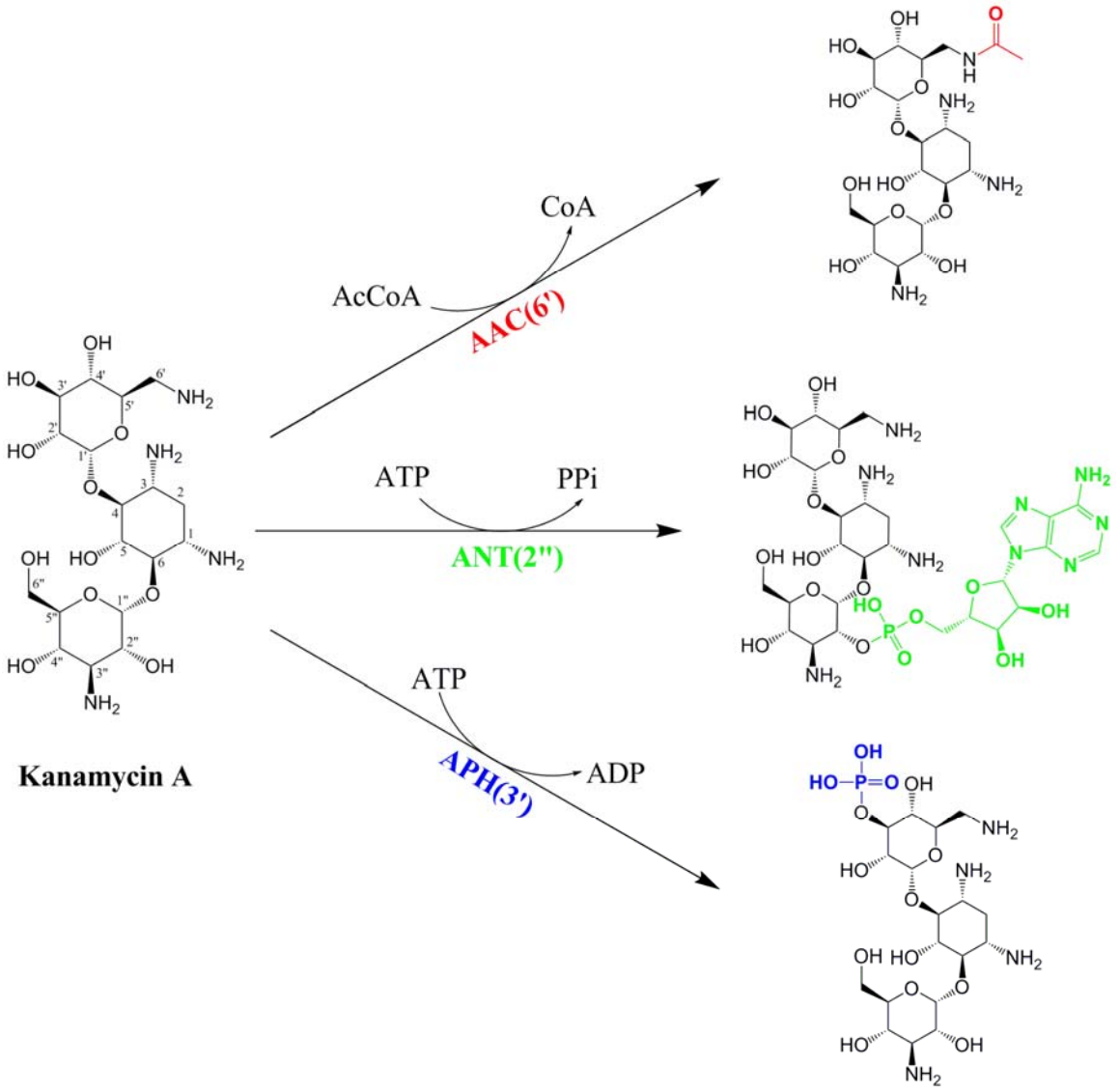

Figure 1-6: Enzymatic modifications of aminoglycosides. Kanamycin A is represented here with appropriate numbered carbons in order to demonstrate regiospecific modifications by three kinds of aminoglycoside modifying enzymes: acetylation at the C6'-OH via AAC(6'), adenylylation at the C2"-OH via ANT(2") and phosphorylation at the C3'-OH via APH(3'). The modifications have been highlighted to correspond with the font colour of the modifying enzyme.

Macrolides have a common structure consisting of a large macrocyclic lactone ring linked to various sugar moieties. They are classified based on the size the lactone ring, which range from 12-16 atoms (Zhanel et al., 2001). Like most antibiotics, the first generation of macrolides were isolated from a number of Actinobacteria; however, after succumbing to the effects of resistance a number of chemical modifications were made to the erythromycin scaffold giving rise to a second and third generations of semi-synthetic antibiotics, such as; clarithromycin, roxithromycin, dirithromycin, the azalide azithromycin and the ketolide telithromycin (Figure 1-7).

The ketolides have been a success story in the field of macrolide antibiotics; the replacement of the L-cladinose sugar in erythromycin with a 3-keto moiety improves the antibiotic activity and the efficacy against resistant organisms (Bryskier, 2000). Recently, anecdotal reports of telithromycin resistant clinical isolates have emerged and could be harbingers of an untimely demise of this new class of ML (Rantala et al., 2006; Reinert et al., 2005).

The action of macrolide antibiotics have been well described, they bind to the 23S rRNA within the 50S ribosomal subunit. Several structures have been solved with macrolides bound to all four ribosomal structures of *T. thermophilus* (Bulkley et al., 2010; Tu et al., 2005), *D. radiodurans* (Berisio et al., 2003; Schlunzen et al., 2001), *E. coli* (Dunkle et al., 2010) and *H. marismortui* (with a G2099A mutation, the equivalent to A2058 in *E. coli* in the 23S rRNA) (Hansen et al., 2002). Although each structure shows subtle differences in the conformation of the lactone ring of the macrolides, they all bind to the same general area of the 50S ribosomal subunit with the same key residue interactions in the peptide exit tunnel near the peptide translocation centre (PTC) (Figure 1-3). This binding region is not unique to macrolides antibiotics, but it is also shared by lincosamide, streptogramin B, ketolide and oxazolidinone antibiotics resulting in classification of MLS_BKO antibiotics, an acronym for antibiotics that bind at this site (Roberts, 2008).

To understand how binding at the peptide exit tunnel effects protein synthesis, we can look at how erythromycin works (Figure 1-8). Erythromycin sits cradled among residues 2057-2059 and U2611 in the 23S rRNA with several strong hydrogen bond contacts formed with the C2'-OH on the desosamine sugar, namely with A2058 (Bulkley et al., 2010; Dunkle et al., 2010). Although the PTC is highly conserved among all orders of life, A2058 is only found among eubacterial species, thus offering a reason why macrolide antibiotics only affect bacterial ribosomes (Tu et al., 2005). The presence of the desosamine sugar in erythromycin causes A2062 to shift position and create a van der

a) Natural 12-membered Macrolides

Methymycin

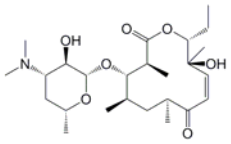

Neomethymycin

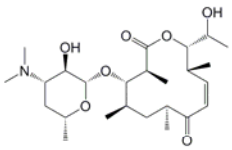

b) Natural 14-membered Macrolides

Pikromycin

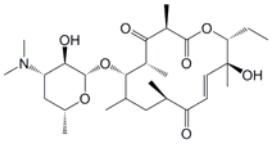

Erythromycin

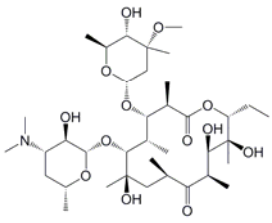

Oleandomycin

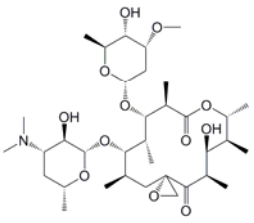

c) Natural 16-membered Macrolides

Spiramycin A

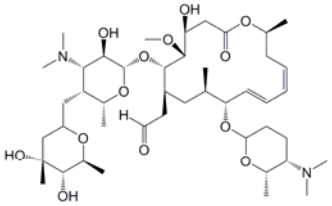

Kitasamycin

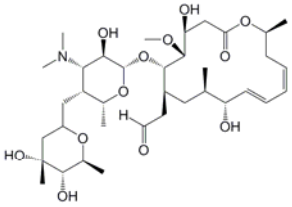

Josamycin

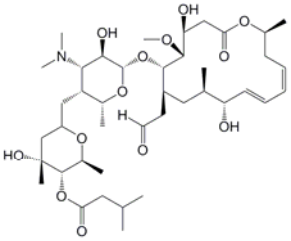

Midecamycin

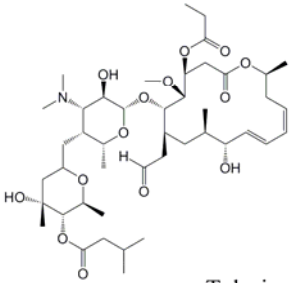

Sporeamicin A

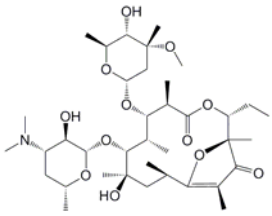

Rosaramicin

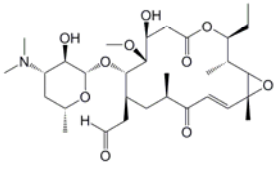

Tylosin

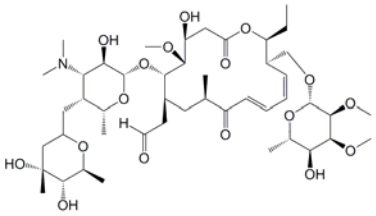

Mycinamicin

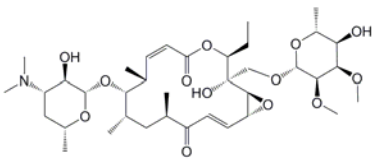

d) Semi-synthetic 14 and 15-membered Macrolides

Clarithromycin

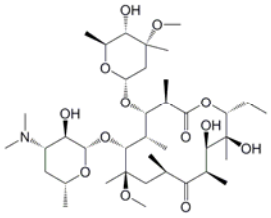

Erythromycalamine

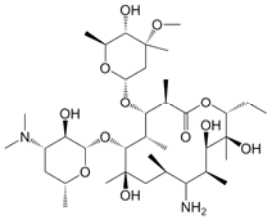

Roxithromycin

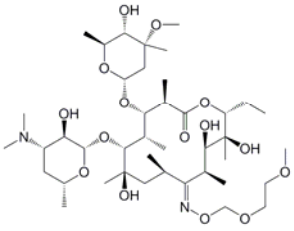

Flurithromycin

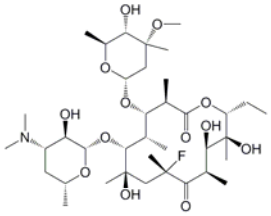

Dirithromycin

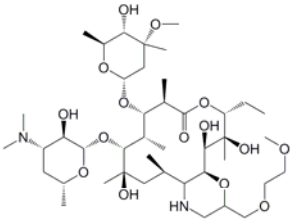

Azithromycin

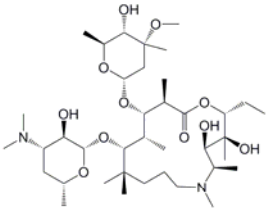

e) Semi-synthetic 16-membered Macrolides

Miokamycin

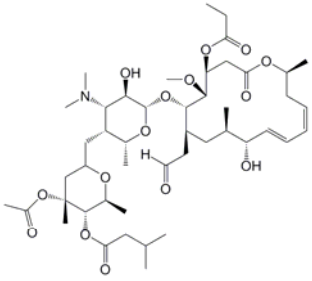

Rokitamycin

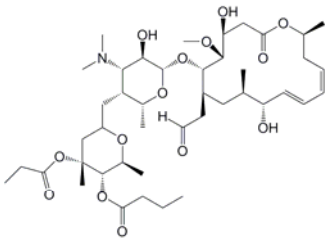

f) Semi-synthetic Ketolides

Telithromycin

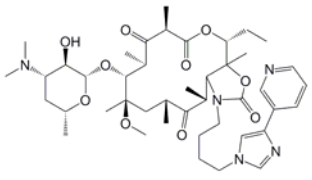

Cethromycin (ABT-773)

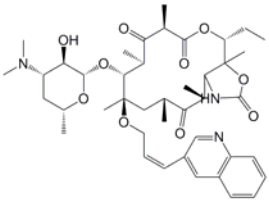

Figure 1-7: Structures of macrolide antibiotics. Macrolides that have been purified from antibiotic producing bacteria typically have either a) 12-membered, b) 14-membered or c) 16-membered lactone rings. These natural products have also been modified to produce semi-synthetic variants, such as the erythromycin-derived d) semi-synthetic 14and 15-membered MLs, the e) semi-synthetic 16-membered ML, and the erythromycin-derived f) ketolides.

Waals contact with the P-site tRNA, this is what is thought to prevent the emerging nascent peptide chain from entering the peptide exit tunnel and halting protein synthesis (Bulkley et al., 2010).

Macrolide Resistance

Macrolide resistance is on the rise within clinical settings. The most prevalent form of resistance is ribosomal protection via rRNA methylases (Erm), there have been 33 variants found in a number of clinical and environmental isolates, all which methylate A2058 (Roberts, 2008). The next most prevalent are MDR efflux pumps, with 14 different variants able to actively export macrolides (Roberts, 2008). One of the less realized methods of macrolide resistance is via inactivating enzymes. There are three modes of inactivation which have been discovered thus far: macrolide esterases (EreA and EreB) (Arthur et al., 1986; Ounissi and Courvalin, 1985), macrolide *O*-glycosyltransferases (GimA, Mgt and OleD) (Arthur et al., 1986; Gourmelen et al., 1998; Hernandez et al., 1993; Jenkins and Cundliffe, 1991) and macrolide *O*-phosphotransferases (MPHs) (Chesneau et al., 2007) (Figure 1-9). Ribosomal binding is severely diminished by the action of all three of these modifications. The hydrolysis of the ester via Ere causes the lactone ring to linearize and undergo a spontaneous hemiacetal formation followed by a condensation yielding a linear molecule that no longer resembles a macrolide (Barthelemy et al., 1984). Both the O-glycosyltransferases and O-phosphotransferases modify the C2'-OH of the desosamine/mycarose sugar which breaks the main hydrogen bond contacts with the A2058 residue, thus abolishing macrolide action. The O-glycosyltransferases have only been found in macrolide producing organisms and are not of clinical significance as of yet, however, the Ere and MPH phenotypes are on the rise clinically. These two resistance phenotypes were originally isolated from *E. coli* (Barthelemy et al., 1984; O'Hara et al., 1988). The presence of macrolide resistance mechanisms within a Gram negative pathogen is surprising since macrolides therapies are seldom used against Gram negative infections, with some exceptions, due to their innate resistance due to their outer cell membrane (Nikaido and Vaara, 1985). This implies that macrolide overuse is leading to these Gram negative organisms harbouring these mode of resistances, which is incidentally on the rise (Phuc Nguyen et al., 2009). Additionally, several MPH variants are also capable of inactivating telithromycin (Chesneau et al., 2007). A pre-emptive strategy is required to curb this new potentially dangerous mode of resistance.

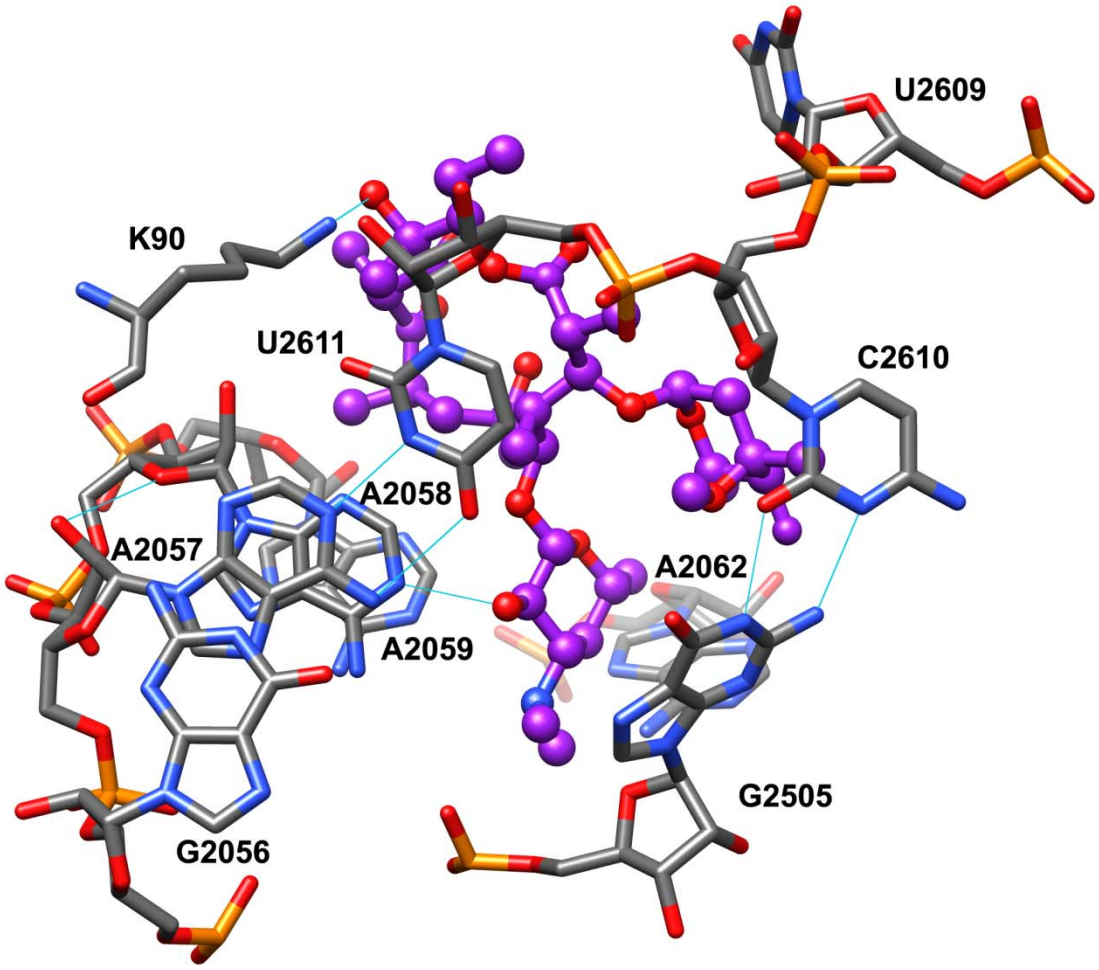

Figure 1-8: Binding of Erythromycin to the 50S ribosome. Erythromycin (magenta), and all other macrolide and ketolide antibiotics, bind to the 50S subunit of the *T. thermophilus* ribosome in the peptide exit tunnel. The critical contacts between 23S rRNA occur at the desosamine sugar moiety of erythromycin and the A2058 residue. (PDB# 3OHJ) (Bulkley et al., 2010)

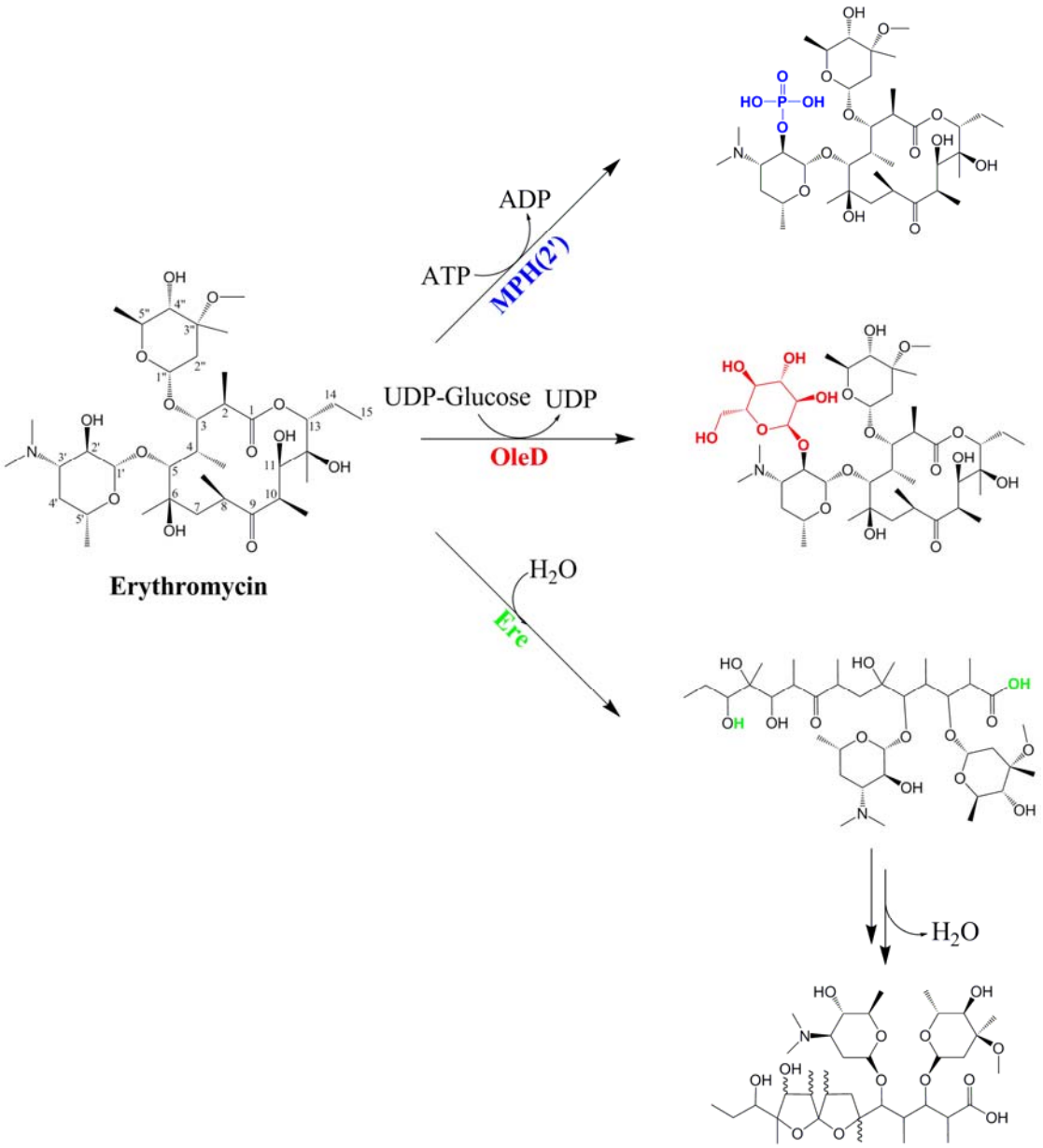

Figure 1-9: Enzymatic modifications of macrolides. The carbons in erythromycin have been numbered in order demonstrate regiospecificity of the enzymatic modifications: phosphorylation at the C2'-OH via MPH(2'), glycosylation at the C2'-OH via OleD and esterification of the lactone ring via Ere. The modifications have been highlighted to correspond with the font colour of the modifying enzyme.

ANTIBIOTIC KINASES

Eukaryotic protein kinases (ePKs) have been of particular interest within eukaryotic biology due to their key involvement in several essential cell processes; including, metabolism, cell division, transcription, apoptosis, cytoskeletal rearrangement, movement and differentiation via complex cell signalling cascades. Kinases constitute the largest family of genes within eukaryotic kingdom and have been intensively studied. They are also of interest because dysregulation or mutation of certain kinases can induce a disease state within the cell, whether it be cancer or neurodegenerative disorders like Alzheimer's and Parkinson's (Capra et al., 2006). This has led to extensive campaigns to find therapies that target these enzymes in hopes of overcoming these afflictions. Although sound in methodology, early attempts showed that the similarity between kinases led to pleiotropic effects of small molecule kinase inhibitors due of to inhibition of other kinases in other pathways (Fabian et al., 2005; Fedorov et al., 2007). Many of these issues are being solved with extensive bioinformatics (Manning et al., 2002), structural studies (Cheek et al., 2005) and screening against diverse panels of kinases (Fabian et al., 2005; Fedorov et al., 2007).

In the prokaryotic kingdom, the majority of cell signalling is not carried out by eukaryotic-like kinases (ELKs), but rather two-component histidine kinases which have a unique structural biology as compared to their eukaryotic counterparts (Wolanin et al., 2002). This does not mean that ELKs are not present in prokaryotes. Several studies have shown the presence of these kinases in Actinobacteria like *Mycobacteria* (Av-Gay and Everett, 2000) and *Streptomycetes* (Petrickova and Petricek, 2003) and play roles in cell signalling. The discovery of ELKs in prokaryotes are also beginning to be realized as important bacterial targets as seen with the Pkn kinases in *Mycobacterium tuberculosis* (Schreiber et al., 2009). In addition to having similar function in both prokaryotes and eukaryotes, the three-dimensional structures of ELKs and ePKs have revealed striking similarities in overall topology and catalytic residues and been collectively grouped as the protein kinase-like (PKL) superfamily (Scheeff and Bourne, 2005). Although PKL enzymes have several diverse domains to allow them to carry out their numerous functions throughout they cell, they all maintain a core kinase domain which is structurally conserved. The kinase core averages at about 300 amino acid residues and is made up of two lobes; a N-terminal lobe that is rich in β-sheets with a single α-helix (~80 aa) and C-terminal lobe that is predominantly α-helices with several shorter β-sheets. These two regions are linked by a hinge which creates a pocket between the two lobes lined with several highly conserved motifs and residues for ATP binding and catalysis (Johnson, 2009). The presence/absence of these motifs were surveyed in all the kinases sequences in the NCBI non-redundant database coupled with a recent global

oceanographic, metagenomic survey which identified 20 unique protein kinase-like (PKL) families (Kannan et al., 2007). This survey looked at the glycine-rich nucleotide positioning loop, the α and β phosphate co-ordinating lysine/arginine residue, the glutamate involved in stabilizing the lysine/arginine, the phosphorylation catalyzing Brenner's Motif (HxDxxxxN), the Mg^{2+} co-ordinating DFG sequence, the DLA sequence involved in stabilizing the Brenner motif and the histidine in LxxLH which hydrogen bonds to the DLA sequence (Kannan et al., 2007) (Figure 1-10).

One of the 20 families described was the choline and aminoglycoside kinase family (CAK) which is the largest and most diverse PKL family described in this survey (Kannan et al., 2007). The aminoglycoside kinases, or aminoglycoside phosphotransferases (APHs), are a major component of this family and were the first microbial kinases discovered to have PKL properties. Early primary sequence analysis suggested that APHs may have a connection to ePKs (Heinzel et al., 1988) and this was only solidified with the determination of the structure of APH(3')-IIIa (Hon et al., 1997). Since its discovery, several other APH structures have been solved including: APH(2")-IIa (Young et al., 2009), APH(2")-IVa (Toth et al., 2010), APH(3')-IIa (Nurizzo et al., 2003), APH(4)-Ia (Stogios et al., 2011) and APH(9)-Ia (Fong et al., 2010), all of which support the same findings (Figure 1-11). These structures each contain the nine key motifs described previously, which are essential for kinase activity. If the remaining APH and the related macrolides phosphotransferase (MPH) families are interrogated, there is a high level of consensus with those same nine regions (Appendix 2). The relationship between APHs and ePKs is further supported by the ability of protein kinase inhibitors (PKIs) to perturb the phosphorylation activity of APHs; this has been noted with isoquinoline sufonamides, wortmannin and a number of flavonoid molecules versus APH(2")-Ia and APH(3')-IIIa (Boehr et al., 2001; Daigle et al., 1997).

Antibiotic phosphorylating enzymes can be generally described as antibiotic kinases (AKs) which occupy a unique space found at the cross-section of the Antibiotic Resistome (D'Costa et al., 2006) and the Microbial Kinome (Kannan et al., 2007) known as the Antibiotic Kinome. This region is composed of microbial kinases that confer, or have the potential to confer, resistance to antibiotics via inactivation by a phosphorylation mechanism with a nucleotide donor. To date, three classes of antibiotics are susceptible to this action, the aforementioned AGs and MLs, and phenicol antibiotics.

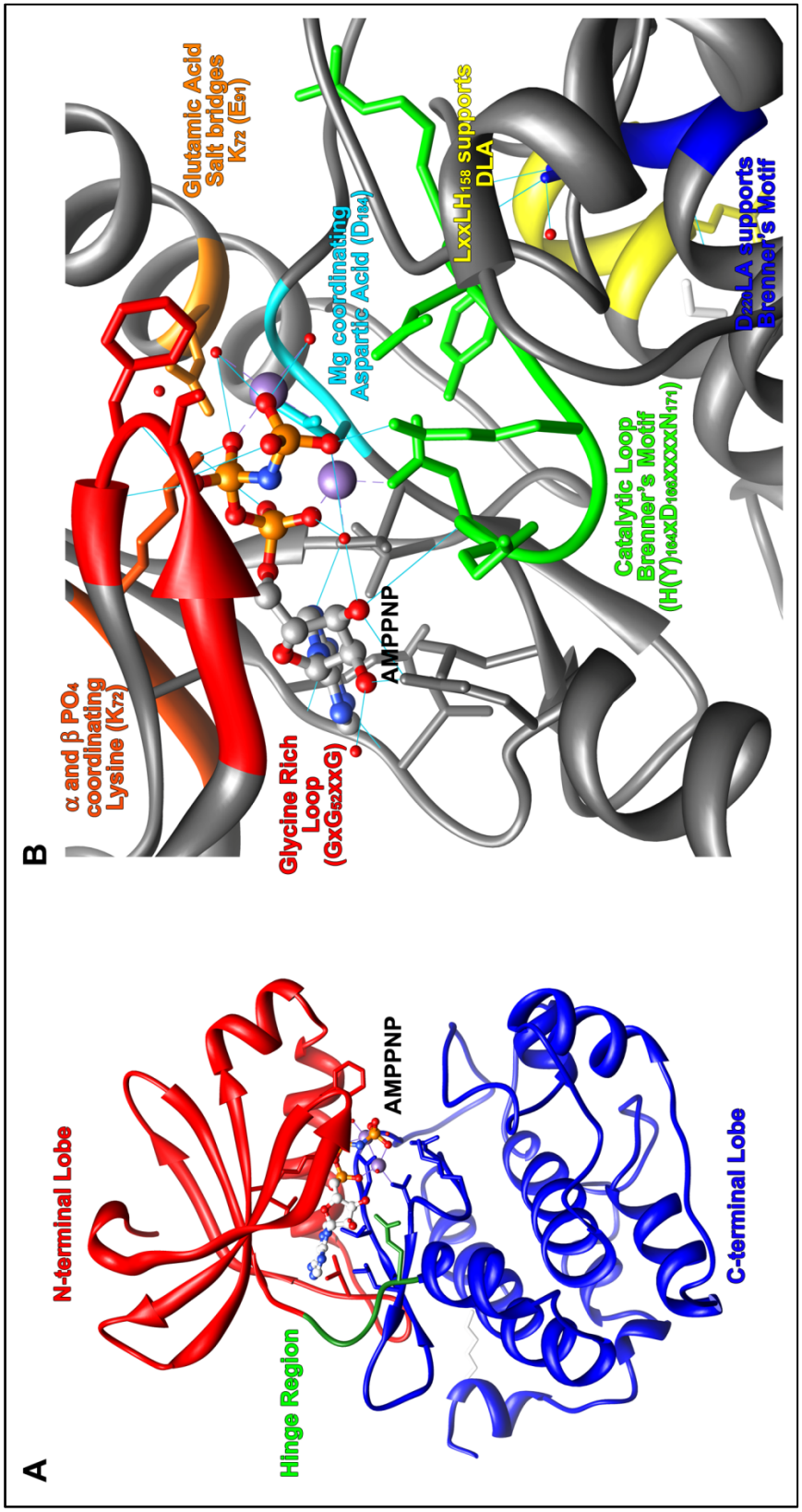

Figure 1-10: Key structural features and motifs in PKL enzymes. The ePK cAMP-dependant protein kinase serves as a typical model (PDB# 1cdk) (Bossemeyer et al., 1993), specifically the kinase domain (residues 38-310), to outline the a) overall shape of the kinase domain with the β-sheet rich N-terminal lobe (red), the hinge region (green), and the α-helix rich C-terminal lobe; and the b) key PKL motifs, which include, the glycine rich loop (red), the PO4 coordinating lysine (orange-red), the salt-bridge forming glutamic acid (orange), the LxxLH motif (yellow), the catalytic loop (green), the Mg^{2+} coordinating aspartic acid (cyan) and the Brenner motif supporting DLA (blue).

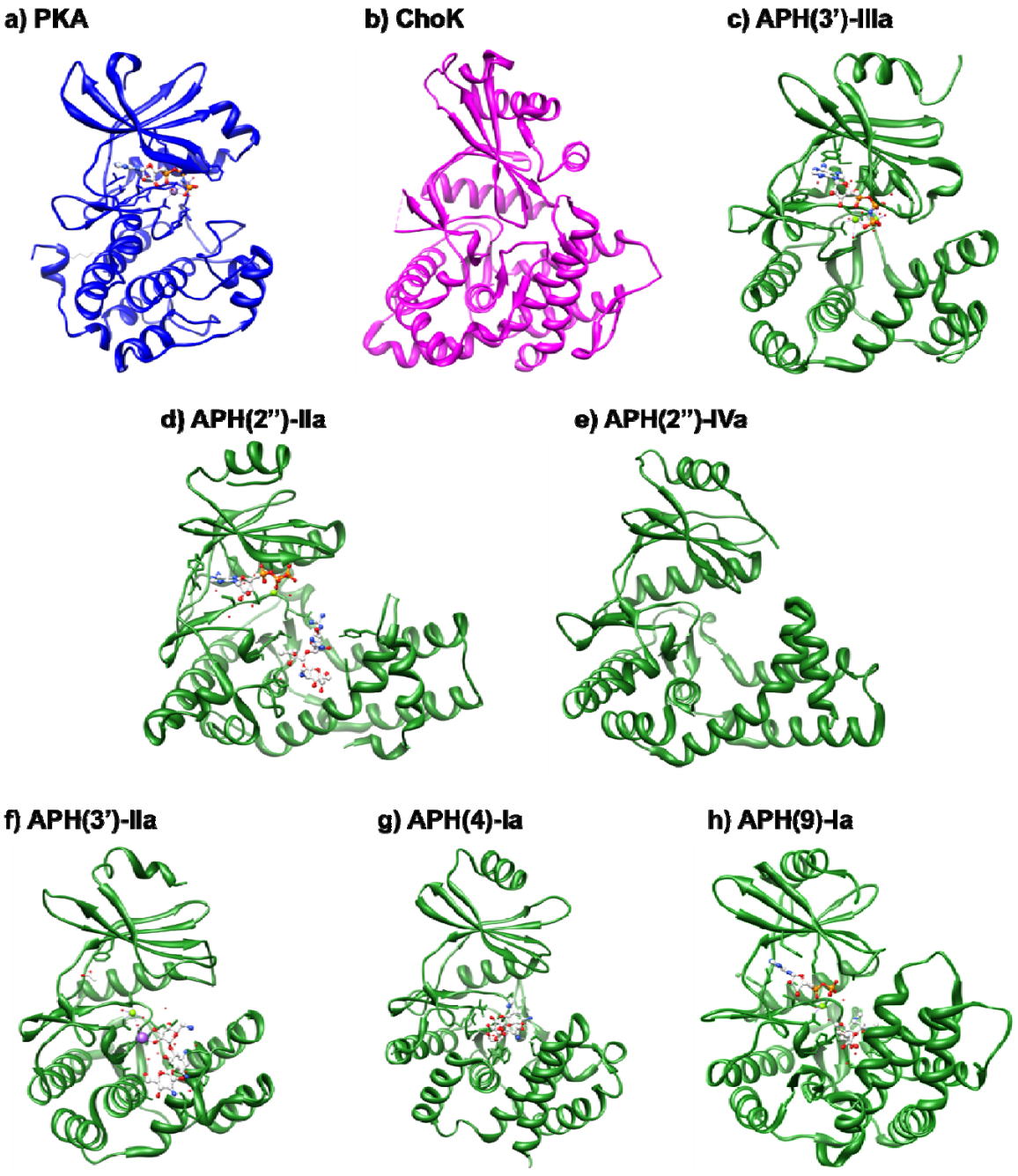

Figure 1-11: Comparison of ePKs to the CAK family of kinases. An overall topological comparison of ePKs (blue), choline kinases (magenta) and aminoglycoside phosphotransferases (green) a) PKA (residues 38-310) bound to AMPPNP (PDB# 1CDK), b) Choline kinase (PDB# 1NWT), c) APH(3')-IIIa bound to AMPPNP (PDB# 1J7U), d) APH(2")-IIa bound to streptomycin and ATP (PDB# 3HAV) , e) APH(2")-IVa (PDB# 3N4T), f) APH(3')-IIa (PDB# 1ND4), g) APH(4)-Ia bound to hygromycin B (PDB# 3OVC) and h) APH(9)-Ia bound to spectinomycin and ADP (PDB# 3I0O)

Chloramphenicol (CM) phosphorylation was originally observed in its producer *Streptomyces venezuelae* as the principal self-protection mechanism via chloramphenicol-3'-*O*-phosphortransferase (CPT) (Mosher et al., 1995). Unlike the other antibiotic kinases discussed here, the three dimensional structure of this enzyme has revealed homology not to the PKL superfamily but rather the P-loop NTPase superfamily, more specifically the non-canonical relatives of the DxTN group of P-loop kinases (Izard and Ellis, 2000; Leipe et al., 2003). This mode of chloramphenicol resistance has mainly been found within non-pathogenic soil dwelling bacteria. However, an annotated hypothetical protein (Rv2636) in *Mycobacterium tuberculosis* H37rv shows 32% identity and 43% similarity to the bona fide CPT (Cole et al., 1998). Although its activity as a CPT has not been demonstrated, this is the only plausible occurrence of a pathogenic variant of this resistance mechanism. So far, CPT appears to be the only known antibiotic kinase to belong to P-loop superfamily. However, the recent discovery of the crystal structure of TmrD, from *Deinococcus radiodurans*, suggests that it may inactivate tunicamycin via a phosphorylation mechanism based on its structural homology with CPT and its sequence identity with the *Bacillus subtilis* TmrB, a protein known to bind tunicamycin (Kapp et al., 2008; Noda et al., 1995).

A STRATEGY TO OVERCOME ANTIBIOTIC KINASES

The revelation that APHs and MPHs share homology to ePKs lends a unique opportunity to exploit this relationship. As previously mentioned, a select number of protein kinase inhibitors have demonstrated the ability to inhibit the action of a few APHs. If a larger spectrum of kinase inhibitors were to be tested against a diverse panel of antibiotic kinases, this could open a new avenue of drug discovery against this class of enzymes. With research on kinase inhibitors on the rise as chemotherapeutic agents against tumour cells, the majority of scaffolds of these molecules have been designed to target the ATP binding site and hold the potential to be repurposed as inhibitors of AKs. Many will argue that by using such compounds as potential therapeutics could lead to pleiotropic effects within the host target via human kinases. Although this claim holds merit, the use of structural biology, combinatorial chemistry and compound counter-screening against other kinases has yielded a number of highly specific kinase inhibitors which are also in clinical use (Johnson, 2009). For example, staurosporine is a notoriously potent promiscuous inhibitor, in recent binding assay conducted against 119 kinases, it was able to bind over 90% of them (Fabian et al., 2005). However, hydroxylation at the C7 yields 7-hydroxystaurosporine, which increases the compound's selectivity as a potent inhibitor of cell division enzyme checkpoint kinase 1. This compound's success has led to phase 1 clinical trials under the name UCN-01. In fact, therapies by kinase inhibitors are increasing with ten compounds already on the market and with an additional 50 compounds under clinical investigation (Johnson, 2009). The

classic example of well known kinase inhibitor is imatinib (Gleevec or Glivec) developed by Novartis. Imatinib selectively inhibits a defective form of ABL tyrosine kinase that is fused to BCR, known as BCR-ABL kinase (Druker et al., 1996) which causes chronic myelogenous leukemia. It has a narrow selectivity spectrum only inhibiting PDGFR kinase and KIT receptor tyrosine kinase (RTK). The inhibition of KIT RTK by imatinib was serendipitous, since the upregulation of KIT RTK leads to gastrointestinal stromal tumours, repurposing imatinib with another role against another form of cancer (Tuveson et al., 2001).

The idea of repurposing kinase inhibitors as antibacterial agents is not unique; success in this area has been demonstrated by scientists at Pfizer. Miller *et al*., have taken the kinase inhibitor pharmacophore of the pyridopyrimidines and used it to target the bacterial fatty acid biosynthesis enzyme biotin carboxylase, a member of the acetyl-CoA carboxylase multi-enzyme complex. The biotin carboxylase also has an active site with structural similarity to ePKs, but harbours enough unique traits to allow for selectivity against human kinases and the eukaryotic acetyl-CoA carboxylase. This discovery did not occur through a directed effort against biotin carboxylase, but through a whole cell screening approach where the target was determined after growth inhibition was observed (Miller et al., 2009). In order to use a directed approach to target AKs with kinase inhibitors several steps are required:

1. Obtain a diverse panel of AKs and subject them to rigorous biochemical characterization to understand their complete substrate spectra.
2. Generate structural data of each representative class bound to its respective substrates to assess the presence/absence of unique motifs and residues for exploitation by novel inhibitor design.
3. Screen these representative enzymes against a preliminary set of well known and characterized kinase inhibitors to search for plausible scaffolds
4. Correlate structural data and screening data to design new highly specific inhibitors of AKs

The work presented here demonstrates the use of the above principles in order to identify novel inhibitors of antibiotic kinases.

REFERENCES

Akova, M., Yang, Y., and Livermore, D.M. (1990). Interactions of tazobactam and clavulanate with inducibly- and constitutively-expressed Class I beta-lactamases. J Antimicrob Chemother *25*, 199-208.

Allen, H.K., Donato, J., Wang, H.H., Cloud-Hansen, K.A., Davies, J., and Handelsman, J. (2010). Call of the wild: antibiotic resistance genes in natural environments. Nat Rev Microbiol *8*, 251-259.

Arthur, M., Autissier, D., and Courvalin, P. (1986). Analysis of the nucleotide sequence of the ereB gene encoding the erythromycin esterase type II. Nucleic Acids Res *14*, 4987-4999.

Av-Gay, Y., and Everett, M. (2000). The eukaryotic-like Ser/Thr protein kinases of Mycobacterium tuberculosis. Trends Microbiol *8*, 238-244.

Baltz, R.H. (2006). Marcel Faber Roundtable: is our antibiotic pipeline unproductive because of starvation, constipation or lack of inspiration? J Ind Microbiol Biotechnol *33*, 507-513.

Ban, N., Nissen, P., Hansen, J., Moore, P.B., and Steitz, T.A. (2000). The complete atomic structure of the large ribosomal subunit at 2.4 A resolution. Science *289*, 905-920.

Barthelemy, P., Autissier, D., Gerbaud, G., and Courvalin, P. (1984). Enzymic hydrolysis of erythromycin by a strain of Escherichia coli. A new mechanism of resistance. J Antibiot (Tokyo) *37*, 1692-1696.

Benveniste, R., and Davies, J. (1973). Aminoglycoside antibiotic-inactivating enzymes in actinomycetes similar to those present in clinical isolates of antibiotic-resistant bacteria. Proc Natl Acad Sci U S A *70*, 2276-2280.

Berisio, R., Schluenzen, F., Harms, J., Bashan, A., Auerbach, T., Baram, D., and Yonath, A. (2003). Structural insight into the role of the ribosomal tunnel in cellular regulation. Nat Struct Biol *10*, 366-370.

Boehr, D.D., Lane, W.S., and Wright, G.D. (2001). Active site labeling of the gentamicin resistance enzyme AAC(6')-APH(2") by the lipid kinase inhibitor wortmannin. Chem Biol *8*, 791-800.

Bossemeyer, D., Engh, R.A., Kinzel, V., Ponstingl, H., and Huber, R. (1993). Phosphotransferase and substrate binding mechanism of the cAMP-dependent protein kinase catalytic subunit from porcine heart as deduced from the 2.0 A structure of the complex with Mn2+ adenylyl imidodiphosphate and inhibitor peptide PKI(5-24). EMBO J *12*, 849-859.

Bryskier, A. (2000). Ketolides-telithromycin, an example of a new class of antibacterial agents. Clin Microbiol Infect *6*, 661-669.

Bulkley, D., Innis, C.A., Blaha, G., and Steitz, T.A. (2010). Revisiting the structures of several antibiotics bound to the bacterial ribosome. Proc Natl Acad Sci U S A *107*, 17158-17163.

Bushby, S.R., and Hitchings, G.H. (1968). Trimethoprim, a sulphonamide potentiator. Br J Pharmacol Chemother *33*, 72-90.

Canton, R. (2009). Antibiotic resistance genes from the environment: a perspective through newly identified antibiotic resistance mechanisms in the clinical setting. Clin Microbiol Infect *15 Suppl 1*, 20-25.

Capra, M., Nuciforo, P.G., Confalonieri, S., Quarto, M., Bianchi, M., Nebuloni, M., Boldorini, R., Pallotti, F., Viale, G., Gishizky, M.L., *et al.* (2006). Frequent alterations in the expression of serine/threonine kinases in human cancers. Cancer Res *66*, 8147-8154.

Carter, A.P., Clemons, W.M., Brodersen, D.E., Morgan-Warren, R.J., Wimberly, B.T., and Ramakrishnan, V. (2000). Functional insights from the structure of the 30S ribosomal subunit and its interactions with antibiotics. Nature *407*, 340-348.

Cheek, S., Ginalski, K., Zhang, H., and Grishin, N.V. (2005). A comprehensive update of the sequence and structure classification of kinases. BMC Struct Biol *5*, 6.

Chesneau, O., Tsvetkova, K., and Courvalin, P. (2007). Resistance phenotypes conferred by macrolide phosphotransferases. FEMS Microbiol Lett *269*, 317-322.

Clemons, W.M., Jr., May, J.L., Wimberly, B.T., McCutcheon, J.P., Capel, M.S., and Ramakrishnan, V. (1999). Structure of a bacterial 30S ribosomal subunit at 5.5 A resolution. Nature *400*, 833-840.

Cole, S.T., Brosch, R., Parkhill, J., Garnier, T., Churcher, C., Harris, D., Gordon, S.V., Eiglmeier, K., Gas, S., Barry, C.E., 3rd, *et al.* (1998). Deciphering the biology of Mycobacterium tuberculosis from the complete genome sequence. Nature *393*, 537-544.

Cundliffe, E., and Demain, A.L. (2010). Avoidance of suicide in antibiotic-producing microbes. J Ind Microbiol Biotechnol *37*, 643-672.

D'Costa, V.M., McGrann, K.M., Hughes, D.W., and Wright, G.D. (2006). Sampling the antibiotic resistome. Science *311*, 374-377.

Daigle, D.M., McKay, G.A., and Wright, G.D. (1997). Inhibition of aminoglycoside antibiotic resistance enzymes by protein kinase inhibitors. J Biol Chem *272*, 24755-24758.

Distler, J., Braun, C., Ebert, A., and Piepersberg, W. (1987). Gene cluster for streptomycin biosynthesis in Streptomyces griseus: analysis of a central region including the major resistance gene. Mol Gen Genet *208*, 204-210.

Druker, B.J., Tamura, S., Buchdunger, E., Ohno, S., Segal, G.M., Fanning, S., Zimmermann, J., and Lydon, N.B. (1996). Effects of a selective inhibitor of the Abl tyrosine kinase on the growth of Bcr-Abl positive cells. Nat Med *2*, 561-566.

Dunkle, J.A., Xiong, L., Mankin, A.S., and Cate, J.H. (2010). Structures of the Escherichia coli ribosome with antibiotics bound near the peptidyl transferase center explain spectra of drug action. Proc Natl Acad Sci U S A *107*, 17152-17157.

Enright, M.C. (2003). The evolution of a resistant pathogen--the case of MRSA. Curr Opin Pharmacol *3*, 474-479.

Eriksen, K.R. (1964). Methicillin-Resistance in Staphylococcus Aureus Apparently Developed during Treatment with Methicillin. Acta Pathol Microbiol Scand *61*, 154-155.

Fabian, M.A., Biggs, W.H., 3rd, Treiber, D.K., Atteridge, C.E., Azimioara, M.D., Benedetti, M.G., Carter, T.A., Ciceri, P., Edeen, P.T., Floyd, M., *et al.* (2005). A small molecule-kinase interaction map for clinical kinase inhibitors. Nat Biotechnol *23*, 329-336.

Fedorov, O., Marsden, B., Pogacic, V., Rellos, P., Muller, S., Bullock, A.N., Schwaller, J., Sundstrom, M., and Knapp, S. (2007). A systematic interaction map of validated kinase inhibitors with Ser/Thr kinases. Proc Natl Acad Sci U S A *104*, 20523-20528.

Fernandez, L., Breidenstein, E.B., and Hancock, R.E. (2011). Creeping baselines and adaptive resistance to antibiotics. Drug Resist Updat.

Fleming, A. (1944). Penicillin: The Robert Campbell Oration. Ulster Med J *13*, 95-122 122.

Fong, D.H., Lemke, C.T., Hwang, J., Xiong, B., and Berghuis, A.M. (2010). Structure of the antibiotic resistance factor spectinomycin phosphotransferase from Legionella pneumophila. J Biol Chem *285*, 9545-9555.

Francois, B., Russell, R.J., Murray, J.B., Aboul-ela, F., Masquida, B., Vicens, Q., and Westhof, E. (2005). Crystal structures of complexes between aminoglycosides and decoding A site oligonucleotides: role of the number of rings and positive charges in the specific binding leading to miscoding. Nucleic Acids Res *33*, 5677-5690.

Gourmelen, A., Blondelet-Rouault, M.H., and Pernodet, J.L. (1998). Characterization of a glycosyl transferase inactivating macrolides, encoded by gimA from Streptomyces ambofaciens. Antimicrob Agents Chemother *42*, 2612-2619.

Hansen, J.L., Ippolito, J.A., Ban, N., Nissen, P., Moore, P.B., and Steitz, T.A. (2002). The structures of four macrolide antibiotics bound to the large ribosomal subunit. Mol Cell *10*, 117-128.

Harms, J., Schluenzen, F., Zarivach, R., Bashan, A., Gat, S., Agmon, I., Bartels, H., Franceschi, F., and Yonath, A. (2001). High resolution structure of the large ribosomal subunit from a mesophilic eubacterium. Cell *107*, 679-688.

Heinzel, P., Werbitzky, O., Distler, J., and Piepersberg, W. (1988). A second streptomycin resistance gene from Streptomyces griseus codes for streptomycin-3"-phosphotransferase. Relationships between antibiotic and protein kinases. Arch Microbiol *150*, 184-192.

Hernandez, C., Olano, C., Mendez, C., and Salas, J.A. (1993). Characterization of a Streptomyces antibioticus gene cluster encoding a glycosyltransferase involved in oleandomycin inactivation. Gene *134*, 139-140.

Hollingshead, S., and Vapnek, D. (1985). Nucleotide sequence analysis of a gene encoding a streptomycin/spectinomycin adenylyltransferase. Plasmid *13*, 17-30.

Hon, W.C., McKay, G.A., Thompson, P.R., Sweet, R.M., Yang, D.S., Wright, G.D., and Berghuis, A.M. (1997). Structure of an enzyme required for aminoglycoside antibiotic resistance reveals homology to eukaryotic protein kinases. Cell *89*, 887-895.

Hutchin, T., and Cortopassi, G. (1994). Proposed molecular and cellular mechanism for aminoglycoside ototoxicity. Antimicrob Agents Chemother *38*, 2517-2520.

Izard, T., and Ellis, J. (2000). The crystal structures of chloramphenicol phosphotransferase reveal a novel inactivation mechanism. EMBO J *19*, 2690-2700.

Jenkins, G., and Cundliffe, E. (1991). Cloning and characterization of two genes from Streptomyces lividans that confer inducible resistance to lincomycin and macrolide antibiotics. Gene *108*, 55-62.

Jenner, L.B., Demeshkina, N., Yusupova, G., and Yusupov, M. (2010). Structural aspects of messenger RNA reading frame maintenance by the ribosome. Nat Struct Mol Biol *17*, 555-560.

Johnson, L.N. (2009). Protein kinase inhibitors: contributions from structure to clinical compounds. Q Rev Biophys *42*, 1-40.

Kannan, N., Taylor, S.S., Zhai, Y., Venter, J.C., and Manning, G. (2007). Structural and functional diversity of the microbial kinome. PLoS Biol *5*, e17.

Kapp, U., Macedo, S., Hall, D.R., Leiros, I., McSweeney, S.M., and Mitchell, E. (2008). Structure of Deinococcus radiodurans tunicamycin-resistance protein (TmrD), a phosphotransferase. Acta Crystallogr Sect F Struct Biol Cryst Commun *64*, 479-486.

Labia, R., Morand, A., Lelievre, V., Mattioni, D., and Kazmierczak, A. (1986). Sulbactam: biochemical factors involved in its synergy with ampicillin. Rev Infect Dis *8 Suppl 5*, S496-502.

Leigh, D.A., Bradnock, K., and Marriner, J.M. (1981). Augmentin (amoxycillin and clavulanic acid) therapy in complicated infections due to beta-lactamase producing bacteria. J Antimicrob Chemother *7*, 229-236.

Leipe, D.D., Koonin, E.V., and Aravind, L. (2003). Evolution and classification of P-loop kinases and related proteins. J Mol Biol *333*, 781-815.

Lund, E. (1953). Erythromycin; a new antibiotic. Acta Pathol Microbiol Scand *33*, 393-400.

Manning, G., Whyte, D.B., Martinez, R., Hunter, T., and Sudarsanam, S. (2002). The protein kinase complement of the human genome. Science *298*, 1912-1934.

McGuire, J.M., Bunch, R.L., Anderson, R.C., Boaz, H.E., Flynn, E.H., Powell, H.M., and Smith, J.W. (1952). [Ilotycin, a new antibiotic]. Schweiz Med Wochenschr *82*, 1064-1065.

Miller, J.R., Dunham, S., Mochalkin, I., Banotai, C., Bowman, M., Buist, S., Dunkle, B., Hanna, D., Harwood, H.J., Huband, M.D., *et al.* (2009). A class of selective antibacterials derived from a protein kinase inhibitor pharmacophore. Proc Natl Acad Sci U S A *106*, 1737-1742.

Mingeot-Leclercq, M.P., and Tulkens, P.M. (1999). Aminoglycosides: nephrotoxicity. Antimicrob Agents Chemother *43*, 1003-1012.

Montefour, K., Frieden, J., Hurst, S., Helmich, C., Headley, D., Martin, M., and Boyle, D.A. (2008). Acinetobacter baumannii: an emerging multidrug-resistant pathogen in critical care. Crit Care Nurse *28*, 15-25; quiz 26.

Mosher, R.H., Camp, D.J., Yang, K., Brown, M.P., Shaw, W.V., and Vining, L.C. (1995). Inactivation of chloramphenicol by O-phosphorylation. A novel resistance mechanism in Streptomyces venezuelae ISP5230, a chloramphenicol producer. J Biol Chem *270*, 27000-27006.

Nikaido, H., and Vaara, M. (1985). Molecular basis of bacterial outer membrane permeability. Microbiol Rev *49*, 1-32.

Noda, Y., Takatsuki, A., Yoda, K., and Yamasaki, M. (1995). TmrB protein, which confers resistance to tunicamycin on Bacillus subtilis, binds tunicamycin. Biosci Biotechnol Biochem *59*, 321-322.

Nordmann, P., Cuzon, G., and Naas, T. (2009). The real threat of Klebsiella pneumoniae carbapenemase-producing bacteria. Lancet Infect Dis *9*, 228-236.

Nurizzo, D., Shewry, S.C., Perlin, M.H., Brown, S.A., Dholakia, J.N., Fuchs, R.L., Deva, T., Baker, E.N., and Smith, C.A. (2003). The crystal structure of aminoglycoside-3'-phosphotransferase-IIa, an enzyme responsible for antibiotic resistance. J Mol Biol *327*, 491-506.

O'Hara, K., Kanda, T., and Kono, M. (1988). Structure of a phosphorylated derivative of oleandomycin, obtained by reaction of oleandomycin with an extract of an erythromycin-resistant strain of Escherichia coli. J Antibiot (Tokyo) *41*, 823-827.

Ounissi, H., and Courvalin, P. (1985). Nucleotide sequence of the gene ereA encoding the erythromycin esterase in Escherichia coli. Gene *35*, 271-278.

Ounissi, H., Derlot, E., Carlier, C., and Courvalin, P. (1990). Gene homogeneity for aminoglycoside-modifying enzymes in gram-positive cocci. Antimicrob Agents Chemother *34*, 2164-2168.

Payne, D.J., Gwynn, M.N., Holmes, D.J., and Pompliano, D.L. (2007). Drugs for bad bugs: confronting the challenges of antibacterial discovery. Nat Rev Drug Discov *6*, 29-40.

Petrickova, K., and Petricek, M. (2003). Eukaryotic-type protein kinases in Streptomyces coelicolor: variations on a common theme. Microbiology *149*, 1609-1621.

Phuc Nguyen, M.C., Woerther, P.L., Bouvet, M., Andremont, A., Leclercq, R., and Canu, A. (2009). Escherichia coli as reservoir for macrolide resistance genes. Emerg Infect Dis *15*, 1648-1650.

Poehlsgaard, J., and Douthwaite, S. (2005). The bacterial ribosome as a target for antibiotics. Nat Rev Microbiol *3*, 870-881.

Ramirez, M.S., and Tolmasky, M.E. (2010). Aminoglycoside modifying enzymes. Drug Resist Updat *13*, 151-171.

Rantala, M., Haanpera-Heikkinen, M., Lindgren, M., Seppala, H., Huovinen, P., and Jalava, J. (2006). Streptococcus pneumoniae isolates resistant to telithromycin. Antimicrob Agents Chemother *50*, 1855-1858.

Reinert, R.R., van der Linden, M., and Al-Lahham, A. (2005). Molecular characterization of the first telithromycin-resistant Streptococcus pneumoniae isolate in Germany. Antimicrob Agents Chemother *49*, 3520-3522.

Roberts, M.C. (2008). Update on macrolide-lincosamide-streptogramin, ketolide, and oxazolidinone resistance genes. FEMS Microbiol Lett *282*, 147-159.

Schatz, A., Bugie, E., and Waksman, S.A. (2005). Streptomycin, a substance exhibiting antibiotic activity against gram-positive and gram-negative bacteria. 1944. Clin Orthop Relat Res, 3-6.

Scheeff, E.D., and Bourne, P.E. (2005). Structural evolution of the protein kinase-like superfamily. PLoS Comput Biol *1*, e49.

Schlunzen, F., Zarivach, R., Harms, J., Bashan, A., Tocilj, A., Albrecht, R., Yonath, A., and Franceschi, F. (2001). Structural basis for the interaction of antibiotics with the peptidyl transferase centre in eubacteria. Nature *413*, 814-821.

Schreiber, M., Res, I., and Matter, A. (2009). Protein kinases as antibacterial targets. Curr Opin Cell Biol *21*, 325-330.

Selmer, M., Dunham, C.M., Murphy, F.V.t., Weixlbaumer, A., Petry, S., Kelley, A.C., Weir, J.R., and Ramakrishnan, V. (2006). Structure of the 70S ribosome complexed with mRNA and tRNA. Science *313*, 1935-1942.

Shaw, K.J., Rather, P.N., Hare, R.S., and Miller, G.H. (1993). Molecular genetics of aminoglycoside resistance genes and familial relationships of the aminoglycoside-modifying enzymes. Microbiol Rev *57*, 138-163.

Stenseth, N.C., Atshabar, B.B., Begon, M., Belmain, S.R., Bertherat, E., Carniel, E., Gage, K.L., Leirs, H., and Rahalison, L. (2008). Plague: past, present, and future. PLoS Med *5*, e3.

Stogios, P.J., Shakya, T., Evdokimova, E., Savchenko, A., and Wright, G.D. (2011). Structure and function of APH(4)-Ia, a hygromycin B resistance enzyme. J Biol Chem *286*, 1966-1975.

Taber, H.W., Mueller, J.P., Miller, P.F., and Arrow, A.S. (1987). Bacterial uptake of aminoglycoside antibiotics. Microbiol Rev *51*, 439-457.

Toth, M., Frase, H., Antunes, N.T., Smith, C.A., and Vakulenko, S.B. (2010). Crystal structure and kinetic mechanism of aminoglycoside phosphotransferase-2"-IVa. Protein Sci *19*, 1565-1576.

Tu, D., Blaha, G., Moore, P.B., and Steitz, T.A. (2005). Structures of MLSBK antibiotics bound to mutated large ribosomal subunits provide a structural explanation for resistance. Cell *121*, 257-270.

Tuveson, D.A., Willis, N.A., Jacks, T., Griffin, J.D., Singer, S., Fletcher, C.D., Fletcher, J.A., and Demetri, G.D. (2001). STI571 inactivation of the gastrointestinal stromal tumor c-KIT oncoprotein: biological and clinical implications. Oncogene *20*, 5054-5058.

Uttley, A.H., Collins, C.H., Naidoo, J., and George, R.C. (1988). Vancomycin-resistant enterococci. Lancet *1*, 57-58.

Vakulenko, S.B., and Mobashery, S. (2003). Versatility of aminoglycosides and prospects for their future. Clin Microbiol Rev *16*, 430-450.

Vicens, Q., and Westhof, E. (2001). Crystal structure of paromomycin docked into the eubacterial ribosomal decoding A site. Structure *9*, 647-658.

Vicens, Q., and Westhof, E. (2002). Crystal structure of a complex between the aminoglycoside tobramycin and an oligonucleotide containing the ribosomal decoding a site. Chem Biol *9*, 747-755.

Vila-Sanjurjo, A., Ridgeway, W.K., Seymaner, V., Zhang, W., Santoso, S., Yu, K., and Cate, J.H. (2003). X-ray crystal structures of the WT and a hyper-accurate ribosome from Escherichia coli. Proc Natl Acad Sci U S A *100*, 8682-8687.

Wolanin, P.M., Thomason, P.A., and Stock, J.B. (2002). Histidine protein kinases: key signal transducers outside the animal kingdom. Genome Biol *3*, REVIEWS3013.

Wright, G.D. (2005). Bacterial resistance to antibiotics: enzymatic degradation and modification. Adv Drug Deliv Rev *57*, 1451-1470.

Wright, G.D. (2010). Antibiotic resistance in the environment: a link to the clinic? Curr Opin Microbiol *13*, 589-594.

Young, P.G., Walanj, R., Lakshmi, V., Byrnes, L.J., Metcalf, P., Baker, E.N., Vakulenko, S.B., and Smith, C.A. (2009). The crystal structures of substrate and nucleotide complexes of Enterococcus faecium aminoglycoside-2"-phosphotransferase-IIa [APH(2")-IIa] provide insights into substrate selectivity in the APH(2") subfamily. J Bacteriol *191*, 4133-4143.

Yusupov, M.M., Yusupova, G.Z., Baucom, A., Lieberman, K., Earnest, T.N., Cate, J.H., and Noller, H.F. (2001). Crystal structure of the ribosome at 5.5 A resolution. Science *292*, 883-896.

Zhanel, G.G., Dueck, M., Hoban, D.J., Vercaigne, L.M., Embil, J.M., Gin, A.S., and Karlowsky, J.A. (2001). Review of macrolides and ketolides: focus on respiratory tract infections. Drugs *61*, 443-498.

CHAPTER TWO
NUCLEOTIDE SELECTIVITY OF ANTIBIOTIC KINASES

CHAPTER TWO PREFACE

The work presented in this chapter was previously published in:

Shakya, T and G.D. Wright. (2010) Nucleotide Selectivity of Antibiotic Kinases. *Antimicrobial Agents and Chemotherapy* 54(5): 1909-1913.

Acknowledgements:

We thank Dr. M. Morar for helpful discussions.

ABSTRACT

Antibiotic kinases, which include aminoglycoside and macrolide phosphotransferases (APHs and MPHs), pose a serious threat to currently used antimicrobial therapies. These enzymes show structural and functional homology with Ser/Thr/Tyr kinases, suggestive of a common ancestor. Surprisingly, recent *in vitro* studies using purified antibiotic kinase enzymes have revealed that a number are able to utilize GTP as the antibiotic phospho-donor; either preferentially or exclusively when compared to ATP, the canonical phosphate donor in most biochemical reactions. To further explore this phenomenon, we examined three enzymes: APH(3')-IIIa, APH(2")-Ib and MPH(2')-I using a competitive assay that mimics *in vivo* nucleotide triphosphate (NTP) concentrations and usage by each enzyme. Downstream analysis of reaction products by HPLC enabled the determination of partitioning of phosphate flux from NTP donors to antibiotics. Using this ratio along with support from kinetic analysis and inhibitor studies, we find that under physiologic concentrations of NTPs, APH(3')-IIIa exclusively uses ATP, MPH(2')-I exclusively uses GTP, and APH(2")-Ib is able to use both species with a preference for GTP. These differences reveal likely different pathways in antibiotic resistance enzyme evolution and can be exploited in selective inhibitor design to counteract resistance.

INTRODUCTION

Antibiotic modification is a major mechanism of resistance that impacts the efficacy of numerous antimicrobial drug classes. The enzymes that catalyze these group transfer mechanisms have evolved from precursor genes that encode proteins used to accomplish numerous metabolic tasks no doubt unrelated to drug resistance. Borrowing nomenclature from the oncogene field, we term such elements proto-resistance genes. Biochemical and structural evidence has shown that proto-resistance genes can be found in a number of key metabolic pathways including cell wall biosynthesis and signal transduction (Wright, 2007). With respect to group transfer antibiotic resistance enzymes, these proto-resistance genes encode protein and other small molecule kinases, acetyltransferases, adenylytransferases, ADP-ribosyltransferases, and glycosyltransferases. The addition of phosphoryl, acyl, adenyl, ribosyl, and glycosyl groups to the antibiotic scaffold alters the interaction with the cellular target to a sufficient degree that the resistance phenotype results (D'Costa and Wright, 2009).

The unifying biochemical logic of group transfer in antibiotic resistance is the co-opting of the normal cellular function of the proto-resistance element by natural selection to include the modification of antibiotic molecules. Because group transfer enzymes require a second substrate (e.g. ATP, acetylCoA, TDP-glucose), these should retain the original specificity of the proto-resistance enzyme since natural selection would not normally be expected to act on this site during resistance gene evolution.

Antibiotic kinases represent a large superfamily of enzymes that covalently modify antibiotics by phosphorylation resulting in addition of both steric bulk and anionic character to the target molecule. Kinases that modify aminoglycoside, macrolide and fenicol antibiotics have been well characterized (D'Costa and Wright, 2009). The latter is a member of the shikimate group of kinases (Izard and Ellis, 2000), whereas the former (APHs and MPHs) share primary sequence, 3D-structure, and enzyme mechanism properties with the Ser/Thr/Tyr/Lipid family of kinases that are chief components of eukaryotic signal transduction (Wright and Thompson, 1999). These antibiotic kinases have largely been seen to use the phosphoryl donor ATP as the second substrate for antibiotic modification, consistent with the primacy of this nucleotide triphosphate in primary metabolism and the intracellular concentration of ~3 mM in bacterial cells (Bochner and Ames, 1982).

During our efforts to characterize the structure and mechanism of macrolide antibiotic kinases, we were struck by the poor activity with ATP, compared to GTP, as a phosphoryl donor substrate *in vitro*, exhibiting a selectivity that had been noted previously but was unexplored (Kono et al., 1992). This preference was surprising to us given the reported intracellular concentrations of ATP vs. GTP, which in bacterial and mammalian cells are reported to be on the order of 3-4 fold in excess of ATP (Buckstein et al., 2008)(Shugar, 1996). In order to explore this further, we have established a competitive HPLC method to establish the NTP selectivity of antibiotic kinases under

conditions that mimic intracellular concentrations of NTPs. We report a new partition co-efficient parameter that functionally discriminates antibiotic kinases based on their NTP preference. This has significant implications on our understanding of the evolution of these kinases from proto-resistance elements and practical application in the development of selective inhibitors of kinases that can reverse resistance.

MATERIALS AND METHODS

Antibiotics and Reagents. Erythromycin A, troleandomycin, clarithromycin, azithromycin, tylosin, spiramycin, NADH, PEP, PK/LDH, ATP, GTP, AMPPNP and GMPPNP were purchased from Sigma-Aldrich (Oakville, ON). Neomycin and kanamycin were purchased from Bioshop Canada (Mississauga, ON) and telithromycin was from Sanofi Aventis.

Expression and Purification of antibiotic kinases. The *mphA* gene was amplified using the polymerase chain reaction from pTZ3509 (Noguchi et al., 1995), a gift from Dr. N. Noguchi, and *aph(2")-Ib* was amplified from pSCH075 (Chow et al., 2001), generously provided by Dr. Joe Chow, using the oligonucleotide primers listed in Appendix 1. The *mphA* gene was ligated into pET28a using *Nde* I and *Hind* III sites and *aph(2")-Ib* was introduced into pDEST17 between the *attR1* and *attR2* sites using the Gateway® system (Invitrogen).

APH(3')-IIIa was purified using the protocol outlined in McKay *et al* (McKay et al., 1994). Both MPH(2')-I and APH(2")-Ib were expressed in *Escherichia coli* BL21(DE3) (Novagen) and grown overnight in the presence of their respective antibiotic (50 μg/mL kanamycin A (Bioshop) for pETMPHa, and 100 μg/mL ampicillin for pDESTAPH(2")-Ib) in Luria Bertani (LB) broth. A 10 mL overnight culture was used to inoculate 1 L of fresh LB broth with antibiotic selection and was grown to OD_{600} ~ 0.6 at 37°C. It was then induced for 16 hours at 16°C with 1 mM isopropyl-β-thiogalactoside (Bioshop). Cells were harvested by centrifugation at 6000 x *g* for 10 min. The cell pellet was resuspended in 15 mL of 50 mM HEPES pH 7.5, 300 mM NaCl, 10 mM imidazole, 1 mM phenylmethanesulfonyl fluoride and 1 μg/mL pancreatic bovine DNAse (Sigma). The resuspended pellet was passed through a 20,000 psi French press cell (Thermo Fisher) four times to create a lysate. The insoluble and soluble fractions were separated by centrifugation at 48,000 x *g* for 30 min. The supernatant was then applied onto 5 mL Ni-NTA Column (Qiagen) equilibrated with 50 mM HEPES pH 7.5, 300 mM NaCl, 10 mM imidazole (Buffer A). A stepwise gradient over 20 column volumes was used to elute each enzyme with 50 mM HEPES pH 7.5, 300 mM NaCl, 250 mM imidazole (Buffer B). The kinase containing fractions were identified by SDS-polyacrylamide gel electrophoresis and were subsequently pooled and dialyzed against 50 mM HEPES pH 7.5, concentrated to approximately 2 mg/mL, and stored at -20°C.

Pyruvate Kinase/Lactate Dehydrogenase Coupled Assay. The phosphorylation of antibiotics was monitored by coupling the release of ADP/GDP with pyruvate kinase/lactate dehydrogenase (PK/LDH) (Pon and Bondar, 1967). The oxidization of NADH (ε = 6220 M^{-1} cm^{-1}) was monitored at 340 nm using a SpectraMax plate reader in a 96-well format. A typical reaction contained 230 μL of reaction buffer (50 mM HEPES pH 7.5, 40 mM KCl, 10 mM $MgCl_2$, 0.3 mM NADH, 3.5 mM phophoenolpyruvate,

0.00125 units PK/LDH, and antibiotic kinase). A 10 μL solution of the appropriate antibiotic was added to the reaction and allowed to incubate for 5 minutes at 37°C. The reaction was initiated with a 10 μL solution of nucleotide (ATP or GTP) and monitored for 5 minutes at 340 nm.

Initial rates were determined by utilizing the linear portion of the progress curve and analyzed by nonlinear least squares fitting of eq. 1,

$$v = V_{max}S/(K_M + S) \quad (1)$$

or eq 2 for substrate inhibited reactions,

$$v = V_{max}S/(K_M + S + S^2/K_i) \quad (2)$$

To further validate interaction of the enzymes with ATP and GTP, their non-hydrolysable analogues, AMPPNP and GMPPNP, were tested against the panel of enzymes using an IC_{50} analysis. Each analogue was diluted in 2-fold dilution and assayed against each enzyme using the PK/LDH coupled assay. Antibiotic concentrations were kept at saturating levels and nucleotide concentrations were held at K_M concentrations. IC_{50}s were determined using Grafit 4.0 and eq. 3,

$$IC_{50} = K_i(1 + K_M/[S]) \quad (3)$$

Paired-Ion Chromatography to Determine Nucleotide Selectivity. The further explore the nucleotide preference of antibiotic kinases using physiological concentrations of ATP and GTP; we established a NTP competition assay with HPLC resolution of products. Concentrations for ATP and GTP reported from *Salmonella enterica* were used to set up the *in vitro* competition assay, and were 3 mM and 0.9 mM respectively (Bochner and Ames, 1982). Enzymes were then incubated at 25°C in the presence of both nucleotides with 50 mM HEPES pH 7.5, 40 mM KCl, 10 mM $MgCl_2$ and 1 mM of appropriate antibiotic in a 50 μL volume. The reaction was stopped by the addition of 150 μL of 8 M urea. The reactions were then filtered through a 10 kDa Pall micro-centrifugation filter at 12,100 *x g* for 20 minutes to remove the protein. The filtrate was collected; diluted two times and 25 μL injected onto a Waters Novapak C18 3.9 X 150 mm reverse-phase column that had been treated with tetrabutylammonium hydrogen sulfate (TBAHS). A linear gradient was used to elute the various forms of the purine nucleotides using a 2 solvent system: solvent A – 15 mM H_2KPO_4/HK_2PO_4, 10 mM TBAHS, solvent B – 35 mM H_2KPO_4/HK_2PO_4, 10 mM TBAHS, 30% (v/v) acetonitrile. The elution was monitored using A_{259}. Once peaks had been identified, they were integrated using the Chromeleon 6.8 HPLC software package to determine the quantity of each of the nucleotide species. The product to substrate ratios were determined for ADP:ATP and GDP:GTP for each time point and plotted on a x-y scatter graph. A line of best fit was applied to each set of data and a partition coefficient (PC) was determined for each enzyme using eq. 4.

$$PC = \Delta d/d\Delta t((ADP:ATP)/(GDP:GTP)) \quad (4)$$

RESULTS

Steady state kinetic analysis of antibiotic kinases. Steady state kinetic constants for APH(3')-IIIa (McKay et al., 1994) and APH(2")-Ib (Toth et al., 2007) as well as antibiotic substrate specificity have been previously reported. Steady state constants for macrolide substrates of MPH(2')-I were determined in this work and are reported in Table 2-1. MPH(2')-I showed a higher selectivity for 14- and 15-membered macrolide antibiotics (e.g. erythromycin, clarithromycin, azithromycin) over the 16-membered ring macrolides spiramycin and tylosin. Of the seven macrolides tested, the ketolide telithromycin was the only one to show substrate inhibition.

TABLE 2-1: KINETIC CONSTANTS FOR MACROLIDE SUBSTRATES OF MPH(2')-I

Substrate	Macrocycle	K_M (μM)	k_{cat} (s^{-1})	K_i (μM)	k_{cat}/K_M ($sec^{-1}*M^{-1}$)
Erythromycin	14	37.2 ± 5.6	0.279	-	7.52×10^3
Clarithromycin	14	45.9 ± 7.4	0.311	-	6.77×10^3
Telithromycin[a]	14	7.4 ± 1.5	0.152	0.622 ± 0.196	2.07×10^4
Azithromycin	15	27.7 ± 3.4	0.292	-	1.05×10^4
Tylosin	16	131 ± 45	0.174	-	1.33×10^3
Spiramycin	16	478 ± 55	0.200	-	4.19×10^2

[a] Telithromycin was the only macrolide to show substrate inhibition
All data were determined in the presence of 0.2 mM GTP

Kinetic constants for the nucleotides were determined for all antibiotic kinases (Table 2-2, Fig. 2-1). These data demonstrate that APH(3')-IIIa is strictly ATP-dependent and MPH(2')-I has a very high selectivity for GTP. In our hands, the N-terminally $(His)_6$-tagged variant of APH(2")-Ib shows a slight selectivity for GTP over ATP but is still able to utilize both NTPs. This contrasts with results reported for untagged APH(2")-Ib that showed a preference for ATP but that GTP was nevertheless a good substrate (4 fold difference in K_m and 4.5 fold in k_{cat}) (Toth et al., 2009) and these results could be the result of minor differences in enzyme and assay conditions.

TABLE 2-2: KINETIC CONSTANTS OF NUCLEOTIDE SUBSTRATES

Substrate	Saturating Antibiotic*	K_M (μM)	k_{cat} (s^{-1})	k_{cat}/K_M ($sec^{-1}*M^{-1}$)
APH(3')-IIIa				
ATP	Neomycin	10.6 ± 1.4	1.59	1.50×10^5
GTP	Neomycin	n.c.	n.c.	n.c
APH(2")-Ib				
ATP	Kanamycin	151 ± 12	0.32	2.30×10^3
GTP	Kanamycin	18.0 ±1.9	0.10	5.40×10^3
MPH(2')-I				
ATP	Erythromycin	1890 ± 510	0.022	1.16×10^1
GTP	Erythromycin	59.2 ± 4.7	0.634	1.07×10^4

*The concentrations of the antibiotics were held as follows: Neomycin (200 μM), Kanamycin (200 μM) and Erythromycin (400 μM). n.c. = no curve

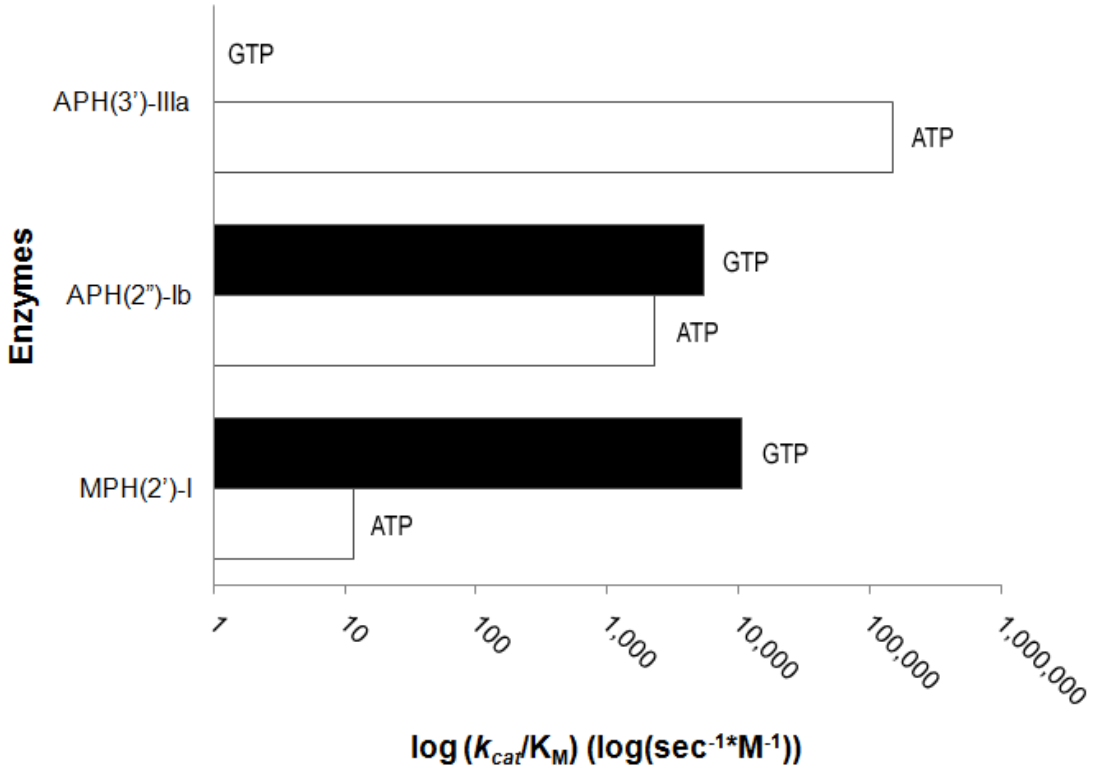

Figure 2-1: Nucleotide specificity of Antibiotic Kinases. The above semi-log bar graph demonstrates the nucleotide specificity of 3 studied antibiotic kinases of ATP (white) vs GTP (black) based upon the Michaelis-Menten constant k_{cat}/K_M ($sec^{-1}*M^{-1}$).

Inhibition profiles of antibiotic kinases as determinants of nucleotide preference. Inhibitory profiles were determined for each enzyme by observing their dose response against the two non-hydrolysable nucleotide analogs AMPPNP and GMPPNP. IC_{50} values were determined, for each of the enzymes and converted to K_i values using equation 3 (Table 2-3). Consistent with our steady state kinetic data, APH(3')-IIIa is only inhibited by AMPPNP, APH(2")-Ib is inhibited by both AMPPNP and GMPPNP and MPH(2')-I is only inhibited by GMPPNP.

TABLE 2-3: K_i VALUES OF INHIBITORS AS PROBES OF NUCLEOTIDE SELECTIVITY

Enzyme	AMPPNP (μM)	GMPPNP (μM)
APH(3')-IIIa	14.2 ± 1.0	No Inhibition
APH(2")-Ib	263.0 ± 55.0	19.3 ± 4.0
MPHa	No Inhibition	19.4 ± 1.4

Antibiotic kinases discriminate nucleotide usage in competition experiments. Although *in vitro* kinetic data demonstrate the selectivity of these enzymes, the conditions within the bacterial cell are very different. Typically ATP and GTP exist in a ratio of about 3:1 in most Gram negative organisms (Bochner and Ames, 1982; Buckstein et al., 2008). Therefore, the ability to use GTP as a phospho-donor in steady state kinetic experiments may not translate to a preference in the cell where ATP dominates. In order to observe how these enzymes would behave *in vivo,* we established an *in vitro* NTP competition assay system with ATP and GTP present under physiological concentrations. NTP utilization was analysed by paired ion chromatography (Patthy et al., 1990) (Fig. 2-2), which uses TBAHS to interact with the phosphates masking the hydrophilic negatively charged groups and improving HPLC resolution.

The conversion of NTPs to NDPs over time under saturating antibiotic conditions was quantitatively assessed using this method. NTP turnover was calculated from the slopes of integrated HPLC data. The slopes for ATP and GTP turnover were used to calculate the partition coefficient (PC) for each enzyme (Figure 2-3). The PC is a ratio that represents the nucleotide selectivity for a given enzyme. If the partition coefficient is equal 1, there is no bias for either ATP or GTP, if it is greater than 1, there is a preference for ATP, and if it is less than 1 the enzyme prefers GTP. MPH(2')-I, although able to utilize ATP in steady state kinetic experiments did not use ATP while there was GTP present at physiological conditions and consequently shows a very low PC. On the other hand APH(2")-Ib utilized both nucleotides and APH(3')-IIIa only used ATP. This experiment demonstrates that under physiological NTP conditions antibiotic kinases demonstrate distinct selectivity for nucleotide substrates.

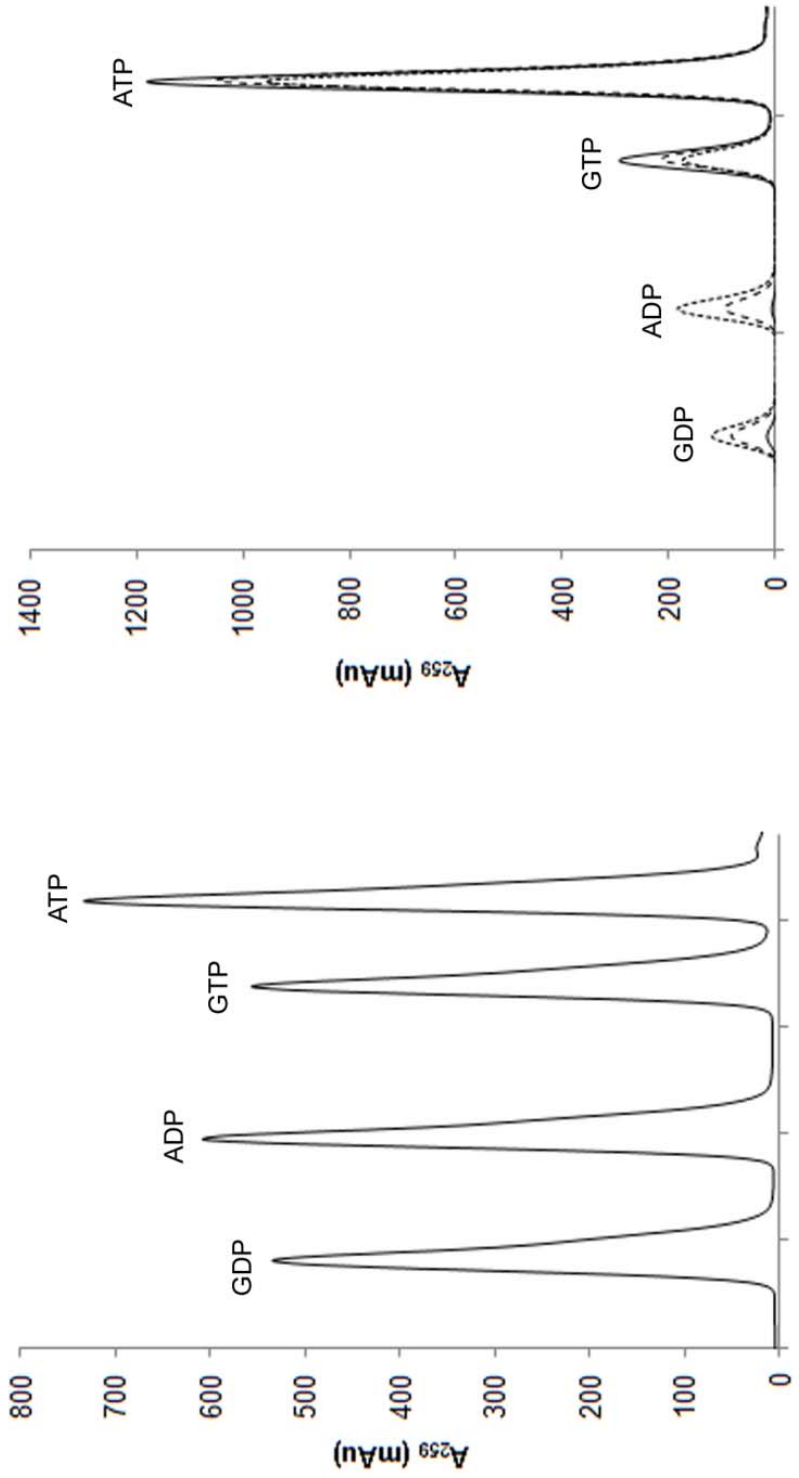

Figure 2-2: Separation of Nucleotides by HPLC. A) Standard curve demonstrating the separation of a mixture of 1 mM GDP, ADP, GTP and ATP. B) A time course comparison of the elution of the various nucleotide species for APH(2")-Ib, Time = 0 mins (------), 60 mins (- - -) and 120 mins (------)

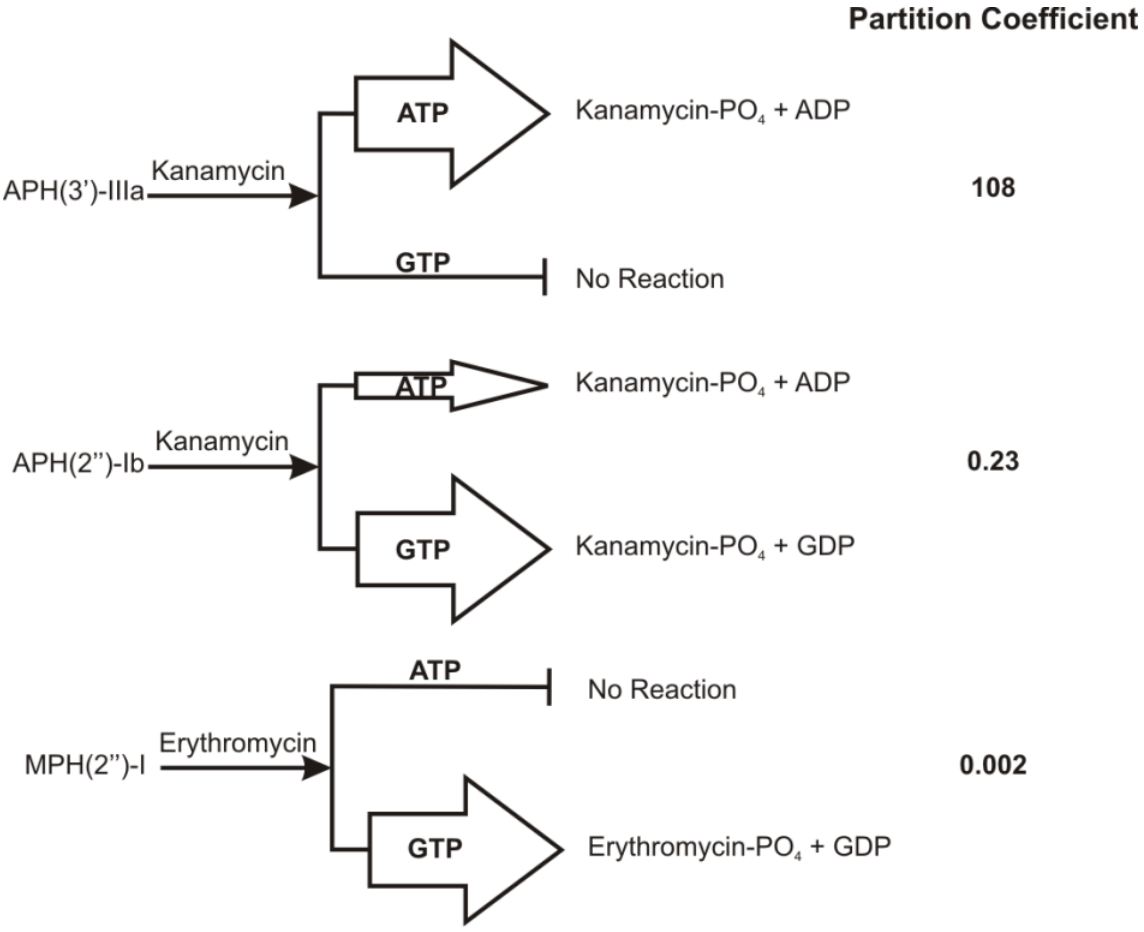

Figure 2-3: NTP Selectivity of Antibiotic Kinases. At physiological concentrations of NTP, antibiotic kinases show either exclusive or preferential usage of ATP or GTP. The width of the arrows approximates the ratio of this selectivity. Calculated partition coefficient listed to the right as calculated from equation 4.

DISCUSSION

Antibiotic resistance enzymes have evolved from precursor proteins, proto-resistance elements, of different origins (Wright, 2007). Elucidation of the structure and function of resistance enzymes has been essential in linking current proteins with ancestral proto-resistance enzymes. For example, the 3D structures and biochemical function analysis of aminoglycoside kinases (APHs) revealed an otherwise unexpected link with Ser/Thr/Tyr protein kinases (Wright and Thompson, 1999). Furthermore, *in silico* analysis of macrolide antibiotic kinase (MPH) amino acid sequences places them in the same family with aminoglycoside and protein kinases. It is therefore highly likely that all these proteins share a common ancestor and that the proto-resistance elements that gave rise to MPHs and APHs fall within their evolutionary tree.

The nucleotide selectivity of protein kinases is almost exclusively in favour of ATP. There are a few exceptions where GTP is either a preferred or equivalent substrate (Shugar, 1996). The best studied example is the Ser/Thr casein kinase-II, CK-2, which shows a 3-5 fold preference for GTP over ATP (Jakobi and Traugh, 1992). Another example is protein kinase C delta, that undergoes 6-fold improved autophosphorylation with GTP (Gschwendt et al., 1995). The human variant of the structurally unrelated small molecule kinase phophoenolpyruvate carboxykinase (PEPCK), which catalyzes the formation of PEP from oxaloacetate, will catalyze this reaction with GTP, while the *E. coli* homolog utilizes ATP (Dunten et al., 2002). Nevertheless, GTP utilization among kinases remains rare.

There is no thermodynamic imperative for the preference by kinases of ATP over other NTPs such as GTP as a phosphodonor. The free energy associated with gamma-phosphate transfer is equivalent. Nature has nevertheless restricted most kinases to ATP utilization and the number of such reactions is reflected in the 3-4 fold stoichiometric excess of cellular ATP versus GTP. GTP is utilized in cell signalling processes, e.g. tightly bound in GTP-protein coupled receptors, and is a major source of energy during translation where each amino acid elongation requires hydrolysis of 2 GTP molecules. Therefore, even though they are thermodynamically equivalent, ATP versus GTP utilization is biochemically segregated. It was therefore surprising that our research as well as several literature reports using purified APH and MPH enzymes revealed that many of these enzymes can use both ATP and GTP (Boehr et al., 2004; Kono et al., 1992; O'Hara et al., 1989). Indeed, this preference was recently used as the basis for a proposed new nomenclature for APH(2”) enzymes (Toth et al., 2009).

However, even though these *in vitro* studies showed that GTP was a substrate for some antibiotic kinases, it did not mean that these observations were biologically relevant where the presence of multiple NTPs at various concentrations presents a different environment than saturating concentrations of NTP in a typical enzyme assay. We therefore established a competition assay using NTPs at physiological concentration to

directly assess this phenomenon. Using this assay, we were able to demonstrate a range of GTP versus ATP utilization by aminoglycoside kinases. APH(3')-IIIa is a 'typical' APH(3'), a class that includes the popular Kan^R (aka NEO) cassette used in molecular and cellular biology, only uses ATP. APH(2")-Ib, which is important for clinical gentamicin resistance in Gram positive cocci and *E. coli* (Chow et al., 2001; Kao et al., 2000), shows a preference, but not exclusive dependence, on GTP in our experiments. On the other hand, the partition experiment shows that the macrolide kinase MPH(2')-I will exclusively use GTP in the cell.

The NTP preference of antibiotic kinases is fascinating and could reflect: 1) the preference of the proto-resistance enzyme ancestor, 2) a structural requirement based on the nature of the second substrate e.g. macrolide or aminoglycoside, or 3) it may offer an evolutionary advantage in the face of antibiotic exposure. The correlation between NTP utilization and sensitivity to NMPPNP inhibitors would suggest that option 2 is unlikely. Macrolides interact with the ribosome and prevent the emergence of the nascent peptide from the P-site (Hermann, 2005), furthermore, GTP is essential for protein synthesis. It could be possible that halting protein synthesis may temporarily increase GTP stores within the cell and this could provide an advantage for the GTP preference of MPHs consistent with option 3. On the other hand aminoglycoside, which cause mistranslation rather than blocking translation, would not be expected to alter GTP levels. We explored changes in NTP and NDP levels in cells exposed to sub-therapeutic antibiotics, but could not detect any significant changes in NTP levels (not shown). While the biological bias of ATP or GTP selectively in antibiotic kinases therefore remains an open question, option 1, where this preference is a reflection of the electivity of the proto-resistance element appears to be the most parsimonious explanation at present.

Whatever the origin, the preference of NTP does provide a useful handle for the development of agents that selectively block antibiotic resistance as we have demonstrated with NMPPNP inhibitors. Targeting the ATP binding site of antibiotic kinases with small molecule inhibitors is possible with known protein kinase inhibitors (Daigle et al., 1997). However, given the non-specific nature of many of these compounds, therapeutic use to circumvent resistance has the potential to also block other off-target cellular kinases, with possible deleterious effects. The GTP utilization of APH(2"), an important gentamicin resistance element, and MPH, a mechanism of growing importance (Phuc Nguyen et al., 2009), reveals an important differentiating property that could be exploited for downstream drug discovery research into agents that block resistance and restore antibiotic function. Obtaining the 3D-strucutre of GTP-utilizing enzymes will greatly enhance this approach.

REFERENCES

Bochner, B.R., and Ames, B.N. (1982). Complete analysis of cellular nucleotides by two-dimensional thin layer chromatography. J Biol Chem *257*, 9759-9769.

Boehr, D.D., Daigle, D.M., and Wright, G.D. (2004). Domain-domain interactions in the aminoglycoside antibiotic resistance enzyme AAC(6')-APH(2"). Biochemistry *43*, 9846-9855.

Buckstein, M.H., He, J., and Rubin, H. (2008). Characterization of nucleotide pools as a function of physiological state in Escherichia coli. J Bacteriol *190*, 718-726.

Chow, J.W., Kak, V., You, I., Kao, S.J., Petrin, J., Clewell, D.B., Lerner, S.A., Miller, G.H., and Shaw, K.J. (2001). Aminoglycoside resistance genes aph(2")-Ib and aac(6')-Im detected together in strains of both Escherichia coli and Enterococcus faecium. Antimicrob Agents Chemother *45*, 2691-2694.

D'Costa, V., and Wright, G.D. (2009). Biochemical Logic of Antibiotic Inactivation and Modification. In Antimicrobial Drug Resistance: Mechanisms of Drug Resistance Vol 1, D. Mayers, S. Lerner, J. Sobel, and M. Ouellette, eds. (New York, Humana Press), pp. 81-96.

Daigle, D.M., McKay, G.A., and Wright, G.D. (1997). Inhibition of aminoglycoside antibiotic resistance enzymes by protein kinase inhibitors. J Biol Chem *272*, 24755-24758.

Dunten, P., Belunis, C., Crowther, R., Hollfelder, K., Kammlott, U., Levin, W., Michel, H., Ramsey, G.B., Swain, A., Weber, D., *et al.* (2002). Crystal structure of human cytosolic phosphoenolpyruvate carboxykinase reveals a new GTP-binding site. J Mol Biol *316*, 257-264.

Gschwendt, M., Kittstein, W., Kielbassa, K., and Marks, F. (1995). Protein kinase C delta accepts GTP for autophosphorylation. Biochem Biophys Res Commun *206*, 614-620.

Hermann, T. (2005). Drugs targeting the ribosome. Curr Opin Struct Biol *15*, 355-366.

Izard, T., and Ellis, J. (2000). The crystal structures of chloramphenicol phosphotransferase reveal a novel inactivation mechanism. EMBO J *19*, 2690-2700.

Jakobi, R., and Traugh, J.A. (1992). Characterization of the phosphotransferase domain of casein kinase II by site-directed mutagenesis and expression in Escherichia coli. J Biol Chem *267*, 23894-23902.

Kao, S.J., You, I., Clewell, D.B., Donabedian, S.M., Zervos, M.J., Petrin, J., Shaw, K.J., and Chow, J.W. (2000). Detection of the high-level aminoglycoside resistance gene aph(2")-Ib in Enterococcus faecium. Antimicrob Agents Chemother *44*, 2876-2879.

Kono, M., O'Hara, K., and Ebisu, T. (1992). Purification and characterization of macrolide 2'-phosphotransferase type II from a strain of Escherichia coli highly resistant to macrolide antibiotics. FEMS Microbiol Lett *76*, 89-94.

McKay, G.A., Thompson, P.R., and Wright, G.D. (1994). Broad spectrum aminoglycoside phosphotransferase type III from Enterococcus: overexpression, purification, and substrate specificity. Biochemistry *33*, 6936-6944.

Noguchi, N., Emura, A., Matsuyama, H., O'Hara, K., Sasatsu, M., and Kono, M. (1995). Nucleotide sequence and characterization of erythromycin resistance determinant that encodes macrolide 2'-phosphotransferase I in Escherichia coli. Antimicrob Agents Chemother *39*, 2359-2363.

O'Hara, K., Kanda, T., Ohmiya, K., Ebisu, T., and Kono, M. (1989). Purification and characterization of macrolide 2'-phosphotransferase from a strain of Escherichia coli that is highly resistant to erythromycin. Antimicrob Agents Chemother *33*, 1354-1357.

Patthy, M., Balla, T., and Aranyi, P. (1990). High-performance reversed-phase ion-pair chromatographic study of myo-inositol phosphates. Separation of myo-inositol phosphates, some common nucleotides and sugar phosphates. J Chromatogr *523*, 201-216.

Phuc Nguyen, M.C., Woerther, P.L., Bouvet, M., Andremont, A., Leclercq, R., and Canu, A. (2009). Escherichia coli as reservoir for macrolide resistance genes. Emerg Infect Dis *15*, 1648-1650.

Pon, N.G., and Bondar, R.J. (1967). A direct spectrophotometric assay for pyruvate kinase. Anal Biochem *19*, 272-279.

Shugar, D. (1996). The NTP phosphate donor in kinase reactions: is ATP a monopolist? Acta Biochim Pol *43*, 9-23.

Toth, M., Chow, J.W., Mobashery, S., and Vakulenko, S.B. (2009). Source of phosphate in the enzymic reaction as a point of distinction among aminoglycoside 2''-phosphotransferases. J Biol Chem *284*, 6690-6696.

Toth, M., Zajicek, J., Kim, C., Chow, J.W., Smith, C., Mobashery, S., and Vakulenko, S. (2007). Kinetic mechanism of enterococcal aminoglycoside phosphotransferase 2''-Ib. Biochemistry *46*, 5570-5578.

Wright, G.D. (2007). The antibiotic resistome: the nexus of chemical and genetic diversity. Nat Rev Microbiol *5*, 175-186.

Wright, G.D., and Thompson, P.R. (1999). Aminoglycoside phosphotransferases: proteins, structure, and mechanism. Front Biosci *4*, D9-21.

CHAPTER THREE
STRUCTURE AND FUNCTION OF APH(4)-Ia: A HYGROMYCIN B RESISTANCE ENZYME

CHAPTER THREE PREFACE

The work presented in this chapter was previously published in:

Stogios, P, Shakya, T, Evdokimova, E, Savchenko, A and G.D. Wright. (2011) Structure and Function of APH(4)-Ia: A Hygromycin B Resistance Enzyme. *J. Biological Chemistry* 286(3):1966-75.

I co-authored this work with Dr. P. Stogios. I conducted all of initial cloning, characterization and mutational analyses of the APH(4)-Ia enzyme.

Acknowledgements:

We would like to acknowledge Yao Fan at beamline 19-ID, Structural Biology Centre, Advanced Photon Source, Argonne National Laboratory for crystal diffraction data collection, and Rosa Di Leo and Laura Rossi in the Savchenko and Wright labs, respectively, for cloning.

ABSTRACT

The aminoglycoside phosphotransferase APH(4)-Ia is one of two enzymes responsible for bacterial resistance to the atypical aminoglycoside antibiotic hygromycin B (hygB). The crystal structure of APH(4)-Ia enzyme was solved in complex with hygB at 1.95 Å resolution. The APH(4)-Ia structure adapts a general two-lobe architecture shared by other APH enzymes and eukaryotic kinases, with the active site located at the inter-domain cavity. The enzyme forms an extended hydrogen bond network with hygB primarily through polar and acidic side chain groups. Individual alanine substitutions of seven residues involved in hygB binding did not have significant effect on APH(4)-Ia enzymatic activity indicating that binding affinity is spread across a distributed network. hygB appeared as the only substrate recognized by APH(4)-Ia among the panel of 14 aminoglycoside compounds. Analysis of the active site architecture and the interaction with the hygB molecule demonstrated several unique features supporting such restricted substrate specificity. Primarily the APH(4)-Ia substrate binding site contains a cluster of hydrophobic residues that provides a complementary surface to the twisted structure of the substrate. Similar to APH(2”) enzymes the APH(4)-Ia is able to utilize either ATP or GTP for phosphoryl transfer. The defined structural features of APH(4)-Ia interactions with hygB and the promiscuity in regard to ATP or GTP binding could be exploited for the design of novel aminoglycoside antibiotics or inhibitors of this enzyme.

INTRODUCTION

With rising incidences of multi-drug resistant bacteria and a decline in the discovery of new antibiotics, attention is returning to 'old' antibiotics that in the past were not selected for clinical development by the pharmaceutical industry. These compounds represent chemical matter that may provide essential scaffolds that could be altered with modern medicinal chemical approaches or may be suitable to be re-introduced into the clinic in this current era of pressing need. For example, the lipopeptide antibiotic daptomycin (Cubicin®) was discovered in the 1980s by Eli Lilly but was not brought to the clinic until 2003 due to the efforts by Cubist Pharmaceuticals which resulted in FDA approval of this 'old' drug (Eisenstein et al., 2010).

Currently analogues of the known aminoglycoside antibiotics such as gentamicin and kanamycin are not seen as favourable drug candidates by the pharmaceutical industry. Discovered in the 1950s, these compounds were acclaimed for their broad-spectrum and potent bactericidal activity. However, they lost favour as front line drugs as a result of toxicity and poor oral availability, and as newer agents with improved pharmacology entered the market. Furthermore, the emergence of resistance provided an additional challenge to the clinical utility of these drugs. Resistance to these antibiotics is most frequently conferred by aminoglycoside-modifying enzymes encoded by transferable gene cassettes. Nevertheless, in this era of acute antibiotic need, the aminoglycoside compounds, particularly the ones that were clinically "underused" in the past are re-emerging as promising drug leads. This in turn necessitates the detailed analysis of mechanisms of resistance to aminoglycosides as an essential part of developing antimicrobial therapies involving this class of antibiotics.

Aminoglycoside-modifying enzymes act through three major chemical mechanisms: acetyltransfer, nucleotidyltransfer or phosphoryltransfer. Each of these classes of enzymes is highly diverse, with numerous representatives featuring different substrate profiles and regiochemical selectivities resulting in a plethora of enzymes with varied and distinct features. The approximately 30 enzymes within the aminoglycoside phosphotransferase class of enzymes typically show less than 35% pair wise identities (Wright and Thompson, 1999).

Hygromycin B (hygB), isolated from *Streptomyces hygroscopicus* (Pittenger, 1953) represents a promising "underused" aminoglycoside antibiotic. It has atypical chemical features in comparison to more common representatives of this antibiotic class. A key structural feature of these common aminoglycosides is the 2-deoxystreptamine core, which is substituted by two amino sugar rings at the 4 and 6 positions (as in gentamicin or tobramycin), or the 4 and 5 positions (as in neomycin or butirosin). HygB is unique in that it is comprised of an N-methyl 2-deoxystreptamine ring (hyosamine), linked through the C5-OH to a talose sugar, which in turn forms an orthoester with the unusual amino acid destomic acid (Figure 3-1), resulting in a distinctive fused ring structure. This unique structure translates into novel mode of action. Where antibiotics like gentamicin bind to the 30S ribosomal subunit resulting in mistranslation of mRNA,

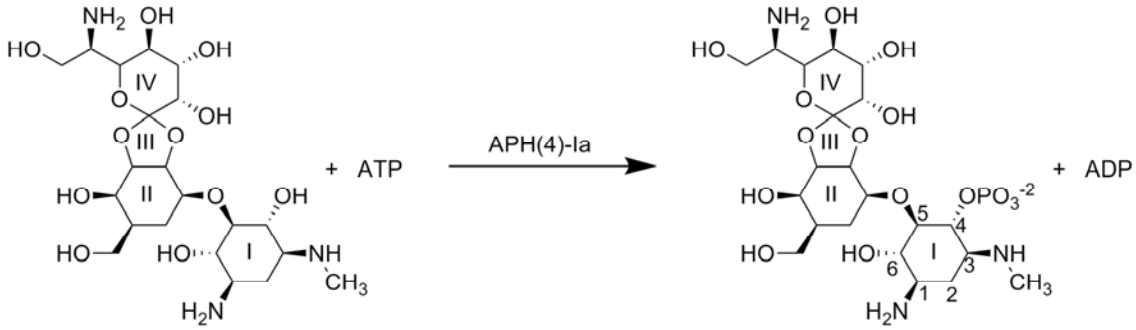

Figure 3-1: Chemical Reaction of APH(4)-Ia. APH(4)-Ia catalyzes the phosphorylation of hygB using the gamma phosphate of ATP with addition of a phosphate group onto the 4-OH on the hyosamine ring (Ring I) yielding an inactivated phospho-hygromycin B and ADP.

hygB binding to this subunit primarily blocks mRNA and tRNA translocation (Borovinskaya et al., 2008; Cabanas et al., 1978). Furthermore, hygB has been shown to also impact translocation in eukaryotic ribosomes (Gonzalez et al., 1978), increasing the spectrum of this antibiotic to eukaryotic pathogens and resulting in its application in agricultural settings as an anthelmintic agent in poultry and swine.

Like all antibiotics, resistance to hygB has emerged. Plasmid-encoded hygB resistance in *Escherichia coli* was reported some 30 years following its introduction (Gritz and Davies, 1983; Rao et al., 1983). This resistance was linked to the aminoglycoside phosphotransferase-(4)-Ia (APH(4)-Ia) enzyme, which catalyzes the ATP-dependent phosphorylation of the hydroxyl moiety on C4 of the hyosamine ring ("Ring I") of hygB (Fig. 1) (Rao et al., 1983). This mechanism differs from the self-protection one described in the hygB-producing *Streptomyces hygroscopicus*, which involves phosphorylation at the 7"-OH of the destomic acid ring ("Ring IV") (Pardo et al., 1985; Zalacain et al., 1987). The enzyme responsible for this activity, APH(7")-Ia, shares only 37% amino acid identify with APH(4)-Ia. This implies that APH(4)-Ia may have evolved distinctly from self-resistance in the producing organism.

The 3D-structures of a number of APHs have been reported (Fong et al., 2010; Hon et al., 1997; Nurizzo et al., 2003; Toth et al., 2010; Young et al., 2009). These structures have demonstrated that despite their sequence diversity, APH enzymes share a common fold that is similar to that of eukaryotic protein kinases. This common fold features a bilobed structure comprised of a primarily β-sheet containing N-terminal domain and a mixed α+β C-terminal domain, with the two domains connected by a linker region. Relative to eukaryotic protein kinases, APH enzymes contain an insertion in the C-terminal domain, which plays an important role in aminoglycoside binding (Hon et al., 1997). Despite structural information about a number of APH enzymes and advances in understanding of the mechanism of phosphorylation reaction (McKay and Wright, 1996), the basis of different substrate specificity toward diverse aminoglycosides between the representatives of APH enzymes remains poorly understood. Low sequence similarity between APH enzymes precludes effective modeling of uncharacterized APH family members and necessitates further structural studies of diverse members of this family.

Given the importance of hygB as a potential scaffold for new drug discovery, we embarked on structural characterization of the APH(4)-Ia•hygB binary complex and investigated the enzymatic properties of this enzyme. The 3D-structure shows that while the APH(4)-Ia enzyme adopts the general features of other APH enzymes, such as the overall eukaryotic protein kinase-like fold and the location of the hygB ligand binding site, it reveals unique structural features that explain its selectivity for this atypical aminoglycoside.

MATERIALS AND METHODS

Expression and Purification of APH(4)-Ia. The *aph(4)-Ia* gene (NCBI Accession #V01499) from the retroviral protein expression vector pQCXIH (Clonetech Laboratories Inc.) was used as the template for preparation of an over-expressing construct. An internal *Nde* I restriction endonuclease site was removed by creating a silent mutation at the site using the Stratagene Quikchange strategy (oligonucleotide primers are shown in Appendix 1). The gene was then amplified with oligonucleotide primers that introduced flanking 5' *Nde* I and 3' *Hind* III sites that were used to clone the gene into vector pET28a to create the expression plasmid pET-APH(4)-Ia.

APH(4)-Ia was expressed in *Escherichia coli* BL21(DE3) (Novagen) and grown overnight in the presence of 50 μg/mL kanamycin A in Luria Bertani (LB) broth. A 10 mL overnight culture was used to inoculate 1 L of fresh LB broth with antibiotic selection and was grown to OD_{600} ~ 0.6 at 37 °C. It was then induced for 16 hours at 16 °C with 1 mM isopropyl-β-thiogalactoside. Cells were harvested by centrifugation at 6000 x *g* for 10 min. The cell pellet was then resuspended in 15 mL of 50 mM HEPES pH 7.5, 300 mM NaCl, 10 mM imidazole, 1 mM phenylmethanesulfonyl fluoride and 1 μg/mL pancreatic bovine DNAse. The resuspended pellet was passed through a T-S series cell disrupter (Constant Systems Inc.) twice at 35,000 psi to create a lysate. The insoluble and soluble fractions were separated by centrifugation at 48,000 x *g* for 30 min. The supernatant was then applied to a 1 mL Ni-NTA Column (Qiagen) equilibrated in ten column volumes 50 mM HEPES pH 7.5, 300 mM NaCl, 10 mM imidazole (Buffer A). A stepwise gradient over five column volumes of each 10%, 25%, 50% and 100% Buffer B (50 mM HEPES pH 7.5, 300 mM NaCl, 250 mM imidazole) was used to elute the enzyme. The APH(4)-Ia containing fractions were identified by SDS-polyacrylamide gel electrophoresis and were subsequently pooled and dialyzed against 50 mM HEPES pH 7.5 overnight at 4 °C with stirring. The protein was then quantified using the Bradford protein assay and was either concentrated or diluted to 0.5 mg/mL, and stored in 50 mM HEPES pH =7.5 and 15% glycerol at -20 °C.

For crystallographic purposes, the *aph(4)-Ia* gene was sub-cloned from pET-APH(4)-Ia into the vector p15Tv-LIC, which codes for a N-terminal $(His)_6$ tag, a TEV protease cleavage site, ampicillin resistance gene and allows ligase-independent cloning. The expression vector was utilized for expression of Se-Met substituted protein using standard M9 high-yield growth procedure according to the manufacturer's instructions (Shanghai Medicilon, catalog MD045004-50), with *E. coli* BL21(DE3) codon plus cells.

Cells were lysed by sonication in 0.3 M NaCl, 50 mM HEPES pH 7.5, 5 mM imidazole, 5% glycerol, 0.5 mM tris[2-carboxyethyl]phosphine and 0.25 mM phenylmethanesulfonyl fluoride. Protein was bound to NiNTA resin at 4° C for two hours, washed with lysis buffer with 30 mM imidazole, and then eluted with lysis buffer with 250 mM imidazole. Eluted protein was supplemented with 1 mM EDTA. The $(His)_6$ tag was removed by cleavage with TEV protease overnight at 4° C in dialysis with the

buffer 0.3 M NaCl, 50 mM HEPES pH 7.5, 5% glycerol and 0.5 mM tris[2-carboxyethyl]phosphine, followed by binding to NiNTA resin and capture of flow-through. Protein was concentrated to at least 10 mg/mL. Protein was flash frozen in liquid nitrogen and stored at -70º C.

Crystallography, Data Collection and Structure Determination. APH(4)-Ia crystals were grown at 22 °C using the hanging drop method, by mixing 1 µL of protein at 6.5 mg/mL with 1 µL of reservoir solution containing 0.2 M di-ammonium hydrogen citrate, 16% PEG3350 and 2 mM hygB. Crystals were cryo-protected with reservoir solution supplemented with 20% paratone prior to flash freezing. Diffraction data at 100 K at the wavelength corresponding to the anomalous scattering peak wavelength of seleno-methionine (0.97915 Å) were collected at beamline 19-BM at the Structural Biology Center, Advanced Photon Source, Argonne National Laboratory. Diffraction data were reduced with HKL2000 (Minor, 1997).

The structure was solved by single-wavelength anomalous dispersion (SAD) using the AutoSol module of Phenix (Adams et al., 2010). Seven of the eight selenomethionine sites in the asymmetric unit were found as judged by occupancy values greater than 0.50. An initial model of the protein was built using Phenix AutoBuild, followed by rounds of manual model building and refinement with Coot (Emsley and Cowtan, 2004) and Phenix.refine. Final rounds of refinement were completed with BUSTER (Blanc et al., 2004) with TLS parameterization (TLS groups were residues 10-99 and 100-301). The final atomic model includes residues 8-301 of APH(4)-Ia, all 25 atoms of hygB, 27 ammonium ions, one chloride ion and seven PEG molecules (with varying numbers of atoms per PEG molecule visible in the electron density). Procheck (Laskowski, 1993) was utilized for the Ramachandran analysis. An iterative composite omit map for verification of position of hygB was generated with Phenix.autobuild with default parameters.

Structure similarity searches of the PDB were performed using the Dali server (Holm et al., 2008). Structure superpositions were performed with the SSM algorithm in Coot or the Dali server as indicated in the manuscript.

Interactions between the protein and hygB were identified in Coot and also using the LIGPLOT program (Wallace et al., 1995).

Electrostatic potential surfaces were calculated using the APBS PyMOL plugin (Petrey and Honig, 2003). Red is negative, white is neutral, blue is positively charged, and surfaces were contoured between -20 and +20 k_BT/e and 10 k_BT/e, where k_B is the Boltzmann constant, T is temperature, and e is the electronic charge. Protein structure images were produced with PyMOL (Delano Scientific).

PDB coordinates. The structure of APH(4)-Ia has been submitted to the PDB with the accession number 3OVC.

Site Directed Mutagenesis of APH(4)-Ia. Site-directed mutagenesis was carried out using the Stratagene Quikchange strategy in the pET-APH(4)-Ia plasmid. The sequences of the oligonucleotide primers can be found in Appendix 1. DNA sequencing using primers for the T7 promoter and terminator were used to verify the success of the mutants. All mutants were purified as previously described above.

Steady State Kinetic Analysis of APH(4)-Ia. The phosphorylation of antibiotics was monitored by coupling the release of ADP or GDP following antibiotic modification with pyruvate kinase/lactate dehydrogenase (PK/LDH) (Pon and Bondar, 1967). The oxidization of NADH (ε = 6220 M^{-1} cm^{-1}) was monitored at 340 nm using a SpectraMax plate reader in a 96-well format. A typical reaction contained 195 μL of reaction buffer (50 mM HEPES pH 7.5, 40 mM KCl, 10 mM $MgCl_2$, 0.3 mM NADH, 3.5 mM phosphoenolpyruvate, 0.00125 units PK/LDH, and ~ 0.1 μM APH(4)-Ia). A 5 μL solution of the appropriate antibiotic was added to the reaction and allowed to incubate for 5 minutes at 25°C. The reaction was initiated with a 50 μL solution of nucleotide and monitored for 5 minutes at 340 nm.

Initial rates (v) were determined by utilizing the linear portion of the progress curve and analyzed by nonlinear least squares fitting to eq. 1,

$$v = V_{max}S/(K_M + S) \qquad (1)$$

Structure determination of Phosphohygromycin B. Large scale preparation of phosphohygromycin B was carried out enzymatically using a 50 mL reaction comprised of 50 mM HEPES pH 7.5, 40 mM KCl, 10 mM $MgCl_2$, 3 mM hygB, 5.4 mM ATP and 2.1 μM APH(4)-Ia. The reaction was monitored using thin-layer chromatography with a mobile phase comprised of 5:2 MeOH:NH_4OH and visualized with ninhydrin. The reaction mixture was passed through a 0.2 μm Millipore filter and a 10 kDa Millipore centrifugal filter to remove precipitated and soluble enzyme respectively. The filtrate was then lyophilized overnight and resuspended in 4 mL of H_2O and applied to a 48 mL AG50W X 8 200-400 Mesh column (78 mm x 28 mm) that had been charged with 1% NH_4OH. The product was recovered with a wash of 0.1% NH_4OH and lyophilized.

RESULTS AND DISCUSSION

Substrate and regio-specificities of APH(4)-Ia. Previous enzyme-based assays indicated that APH(4)-Ia is highly specific for hygromycin B and close analogs (Rao et al., 1983). Using purified recombinant APH(4)-Ia, we screened a diverse panel of aminoglycoside antibiotics as potential substrates including the 4,6-disubstituted 2-deoxystreptamine-based aminoglycosides (amikacin, kanamycin A, gentamicin C complex, and tobramycin), the 4,5-disubtituted 2-deoxystreptamine-based aminoglycosides (butirosin, neomycin B, paromomycin, ribostamycin and lividomycin) and the atypical aminoglycosides (neamine, apramycin, streptomycin, spectinomycin and hygromycin B). Only hygB was susceptible to phosphorylation by APH(4)-Ia (Table 3-2). Such narrow substrate specificity is unusual for APHs, which often have very broad aminoglycoside substrate profiles (Daigle et al., 1999; McKay et al., 1994b; Siregar et al., 1995; Toth et al., 2007; Tsai et al., 1998). In contrast, APH(4)-Ia demonstrated the ability to utilize both ATP and GTP as a phosphate donor with ~5-fold preference towards ATP based upon the k_{cat}/K_m values of 5.42 X 10^4 and 1.04 X 10^4, respectively. Similar nucleotide promiscuity has been previous observed for the APH(2") class of enzymes (Shakya and Wright, 2010; Toth et al., 2009). In eukaryotic protein kinases the capacity to utilize GTP is rare and this difference could be exploited in the development of specific inhibitors.

High resolution mass spectrometry of phosphorylated hygB gave a mass of 607.1990 consistent with mono-phosphorylation of hygB. Regiospecificity of phosphoryl transfer was confirmed to be at position 4 by multidimensional NMR as predicted (Figure 3-1) (Rao et al., 1983).

Overall structure of APH(4)-Ia. APH(4)-Ia shares relatively low sequence similarity with previously characterized APH enzymes (maximum of 16% identity across the full-length enzymes) (Fong et al., 2010; Hon et al., 1997; Nurizzo et al., 2003; Toth et al., 2010; Young et al., 2009). In order to gain further understanding of the unique substrate selectivity of this enzyme, the structure of APH(4)-Ia was solved by the SAD method using Se-Met derivatized APH(4)-Ia protein co-crystallized with hygB. The final model contained one polypeptide chain in the asymmetric unit, with residues 8 to 301 resolved in the electron density, along with all atoms of the antibiotic (structure statistics are summarized in Table 3-1).

The analysis of the APH(4)-Ia structure demonstrated that like previously characterized APH enzymes APH(4)-Ia adopts a general eukaryotic protein kinase fold. Thus to simplify comparative structural analysis we labelled the secondary structure elements of the APH(4)-Ia structure according to those in the original APH structure, APH(3')-IIIa (Hon et al., 1997). The N-terminal domain (residues 7 to 92) and C-terminal domain (residues 99 and 301) are connected by a short loop (residues 93 to 98) also known as a hinge (Figure 3-2a). The C-terminal domain can be further divided into two sub-domains, each comprised of two non-contiguous sequences. The core sub-domain spans residues 99 to 143 and 190 to 258. The second sub-domain is exclusively

α-helical and is made up of residues 144 to 189 and 259 to 301.

TABLE 3-1: REFINEMENT DATA FOR CRYSTAL STRUCTURE OF APH(4)-IA + HYGB

	APH(4)-Ia + hygB (3OVC)
Data collection	
Wavelength (Å)	0.9798 (peak)
Resolution range (Å)	50.0 – 1.95
Space group	P 3_2 2
a = *b* (Å)	70.64
c (Å)	125.88
R_{merge}	0.068 (0.697)[a]
$\langle I \rangle / \sigma I$	52.2 (3.46)
Completeness (%)	99.9 (100)
Redundancy	10.3 (7.6)
Refinement	
Resolution range (Å)	23.54 – 1.95
Number of reflections	
Working set	25785
Test set	1360
R_{work}/R_{free} [b]	0.176/0.218
Number of non-hydrogen atoms	
Protein	2330
Substrate	25
Ion/solvent	131
Water	249
Root mean square deviation	
Bond length (Å)	0.010
Bond angle (°)	0.98
Average thermal factor (Å^2)	
Protein	38.6
Substrate	29.6
Ion/solvent	52.8
Water	48.2
Ramachandran analysis (%)	
Most favoured regions regions	92.1
Additionally allowed regions	7.5
Generously allowed regions	0.4
Disallowed regions[c]	0

[a]Values in parantheses refer to highest resolution shell of 1.98-1.95 Å.
[b]R_{free} was calculated by randomly omitting 5% of the observed reflections from the refinement.
[c]According to the Ramachandran plot in Procheck (Laskowski, 1993)

Pair-wise superposition of APH(4)-Ia with the full-length structures of APH(2'')-IIa (Young et al., 2009), APH(2'')-IVa (Toth et al., 2010), APH(3')-IIa (Nurizzo et al., 2003), APH(3')-IIIa (Burk et al., 2001; Hon et al., 1997) and APH(9)-Ia (Fong et al., 2010), show RMSD values between 2.6-3.3 Å (over 182-229 matching Cα atoms), reflecting the conservation of the general APH fold in the APH(4)-Ia structure. However,

the C-terminal core sub-domain of APH(4)-Ia shows particularly high fold conservation and superimposes with the equivalent domain of other APH enzymes with a lower range of RMSD values (between 2.0 and 2.6 Å, over 89-95 matching Cα atoms). This similarity is reflected in the strict spatial conservation of common catalytic residues, many of which are localized to the C-terminal core subdomain. The N-terminal domain of APH(4)-Ia is also more highly conserved in structure than the full enzyme structure overall and superimposes with the equivalent domain of other APH enzymes with RMSD values between 2.1-2.6 Å (over 67-75 matching Cα atoms). This is reflected in the high conservation of the ATP binding site, which is largely formed by this subdomain. Taken together, these observations suggest that the structural variation in APH enzymes can be attributed to the C-terminal helical subdomain. This domain is involved in substrate recognition, this led to the analysis of its topology and conformation.

Role of the C-terminal helical subdomain in the narrow substrate specificity of APH(4)-Ia. Primary sequence alignment suggested that residues 156 to 171 of APH(4)-Ia should correspond to the aminoglycoside-binding loop of APH(3')-IIIa, but according to tertiary structure analysis the region corresponding to these residues is largely displaced away from the antibiotic binding site. Instead, the space corresponding to the aminoglycoside-binding loop in APH(3')-IIIa structure is occupied by α9 and α10 helices in the APH(4)-Ia (Figure 3-3). A similar feature had been shown for the APH(2")-IIa structure (Young et al., 2009); our superposition verified that the C-terminal helical subdomain of APH(2")-IIa is a better match to this subdomain of APH(4)-Ia (Figure 3-3).

While substitution of the aminoglycoside-binding loop by helices α9 and α10 in APH(4)-Ia positions amino acids largely in the same vicinity in the aminoglycoside binding site, this replacement introduces numerous differences. The helical periodicity and the specific residue content of α9 and α10 result in different residues accessible for interaction with the substrate. These structural features may contribute to the narrow substrate specificity of APH(4)-Ia. Notably, APH(3')-IIa Asp159, which interacts with the C ring of kanamycin, corresponds to Trp288 in the APH(4)-Ia structure. The presence of this bulky sidechain would preclude binding of 4,6-disubstituted aminoglycosides to APH(4)-Ia, a notion consistent with the substrate specificity studies. Furthermore, modeling of aminoglycosides with additional chemical groups at the position 1 of the 2-deoxystreptamine ring, such as the 4-amino-2-hydroxy-butyryl group of butirosin, into the APH(4)-Ia active site resulted in clashes with helix α10.

While the overall structure topology of the C-terminal helical subdomain of APH(4)-Ia is similar to that of corresponding subdomain in APH(2")-IIa structure, there are notable differences in the active site between these enzymes that may be responsible for their different substrate preference. Compared to the APH(2")-IIa structure, the α9 helix in APH(4)-Ia is rotated towards the active site by ~30°, which results in the Trp288

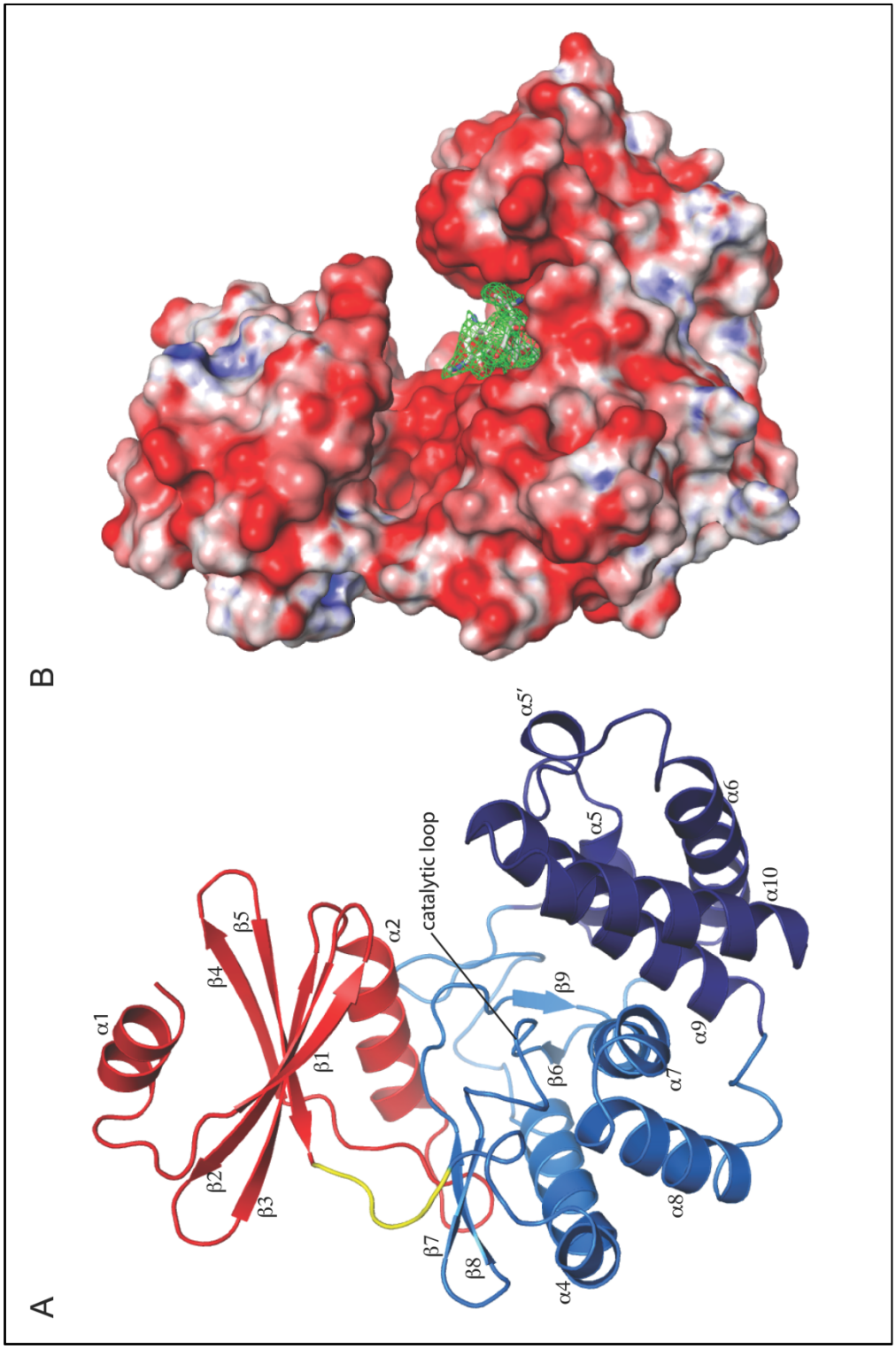

Figure 3-2: Structure of APH(4)-Ia in complex with hygB. *A*, Structure of APH(4)-Ia, coloured by domain (red = N-terminal domain, yellow = linker/hinge, light blue = C-terminal core sub-domain, dark blue = C-terminal helical sub-domain). Secondary structures and catalytic loop are labeled according to the definitions of Hanks *et al.* (Hanks et al., 1988) *B*, Electrostatic surface representation of APH(4)-Ia showing bound hygB (ligand in stick representation). Electron density around hygB shown is from a *Phenix* iterative omit $2F_o$-F_c map at 1.0 σ.

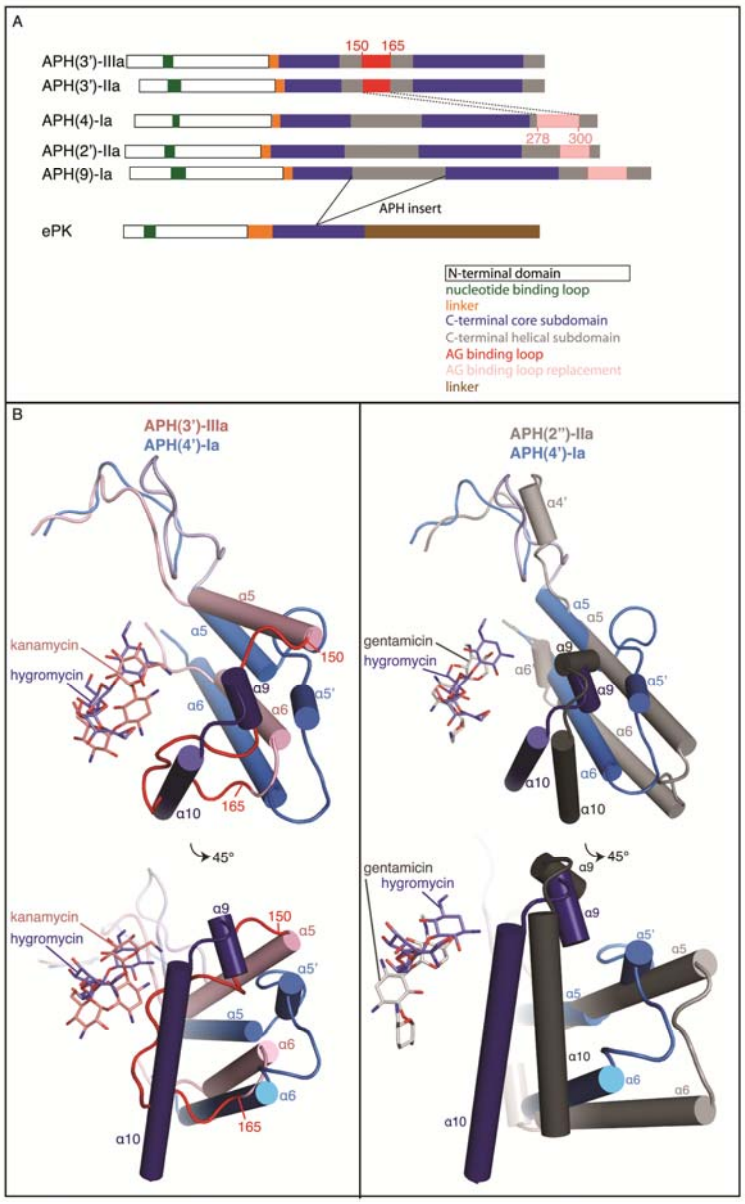

Figure 3-3: Domain architecture of APH enzymes and secondary structure topology of the C-terminal helical sub-domain. a) Domain architecture of APH enzymes and a representative eukaryotic protein kinase (ePK) enzyme CAPK (Zheng et al., 1993). The space occupied by the aminoglycoside binding loop from APH(3') enzymes (shaded red) is replaced by the C-terminal region shaded pink in the APH(4)-Ia, APH(2'')-IIa and APH(9)-Ia enzymes, as indicated by dashed lines connecting these regions. b) Zoom in view of the C-terminal helical sub-domain, showing the aminoglycoside binding loop of APH(3') enzymes is replaced by extreme C-terminal helices in APH(4)-Ia, APH(2'')-IIa and APH(9)-Ia enzymes. Left panel = superposition of the structures of APH(3')-IIIa (residues 125-182), coloured pink, and APH(4)-Ia (residues 125-189 and 278-300), coloured blue. Aminoglycoside binding loop of APH(3')-IIIa (residues 150-165) is coloured red and the region of APH(4)-Ia (residues 278-300) that fills the equivalent volume is coloured dark blue. Right panel = superposition of the structures of APH(2")-IIa (residues 122-184 and 275-291), coloured grey, and APH(4)-Ia (125-189 and 278-300), coloured blue.

side chain approaching the active site by ~5 Å relative to its equivalent residue (Gly285) in APH(2")-IIa. As in the comparison with APH(3')-IIa, the presence of this large aromatic side chain and the noted movement would prevent the binding of 4,6-disubstituted aminoglycosides due to spatial constraints. Also, the α-helix defining the border of the active site (α9 in APH(2'')-IIa, α7 in APH(4)-Ia) is 4 Å closer to the position of the aminoglycoside ligand in APH(4)-Ia; Trp235 in this helix would interfere with the ring at the 6-position of a 4,6-disubstituted ligand in the active site of APH(4)-Ia.

Comparative structural analysis have demonstrated that the APH(4)-Ia enzyme features a distinctive topological variation in the aminoglycoside-binding loop region and specific sequence determinants that disfavour the binding of 4,5- or 4,6-disubstituted aminoglycosides. These structural observations are consistent with the steady state kinetic studies presented here.

APH(4)-Ia contains a unique cluster of hydrophobic residues that complements the twisted shape of hygB. Having established that the active site of APH(4)-Ia is not comprised of an aminoglycoside binding loop structure, we analyzed the specific interactions between the enzyme and hygB.

As with other APH enzymes (Burk et al., 2001; Fong et al., 2010; Hon et al., 1997; Nurizzo et al., 2003; Toth et al., 2010; Young et al., 2009), the substrate binding site in the APH(4)-Ia structure is found in a negatively charged pocket between the C-terminal core and helical sub-domains (Figure 3-2b). In the structure the hygB adopts a conformation such that rings II, III and IV are not coplanar, in contrast to the equivalent rings of 4,6-disubstituted ligands when bound to APH(2") or APH(3') enzymes. The plane defined by ring I of hygB is nearly perpendicular to a plane through rings II and III. Ring I is also nearly perpendicular in the other axis to the plane of ring IV, due to the twist introduced by the orthoester between rings III and IV. Interestingly, rings I and IV of hygB superimpose well with rings A and C of the spectinomycin bound to APH(9)-Ia (Fong et al., 2010). This is due to the fact that ring IV of hygB is twisted relative to rings II and III, in the same way as the twist of the spectinomycin ring C relative to rings A and B.

Ring I of hygB is prominently separated from the other rings with the C4-OH (oxygen 11/O11) phosphorylation site positioned at a distance of 2.2 Å from the catalytic Asp198 (Figure 3-4). When other APH/aminoglycoside complex structures are superimposed onto the APH(4)-Ia/hygB structure, ring I of hygB occupies the position corresponding to the phosphorylated rings of spectinomycin bound to APH(9)-Ia, and ring C or ring A of 4,6-disubstituted aminoglycoside ligands bound to APH(2") enzymes and APH(3') enzymes, respectively. On the enzyme side this feature is reflected in the strict conservation of the C-terminal core sub-domain conformation and that of the catalytic residues across all APH enzymes.

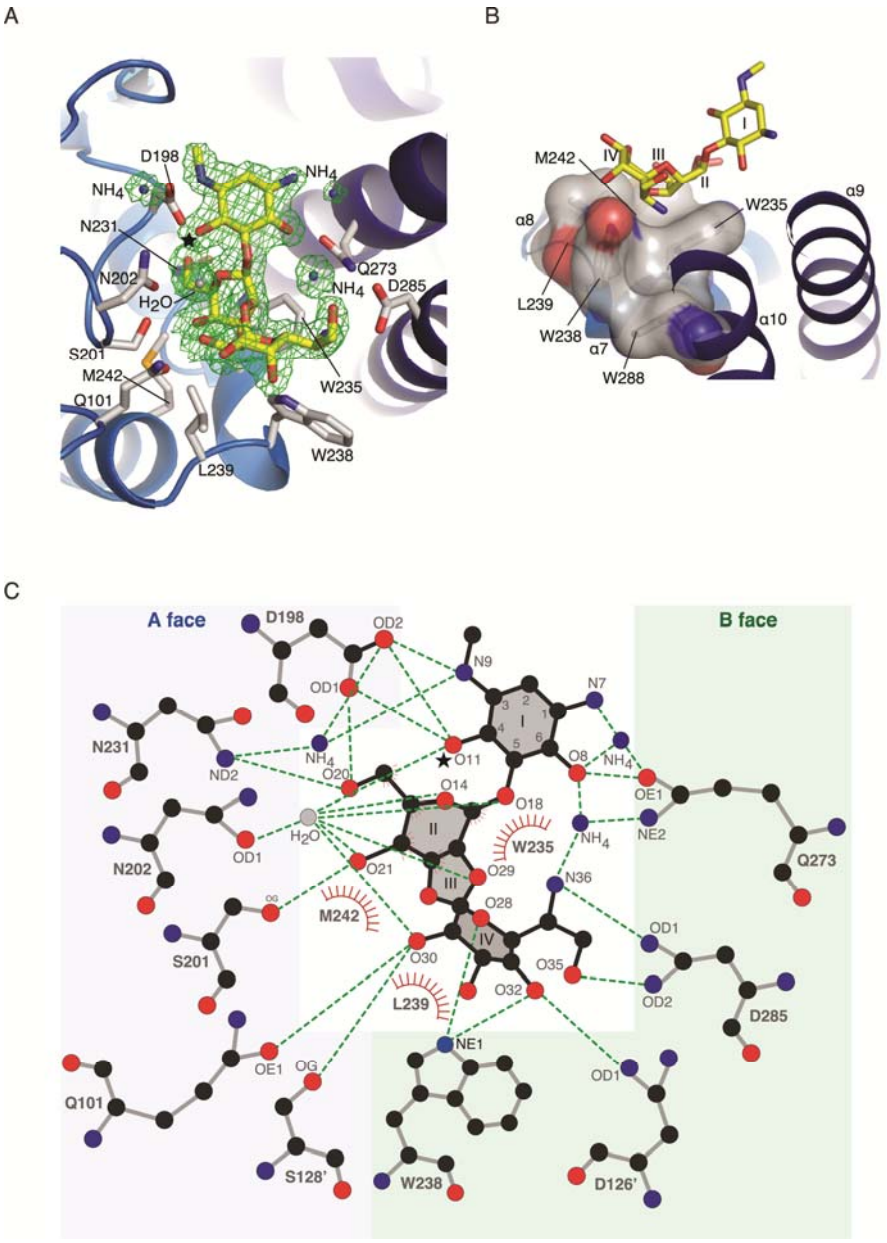

Figure 3-4: HygB binding to APH(4)-Ia. *A*, HygB (shown in yellow sticks) bound to APH(4)-Ia. Electron density shown is from a *Phenix* iterative omit $2F_o$-F_c map at 1.0 σ. Ammonium ions, water molecules, and enzyme sidechains that form H-bond or van der Waals interactions with hygB are shown. The phosphorylation site on hygB is labeled with a black star. *B*, Hydrophobic interactions between APH(4)-Ia and hygB. Surface representation is shown for Trp235, Trp238, Leu239, Met242 and Trp288. Surface colouring: grey = uncharged, blue = nitrogen atoms, red = oxygen atoms. *C*, All interactions between APH(4)-Ia and hygB. Hydrogen bonds are indicated with green dashed lines and van der Waals interactions indicated by red fans. The phosphorylation site O11 is labeled with a black star. Carbon, nitrogen, oxygen atoms, water and ammonium molecules are coloured black, blue, red, grey and blue, respectively. The interactions from Asp126 and Ser128, residues from a symmetry-related chain in the crystal are indicated by an apostrophe.

The APH(4)-Ia enzyme forms a pocket that is complementary to the twisted shape of hygB (Figure 3-4). There are thirteen direct hydrogen bonds between hygB and nine residues of this APH enzyme (Figure 3-4c). These interactions are nearly equally distributed between the two "faces" of the substrate: an "A face" that interacts with six residues from the catalytic and NTP binding sites, and a "B face" that interacts with five residues from the C-terminal helical subdomain.

The interaction between the enzyme and hygB is bridged by a water molecule and three ammonium ions. The water molecule interacts with the Asn202 side chain and forms six interactions with the A face of the ligand, including the phosphorylation site O11. One of the ammonium ions is found proximal to the A face and bridges interactions between Asp198 and Asn231 with N9 of the ligand. On the B face of the ligand, the other two ammonium ions interact with Gln273 and atoms in rings I and IV of hygB.

Specific interactions between hygB and APH(4)-Ia Ser201 appear to be responsible for straining of the backbone ϕ/ψ angles of this residue (Table 3-1), Ser201 is the only residue in the "generously allowed" region of the Ramachandran plot. This strained nature of Ser201 does not have an analog in previously characterized APH-substrate complex structures, thus this residue plays a unique role in this APH enzyme.

In addition to an extensive network of electrostatic/H-bonding interactions, the APH(4)-Ia binding pocket also supplies a significant hydrophobic surface to complement the structure of the substrate (Figure 3-4b). Residues Trp235, Trp238, Leu239 and Met242 provide hydrophobic and stacking interactions with rings II, III and IV of hygB. Trp235 is positioned directly under and stacks with ring II of hygB. The edge of Trp238 defined by atoms NE1 and CD1, along with Leu239 form a surface accommodating ring IV of hygB. The CE atom of Met242 interacts with an edge of ring II. Trp235 and Trp238 in turn pack against Trp288 from α9 of the enzyme. The hydrophobic patch formed by these three tryptophan residues represents a distinctive feature of the APH(4)-Ia structure when compared to other structures of APH enzymes. The three tryptophan residues likely contribute to the conformation of the other residues making up this hydrophobic patch, therefore determining selectivity for the atypical chemical architecture of hygB.

HygB occupies only a portion of the large cleft between the APH(4)-Ia N- and C-terminal domains. This cleft contains residues Pro135, Tyr144, Phe150, Ala197, Met221, Tyr227, Asn231, Arg268 and Ile269, belonging to both C-terminal sub-domains.

Nucleotide binding site of APH(4)-Ia resembles that of APH(2'')-IIa. At least seven residues involved in nucleotide binding in APH(2'')-IIa (Young et al., 2009), APH(3')-IIIa (Burk et al., 2001; Hon et al., 1997) and APH(9)-Ia (Fong et al., 2010) are also conserved in the APH(4)-Ia. These include the Brenner motif, a sequence that is distinctive of enzymes that catalyze phosphoryl transfer (Brenner, 1987) and the DFG

sequence that is conserved in eukaryotic protein kinases. APH(4)-Ia Glu288 corresponds to a highly conserved Asp/Glu residue in α7 that forms interactions with the backbone amides of the H-X sequence of the Brenner motif. APH(4)-Ia contains a conserved glycine (Gly31) in the β2-β3 loop corresponding to the nucleotide positioning loop (NPL)/Gly-rich loop). The enzyme contains the conserved Leu48-Arg49 sequence in β3, shown to be involved in interactions with bound nucleotides and forming a salt-bridge with a highly conserved acidic residue in α2. The enzyme also contains the highly conserved IDWS sequence in the β7-β8 loop; side chains of the ID pair form interactions with bound nucleotides.

APH(4)-Ia did not crystallize in complex with ATP or its non-hydrolysable analogs such as AMPPNP or AMPPCP. To gain some insight about APH(4)-Ia interactions with this substrate, the ATP molecule was manually docked in the nucleotide binding site of APH(4)-Ia using a superposition with the structure of APH(2'')-IIa in complex with ATP and streptomycin (Young et al., 2009). This superposition was accomplished by aligning Cα atoms in the region between β6 and β9, comprising the Brenner and DFG motifs (RMSD = 0.85 Å). This superposition showed that the APH(4)-Ia and APH(2')-IIa N-terminal domains differ by a rotation of approximately 10° about the hinge region and we therefore adjusted the ATP position to compensate for this variation.

Based on this positioning of the nucleotide, most of the conserved nucleotide binding elements in the APH(4)-Ia structure are properly positioned for interactions with ATP except for the side chains of Arg49 and Asp216. In ATP-bound forms of APH enzymes, the positively charged group of the conserved Lys/Arg residue is positioned to interact with non-bridging oxygen atoms of the α and β-phosphates of ATP (Burk et al., 2001; Fong et al., 2010; Scheeff and Bourne, 2005; Young et al., 2009). APH(4)-Ia Asp216 corresponds to the residue that would interact with Mg^{2+} and a non-bridging oxygen of the α-phosphate of ATP in an APH(4)-Ia-Mg-ATP complex. In the APH(4)-Ia ATP binding model, changes in the side chain rotamers of Arg49 and Asp216 would be needed to initiate such interactions.

The model also indicated that the nucleotide positioning loop (NPL) of APH(4)-Ia would form interactions with the nucleotide that resemble those seen between the NPL of APH(2")-IIa and ATP (Young et al., 2009). The NPL sequence is conserved between APH(4)-Ia and APH(2")-IIa, and includes two serines involved in interactions with phosphates of ATP. Therefore, the NPL of APH(4)-Ia likely does not undergo significant conformational changes and would not clamp over the nucleotide as seen in the nucleotide-bound APH(3') and APH(9) complexes (Burk et al., 2001; Fong et al., 2010; Thompson et al., 2002).

This similarity between the nucleotide binding pocket of APH(4)-Ia and APH(2")-IIa could also explain why APH(4)-Ia shows promiscuity towards the nucleotide substrates ATP and GTP. APH(2'')-IIa was recently shown to utilize both nucleotides in

its reaction (Toth et al., 2009). It has been suggested that a larger nucleotide binding pocket in the APH(2'') enzymes could offer an alternative binding mode for GTP as compared to ATP (Toth et al., 2010). APH(3')-IIIa on the other hand shows exclusivity for ATP (Shakya and Wright, 2010), which could be due to a tighter binding pocket, and a large conformational change of the NPL upon nucleotide binding (Burk et al., 2001).

Site-directed Mutagenesis of APH(4)-Ia. In order to confirm the results of the structural analysis, several APH(4)-Ia active site residues were probed by site-directed mutagenesis. Eleven active site residues, Gln101, Asp126, Ser201, Asn231, Trp238, Gln273, and Asp285 (all involved in hygB binding), Arg49, Asn203, Asp216 (participating in nucleotide binding) and Asp198 (involved in γ-phosphate transfer from ATP to hygB) were selected. Each of these residues was individually mutated to an alanine, with the exception of Trp238, which was converted to leucine in order to retain similar hydrophobic and volume properties. Of the eleven mutations studied, the four expected to participate in ATP binding and catalysis (R49A, D216A, N203A and D198A) showed the greatest level of impairment in hygB modifying activity as compared to the wild-type enzyme (Table 3-2). Among these, the D216A, N203A and D198A variants showed complete loss of activity. R49A variant showed no change in its ability to recognize hygB but was severely impaired in ATP binding with a 30-fold increase in its K_m as compared to the wild-type. The residues involved in nucleotide binding are well conserved across all the APH enzymes with the exception of the substitution of the α–β phosphate coordinating lysine with an arginine (Arg49). This substitution is also seen in APH(2'')-IIIa and the macrolide phosphotransferases MPHa and MPHb. Arg49 shows the same level of indispensability as compared to its lysine counterparts in other APH enzymes (Hon et al., 1997; McKay et al., 1994a), where its removal leads to severe impairment in ATP utilization.

The seven APH(4)-Ia variants with alanine substitutions of residues involved in hygB binding showed nominal changes (no greater than a 2-fold increase) in K_m and k_{cat}/K_m as compared to the wild-type enzyme for hygB utilization. This reflects the extensive and distributed hydrogen-bonding network used to bind hygB. In such a network, removal of one or even two hydrogen bonds in the network of 13 total bonds is not predicted to have a significant effect.

TABLE 3-2: KINETIC CONSTANTS OF APH(4)-IA MUTANTS

Enzyme	Substrate Tested	K_m (μM)	k_{cat} (sec^{-1})	k_{cat}/K_m ($sec^{-1}*M^{-1}$)
Wild-type	HygB	6.8 ± 1.1	3.18	4.68×10^5
	ATP	57.2 ± 7.2	3.10	5.42×10^4
	GTP	339 ± 43	3.53	1.04×10^4
R49A	HygB	3.7 ± 0.3	0.37	1.00×10^5
	ATP	1708 ± 677	0.84	4.93×10^2
Q101A	HygB	34.5 ± 1.8	4.21	1.22×10^5
	ATP	314 ± 11	5.11	1.63×10^4
D126A	HygB	3.5 ± 0.7	1.36	3.89×10^5
	ATP	31 ± 3.4	1.17	3.77×10^4
D198A	HygB	No Activity		
	ATP	No Activity		
S201A	HygB	15 ± 4.6	3.75	2.50×10^5
	ATP	96.3 ± 6.7	3.73	3.88×10^4
N203A	HygB	No Activity		
	ATP	No Activity		
D216A	HygB	No Activity		
	ATP	No Activity		
N231A	HygB	18 ± 2.4	2.13	1.18×10^5
	ATP	73 ± 9.0	2.18	2.99×10^4
W238L	HygB	7 ± 2.1	2.68	3.83×10^5
	ATP	52.2 ± 6.2	2.40	4.59×10^4
Q273A	HygB	11.2 ± 1.6	2.77	2.48×10^5
	ATP	255 ± 15	3.28	1.29×10^4
D285A	HygB	12.6 ± 1	3.22	2.55×10^5
	ATP	70.5 ± 8.0	3.19	4.52×10^4

For hygB K_ms, the [ATP] = 1 mM, for ATP K_ms, the [hygB] = 0.5 mM.

CONCLUSION

This study presents a structural and functional analysis of APH(4)-Ia interactions with its substrate, the atypical aminoglycoside antibiotic hygromycin B. APH(4)-Ia adopts the common eukaryotic protein-kinase like fold seen in all APH enzyme structures. However, the APH(4)-Ia structure also demonstrates unique features that provides molecular insight into the high substrate specificity of this enzyme. Primarily, the APH(4)-Ia substrate binding site is lined by hydrophobic residues, including a cluster of Trp residues, absent in previously characterized APH enzymes. These residues provide a structural and chemical complement to the structure of hygB and also prohibits binding of 4,6- or 4,5-disubstituted 2-deoxystreptamine-based aminoglycosides.

Through comparative structural analysis, it was shown that the aminoglycoside binding site of APH(4)-Ia is made up of residues found towards the C-terminal portion of the C-terminal helical subdomain, and not the region corresponding to the "aminoglycoside binding loop", found in the N-terminal portion of the C-terminal helical subdomain in otherwise homologous APH(3') enzymes. This topology is shared with APH(2") and APH(9) groups of enzymes. APH(4)-Ia can also utilize GTP in its phosphorylation reaction, which is a property previously observed only for APH(2") enzymes (Toth et al., 2009).

HygB has broad antimicrobial activity and is only targeted by two known modifying enzymes, APH(7")-Ia and APH(4)-Ia, making it a good scaffold for novel antibiotic development in comparison with other aminoglycoside antibiotics such as kanamycin A, which is targeted by over 18 different modifying enzymes. The presented structural and mutational analysis opens the possibility for the design of hygB derivatives that would be less prone to modification by APH(4)-Ia, further improving the prospects for generation of novel phosphorylation-proof aminoglycoside antibiotics.

REFERENCES

Adams, P.D., Afonine, P.V., Bunkoczi, G., Chen, V.B., Davis, I.W., Echols, N., Headd, J.J., Hung, L.W., Kapral, G.J., Grosse-Kunstleve, R.W., *et al.* (2010). PHENIX: a comprehensive Python-based system for macromolecular structure solution. Acta Crystallogr D Biol Crystallogr *66*, 213-221.

Blanc, E., Roversi, P., Vonrhein, C., Flensburg, C., Lea, S.M., and Bricogne, G. (2004). Refinement of severely incomplete structures with maximum likelihood in BUSTER-TNT. Acta Crystallogr D Biol Crystallogr *60*, 2210-2221.

Borovinskaya, M.A., Shoji, S., Fredrick, K., and Cate, J.H. (2008). Structural basis for hygromycin B inhibition of protein biosynthesis. RNA *14*, 1590-1599.

Brenner, S. (1987). Phosphotransferase sequence homology. Nature *329*, 21.

Burk, D.L., Hon, W.C., Leung, A.K., and Berghuis, A.M. (2001). Structural analyses of nucleotide binding to an aminoglycoside phosphotransferase. Biochemistry *40*, 8756-8764.

Cabanas, M.J., Vazquez, D., and Modolell, J. (1978). Dual interference of hygromycin B with ribosomal translocation and with aminoacyl-tRNA recognition. Eur J Biochem *87*, 21-27.

Daigle, D.M., Hughes, D.W., and Wright, G.D. (1999). Prodigious substrate specificity of AAC(6')-APH(2"), an aminoglycoside antibiotic resistance determinant in enterococci and staphylococci. Chem Biol *6*, 99-110.

Eisenstein, B.I., Oleson, F.B., Jr., and Baltz, R.H. (2010). Daptomycin: from the mountain to the clinic, with essential help from Francis Tally, MD. Clin Infect Dis *50 Suppl 1*, S10-15.

Emsley, P., and Cowtan, K. (2004). Coot: model-building tools for molecular graphics. Acta Crystallogr D Biol Crystallogr *60*, 2126-2132.

Fong, D.H., Lemke, C.T., Hwang, J., Xiong, B., and Berghuis, A.M. (2010). Structure of the antibiotic resistance factor spectinomycin phosphotransferase from Legionella pneumophila. J Biol Chem *285*, 9545-9555.

Gonzalez, A., Jimenez, A., Vazquez, D., Davies, J.E., and Schindler, D. (1978). Studies on the mode of action of hygromycin B, an inhibitor of translocation in eukaryotes. Biochim Biophys Acta *521*, 459-469.

Gritz, L., and Davies, J. (1983). Plasmid-encoded hygromycin B resistance: the sequence of hygromycin B phosphotransferase gene and its expression in Escherichia coli and Saccharomyces cerevisiae. Gene *25*, 179-188.

Hanks, S.K., Quinn, A.M., and Hunter, T. (1988). The protein kinase family: conserved features and deduced phylogeny of the catalytic domains. Science *241*, 42-52.

Holm, L., Kaariainen, S., Rosenstrom, P., and Schenkel, A. (2008). Searching protein structure databases with DaliLite v.3. Bioinformatics *24*, 2780-2781.

Hon, W.C., McKay, G.A., Thompson, P.R., Sweet, R.M., Yang, D.S., Wright, G.D., and Berghuis, A.M. (1997). Structure of an enzyme required for aminoglycoside antibiotic resistance reveals homology to eukaryotic protein kinases. Cell *89*, 887-895.

Laskowski, R.A., MacArthur, M. W., Moss, D. S. and Thornton, J. M. (1993). PROCHECK: a program to check the stereochemical quality of protein structures. Journal of Applied Crystallography *26*, 283-291.

McKay, G.A., Robinson, R.A., Lane, W.S., and Wright, G.D. (1994a). Active-site labeling of an aminoglycoside antibiotic phosphotransferase (APH(3')-IIIa). Biochemistry *33*, 14115-14120.

McKay, G.A., Thompson, P.R., and Wright, G.D. (1994b). Broad spectrum aminoglycoside phosphotransferase type III from Enterococcus: overexpression, purification, and substrate specificity. Biochemistry *33*, 6936-6944.

McKay, G.A., and Wright, G.D. (1996). Catalytic mechanism of enterococcal kanamycin kinase (APH(3')-IIIa): viscosity, thio, and solvent isotope effects support a Theorell-Chance mechanism. Biochemistry *35*, 8680-8685.

Minor, Z.O.a.W. (1997). Processing of X-ray Diffraction Data Collected in Oscillation Mode, Vol 276.

Nurizzo, D., Shewry, S.C., Perlin, M.H., Brown, S.A., Dholakia, J.N., Fuchs, R.L., Deva, T., Baker, E.N., and Smith, C.A. (2003). The crystal structure of aminoglycoside-3'-phosphotransferase-IIa, an enzyme responsible for antibiotic resistance. J Mol Biol *327*, 491-506.

Pardo, J.M., Malpartida, F., Rico, M., and Jimenez, A. (1985). Biochemical basis of resistance to hygromycin B in Streptomyces hygroscopicus--the producing organism. J Gen Microbiol *131*, 1289-1298.

Petrey, D., and Honig, B. (2003). GRASP2: visualization, surface properties, and electrostatics of macromolecular structures and sequences. Methods Enzymol *374*, 492-509.

Pittenger, R.C.W., RN; Hoehn, PN; Daily, WA; McGuire, JM (1953). Hygromycin. I. Preliminary studies in the production and biologic activity on a new antibiotic. Antimicro Chemother *3*, 1268-1278.

Pon, N.G., and Bondar, R.J. (1967). A direct spectrophotometric assay for pyruvate kinase. Anal Biochem *19*, 272-279.

Rao, R.N., Allen, N.E., Hobbs, J.N., Jr., Alborn, W.E., Jr., Kirst, H.A., and Paschal, J.W. (1983). Genetic and enzymatic basis of hygromycin B resistance in Escherichia coli. Antimicrob Agents Chemother *24*, 689-695.

Scheeff, E.D., and Bourne, P.E. (2005). Structural evolution of the protein kinase-like superfamily. PLoS Comput Biol *1*, e49.

Shakya, T., and Wright, G.D. (2010). Nucleotide selectivity of antibiotic kinases. Antimicrob Agents Chemother *54*, 1909-1913.

Siregar, J.J., Miroshnikov, K., and Mobashery, S. (1995). Purification, characterization, and investigation of the mechanism of aminoglycoside 3'-phosphotransferase type Ia. Biochemistry *34*, 12681-12688.

Thompson, P.R., Boehr, D.D., Berghuis, A.M., and Wright, G.D. (2002). Mechanism of aminoglycoside antibiotic kinase APH(3')-IIIa: role of the nucleotide positioning loop. Biochemistry *41*, 7001-7007.

Toth, M., Chow, J.W., Mobashery, S., and Vakulenko, S.B. (2009). Source of phosphate in the enzymic reaction as a point of distinction among aminoglycoside 2"-phosphotransferases. J Biol Chem *284*, 6690-6696.

Toth, M., Frase, H., Antunes, N.T., Smith, C.A., and Vakulenko, S.B. (2010). Crystal structure and kinetic mechanism of aminoglycoside phosphotransferase-2"-IVa. Protein Sci *19*, 1565-1576.

Toth, M., Zajicek, J., Kim, C., Chow, J.W., Smith, C., Mobashery, S., and Vakulenko, S. (2007). Kinetic mechanism of enterococcal aminoglycoside phosphotransferase 2"-Ib. Biochemistry *46*, 5570-5578.

Tsai, S.F., Zervos, M.J., Clewell, D.B., Donabedian, S.M., Sahm, D.F., and Chow, J.W. (1998). A new high-level gentamicin resistance gene, aph(2")-Id, in Enterococcus spp. Antimicrob Agents Chemother *42*, 1229-1232.

Wallace, A.C., Laskowski, R.A., and Thornton, J.M. (1995). LIGPLOT: a program to generate schematic diagrams of protein-ligand interactions. Protein Eng *8*, 127-134.

Wright, G.D., and Thompson, P.R. (1999). Aminoglycoside phosphotransferases: proteins, structure, and mechanism. Front Biosci *4*, D9-21.

Young, P.G., Walanj, R., Lakshmi, V., Byrnes, L.J., Metcalf, P., Baker, E.N., Vakulenko, S.B., and Smith, C.A. (2009). The crystal structures of substrate and nucleotide complexes of Enterococcus faecium aminoglycoside-2"-phosphotransferase-IIa [APH(2")-IIa] provide insights into substrate selectivity in the APH(2") subfamily. J Bacteriol *191*, 4133-4143.

Zalacain, M., Pardo, J.M., and Jimenez, A. (1987). Purification and characterization of a hygromycin B phosphotransferase from Streptomyces hygroscopicus. Eur J Biochem *162*, 419-422.

Zheng, J., Trafny, E.A., Knighton, D.R., Xuong, N.H., Taylor, S.S., Ten Eyck, L.F., and Sowadski, J.M. (1993). 2.2 A refined crystal structure of the catalytic subunit of cAMP-dependent protein kinase complexed with MnATP and a peptide inhibitor. Acta Crystallogr D Biol Crystallogr *49*, 362-365.

CHAPTER FOUR
A SMALL MOLECULE DISCRIMINATION MAP OF THE ANTIBIOTIC RESISTANCE KINOME

CHAPTER FOUR PREFACE

The work presented in this chapter is currently being prepared for publication and has been the result of an extensive collaboration between:

Tushar Shakya[1], Peter Stogios[2], Nicolas Todorovic[3], Nick Waglechner[1], Elena Evdokimova[2], Jan Blanchard[4], Andrew McArthur[5], Alfredo Capretta[3], Alexei Savchenko[2] and Gerard D. Wright[1]

[1]M.G. DeGroote Institute for Infectious Disease Research, Department of Biochemistry and Biomedical Sciences, McMaster University, Hamilton, ON, L8S 3Z5, Canada
[2]Banting and Best Department of Medical Research, University of Toronto, Toronto, ON, M5G 1L6
[3]Department of Chemistry, McMaster University, Hamilton, ON L8S 3Z5, Canada
[4]High-throughput Screening Lab, Centre for Microbial and Chemical Biology, McMaster University, Hamilton, ON, L8S 3Z5, Canada
[5]Andrew McArthur Consulting, Hamilton, ON, Canada

My contributions to this work have been specifically towards the cloning, expression, purification and characterization of all of the enzymes within this study. In addition to this, I conducted all of the compound screening including follow-up studies. Chemical synthesis was conducted by Nick Todorovic under the supervision of Dr. Fred Capretta; structural studies were conducted by Dr. Peter Stogios and Elena Evdokimova under the supervision of Dr. Alexei Savchenko; and the phylogenetic analysis of the kinases was conducted by Nick Waglechner under the supervision of Dr. Andrew McArthur.

Acknowledgements:
Generous gift of the plasmids for the templates of *aph(2")-IIa, aph(2")-IIIa, aph(2")-IVa* and *aph(3')-IIa* from Dr. Sergei Vakulenko and Dr. Shahriar Mobashery. The *aph(9)-Ia* expression plasmid was from Dr. Albert Berghuis. The *mphA* and *mphB* plasmids were from Dr. Norihisa Noguchi. Dr. Tomohiro Tamura supplied all strains and plasmids required for protein expression in *Rhodococcus* and Peter Spanogiannopolous for implementation of the *Rhodococcus expression system.* Yao Fan at beamline 19-ID, Structural Biology Centre, Advanced Photon Source, Argonne National Laboratory for crystal diffraction data collection, and Rosa Di Leo in the Savchenko lab for cloning all constructs used in crystallography.

ABSTRACT

Antibiotic resistance kinases are a major cause of clinical failure of antibiotics including the aminoglycosides and macrolides. Structure and function studies have demonstrated that these enzymes share the same characteristic protein fold and motifs as Ser/Thr/Try protein kinases offering the possibility that they would be targets for known protein kinase inhibitors. This would enable chemo-profiling of resistance kinases for discrimination of inhibitor scaffold selectivity and leads for molecules that could block resistance. We have interrogated fourteen resistance kinases against a set of 80 well characterized kinase inhibitors. Compounds with both broad and narrow inhibition profiles were identified that could be eventual leads for co-drug therapy. We found that compound specificity against a set of enzymes is not necessarily dictated by molecular phylogeny, and that enzyme promiscuity can vary regardless of ancestral origin, antibiotic substrate- and regio-specificity. We also show how these data can be used in conjunction with structural data to predict interactions between small molecules and enzymes where co-structures do not exist.

INTRODUCTION

Resistance to antibiotics is a problem of global scope with massive impact on clinical outcomes. The emergence of resistance to all classes of antibiotics in current use and the gathering of multiple resistance mechanisms in individual pathogens has resulted in strains resistant to all available drugs. This regression towards the pre-antibiotic era continues unabated as efforts to bring new antibiotics to market are diminishing. New drugs and antibiotic strategies are urgently needed to fill this growing gap in infectious disease control.

One of the challenges facing the drug discovery community is the lack of readily available new chemical scaffolds with antibiotic activity. This has led to the open question of whether all easily implementable antibiotic chemical scaffolds have already been exploited over the last 50 years: the so-called 'low hanging fruit' (Baltz, 2006; Fischbach and Walsh, 2009). One option to meet the challenge of new scaffold discovery is to rescue 'old' or orphaned antibiotics by inhibiting antibiotic resistance proteins. Indeed, this strategy has been highly successful in the β-lactam field. Synthetic and natural product inhibitors of β-lactamases have proven to be highly successful β-lactam adjuvants; some examples of such combinations are: Augmentin® (amoxicillin-clavulanate) (Leigh et al., 1981), Zozysn® (Piperacillin-tazobactam) (Akova et al., 1990) and Unasyn® (ampillicin-sulbactam) (Labia et al., 1986). New combinations are also actively being pursued; for example, meropenem and clavulanate have recently been shown to have potent activity against *Mycobacterium tuberculosis* (Hugonnet et al., 2009). Also, the novel β-lactamase inhibitor NXL104 and the cephalosporin ceftazidime have shown potency against several *Enterobacteriaceae* harboring extended-spectrum β-lactamases and carbapenemases (Livermore et al., 2008). The later combination is scheduled to complete phase II clinical trials in 2011. The success of these combination therapies in combating β-lactam resistance via β-lactamase inhibition suggests the same strategy could be applied to other resistance mechanisms. Aminoglycosides and macrolides are clinically relevant antibiotics that are susceptible to inactivation via numerous, ubiquitous modifying enzymes, as described below. To date, no combination therapies are available to rescue the activity of these antibiotics.

The Antibiotic Resistance Kinome represents a unique space found at the cross-section of the Microbial Kinome (Kannan et al., 2007) and Antibiotic Resistome (D'Costa et al., 2006). This subset of genes is comprised of antibiotic kinases (AKs), prevalent in microbes in both the clinic and the environment, that confer, or have the potential to confer, resistance to important antibiotics such as aminoglycosides (e.g. gentamicin, amikacin) and macrolides (e.g. erythromycin, azithromycin, telithromycin). These kinases show modest primary sequence similarity making phylogenic classification difficult; however, they all adopt the Ser/Thr/Tyr protein kinase three-dimensional fold (Fong et al., 2010; Hon et al., 1997; Nurizzo et al., 2003; Stogios et al., 2011; Toth et al.,

2010; Young et al., 2009). In particular, the nucleotide-binding site contains several conserved key catalytic residues (Kannan et al., 2007). This finding suggests that protein kinase inhibitors have the potential to also inhibit AKs, as demonstrated by isoquinoline sulfonamides and flavonoid protein kinase inhibitors that have been shown to successfully inhibit several aminoglycoside kinases (Daigle et al., 1997).

Susceptibility to protein kinase inhibitors has been previously used to quantitatively explore the phylogenetic relationship among human protein kinase inhibitors using novel high–throughput platforms (Fabian et al., 2005; Metz et al., 2011). These efforts provide a quantitative map of inhibitor-kinase space, establishing an inhibitor-based phylogeny that can be leveraged in drug discovery. This approach allows simultaneous evaluation of the kinase spectrum of activity among a panel of enzymes and facilitates selection of compounds based on downstream requirements as probes of biology or, more importantly, as plausible drug leads.

Protein kinase inhibitors are currently in clinical use for the treatment of cancer and have great potential for additional therapies (Knight et al., 2010; Zhang et al., 2009). The pharmaceutical industry has invested significantly in the design and synthesis of large libraries of compounds that target protein kinases, representing an untapped small molecule resource that could potentially be repurposed for blocking antibiotic resistance. Similar efforts have been successful, as seen with the use of pyridopyrimidines, a eukaryotic kinase pharmacophore, to inhibit bacterial biotin carboxylase in prokaryotic fatty acid biosynthesis (Miller et al., 2009). We have screened a library of 80 well characterized protein kinase inhibitors against a panel of fourteen bona fide AKs, and show that these inhibitors can be used to quantitatively distinguish among resistance kinases and expose active site similarities and differences that can be exploited in the discrimination of molecules that block antibiotic resistance.

MATERIALS AND METHODS

Phylogenetic Analysis of AKs. A comprehensive list of 34 known AKs was compiled in order to determine their phylogenetic relationship: APH(2")-Ia (Acc # AAA26865, residues 175-479), APH(2")-IIa (Acc # AAK63040), APH(2")-IIIa (Acc # AAB49832), APH(2")-IVa (Acc # AAC14693), APH(2")-Ie (Acc # AAW59417), APH(3')-Ia (Acc # CAA23656), APH(3')-IIa (Acc # CAA23892), APH(3')-IIb (Acc # AAG07506), APH(3')-IIIa (Acc # CAA24789), APH(3')-IVa (Acc # P00553), APH(3')-Va (Acc # P00555), APH(3')-Vb (Acc # P13250), APH(3')-Vc (Acc # AAB21326), APH(3')-Vd (Acc # YP_482452), APH(3')-VIa (Acc # CAA30578), APH(3')-VIb (Acc # CAF29483), APH(3')-VIIa (Acc # P14508), APH(3')-VIIIa (Acc # AAA26412), APH(3")-Ia (Acc # CAA37605), APH(3")-Ib (Acc # AAA26442), APH(3")-Ic (Acc # ABC68330), APH(4)-Ia (Acc # P00557), APH(4)-Ib (Acc # CAA52372, residues 179 - 420), APH(6)-Ia (Acc # P08077), APH(6)-Ib (Acc # P18622), APH(6)-Ic (Acc # CAA25854), APH(6)-Id (Acc # AAA26443), APH(7")-Ia (Acc # P09979), APH(9)-Ia (Acc # AAB58447), APH(9)-Ib (Acc # AAB66655), APH(9)-Ic (Acc # AAD50455), MPH(2')-Ia (Acc # BAA03776), MPH(2')-IIa (Acc # BAA12910), MPH(2')-IIIa (Acc # BAA34540).

A preliminary alignment was conducted with a Pfam group for APHS (Pf01636, Pfam data base at the Welcome Trust Sanger Institute) in order to align all of the core APH motifs using HMMER 3.0 (Eddy, 2008) at default parameters. It was then followed by five rounds of refinement with MUSCLE v3.7 (Edgar, 2004) followed with manual adjustment of APH(4)-Ia, APH(6)-Id and APH(9)-Ia to return consensus in the conserved regions (Appendix 2).

The tree was estimated with two runs of 5 million generations of a Metropolis coupled Markov chain Monte Carlo (MCMCMC) algorithm (Altekar et al., 2004) with four chains per run in Mr. Bayes v3.1.2 (Ronquist and Huelsenbeck, 2003) using a gamma model and estimating a proportion of invariant sites using the empirical WAG amino acid substitution model (Whelan and Goldman, 2001). Random topology trees were sampled every 100 generations. The consensus tree was constructed using a burn-in of 1000 samples for every 50,000 trees sampled such they followed the 50% majority rule.

Cloning, Expression and Purification of Antibiotic Kinases. A summary of the strains used in this study are in Table 4-1 and the oligonucleotide primers used to construct specific expressing clones can be seen in Appendix 1. APH(2")-Ia (Boehr et al., 2001), APH(2")-IIa (Shakya and Wright, 2010), APH(3')-IIIa (McKay et al., 1994), APH(4)-Ia (Stogios et al., 2011), APH(9)-Ia (Lemke et al., 2005) and MPH(2')-Ia (Shakya and Wright, 2010) were expressed and purified as previously described. The remaining genes were all cloned into their respective expression vectors using standard restriction endonuclease digestion and ligation techniques, with the exception of APH(3')-Va which

was cloned into pDEST17 expression vector using the homologous recombination technique as described by the Gateway® Cloning System (Invitrogen).

TABLE 4-1:. CONSTRUCTS USED IN THIS STUDY

Gene	Original Organism	Source	Backbone	Reference
aac(6')-Ie - aph(2")-Ia	*S. aureus*	HisAAC(6')-APH(2'')*	pET15b	(Boehr et al., 2001)
aph(2")-IIa	*E. coli*	pD17-APH(2")-Ib*	pDEST17	(Shakya and Wright, 2010)
aph(2")-IIIa	*E. gallinarium*	pAM3606	pET28a	(Chow et al., 1997)
aph(2")-IVa	*E. casseflavius*	NC95	pET28a	(Tsai et al., 1998)
aph(3')-Ia	*A. baumannii*	gDNA	pET28a	(Fournier et al., 2006)
aph(3')-IIa	*S. enterica*	pGEME182	pET28a	(Siregar et al., 1994)
aph(3')-IIIa	*E. faecalis*	pETSACG1*	pET22b	(McKay et al., 1994)
aph(3')-Va	*S. fradiae*	gDNA	pDEST17	(Thompson and Gray, 1983)
aph(3'')-Ia	*S. griseus*	gDNA	pET28a	(Trower and Clark, 1990)
aph(4)-Ia	*E. coli*	pET28a-APH(4)-Ia*	pET28a	(Stogios et al., 2011)
aph(6)-Ia	*S. griseus*	gDNA	pTipQC.1	(Distler et al., 1987)
aph(9)-Ia	*L. pneumophila*	pET21b-APH(9)H*	pET21b	(Lemke et al., 2005)
mphA	*E. coli*	pET28a-MPH(2')-I	pET28a	(Shakya and Wright, 2010)
mphB	*E. coli*	pTZ3716	pET28a	(Noguchi et al., 1996)

*The same constructs were used as stated in the cited papers. Remaining genes were cloned from the respective sources into the stated plasmid backbones.

All of the enzymes, with the exception of APH(6)-Ia were purified using a standard protocol. Each enzyme was expressed in *E. coli* BL21(DE3) (Novagen) and grown overnight in the presence of 50 μg/mL kanamycin A (100 μg/mL of Ampicillin for pD17-aph(3')-Va) in Luria Bertani (LB) broth. A 10 mL overnight culture was used to inoculate 1 L of fresh LB broth with antibiotic selection and was grown to OD_{600} ~ 0.6 at 37°C. It was then induced for 16 hours at 16°C with 1 mM isopropyl-β-thiogalactoside. Cells were harvested by centrifugation at 6000 x *g* for 10 min. The cell pellet was then resuspended in 15 mL of 50 mM HEPES pH 7.5, 300 mM NaCl, 10 mM imidazole, 1 mM phenylmethanesulfonyl fluoride and 1 μg/mL pancreatic bovine DNAse. The resuspended pellet was passed through a T-S series cell disrupter (Constant Systems Inc.) twice at 35,000 psi to create a lysate. The insoluble and soluble fractions were separated by centrifugation at 48,000 x *g* for 30 minutes. The supernatant was then applied to a 1 mL Ni-NTA Column (Qiagen) equilibrated in ten column volumes 50 mM HEPES pH 7.5, 300 mM NaCl, 10 mM imidazole (Buffer A). A stepwise gradient over five column volumes each of 10%, 25%, 50% and 100% Buffer B (50 mM HEPES pH 7.5, 300 mM NaCl, 250 mM imidazole) was used to elute the enzyme. The kinase containing fractions were identified by SDS-polyacrylamide gel electrophoresis and were subsequently pooled and dialyzed against 50 mM HEPES pH 7.5 overnight at 4°C with stirring. The protein was then quantified using the Bradford protein assay and was either concentrated or diluted ~2 mg/mL, and stored in 15% glycerol at -20°C.

APH(6)-Ia was expressed in a unique fashion due to poor expression and solubility in standard *E. coli* expression systems. The plasmid pTip-aph(6)-Ia ($Thio^R$,

Cm^R) was constructed in order to facilitate APH(6)-Ia expression in *Rhodococcus erythropolis* L-88 (Mitani et al., 2005), a lysozyme susceptible mutant. The plasmid was prepared in *E. coli* DH5α cells with chloramphenicol (35 μg/mL) selection in order maintain stability of the pTip-QC1 plasmid (Nakashima and Tamura, 2004). To facilitate transformation into *Rhodococcus spp.* 300-500 ng of the pTip-aph(6)-Ia plasmid was prepared and transformed into electro-competent cells (Shao et al., 1995) cell using a 2 mm BioRad electrocuvette in the BioRad Gene pulser system with a 2.5 kV pulse. Transformants were grown on LB agar plates containing 35 μg/mL chloramphenicol for 5 days at 30°C. Post selection, several single colonies were selected and inoculated in 100 mL of LB supplemented with 35 μg/mL chloramphenicol for 2-3 days at 30°C until a saturated culture was achieved. The total culture was then diluted 1:10 into 1 L of LB with 35 μg/mL chloramphenicol and 1 μg/mL thiostrepton. The culture was grown at 30°C with shaking at 250 rpm for 16-20 hours. Cells were harvested by centrifugation at 5000 x *g* for 45 minutes, and then resuspended in 30 mL of 0.85% saline and centrifuged again at 10 000 x *g* for 10 minutes and stored at -20°C. For lysis, cells were resuspended in 25 mL of 50 mM HEPES pH 7.5, 300 mM NaCl, 10 mM imidazole, 1 mM phenylmethanesulfonyl fluoride, 1 μg/mL pancreatic bovine DNAse and 2 mg/mL of lysozyme. Cells were incubated for 1 hour on ice and then passed through a T-S series cell disrupter (Constant Systems Inc.) twice at 35,000 psi to create a lysate. The insoluble and soluble fractions were separated by centrifugation at 48,000 x *g* for 30 minutes and purified using a 1 mL Ni-NTA column as described above.

Pyruvate Kinase/Lactate Dehydrogenase Coupled Enzyme Assay. The phosphorylation of antibiotics was monitored by coupling the release of ADP or GDP with pyruvate kinase/lactate dehydrogenase (PK/LDH) (Pon and Bondar, 1967). The oxidization of NADH (ε= 6220 M^{-1} cm^{-1}) was monitored at 340 nm using a SpectraMax microtitre plate reader in a 96-well format. A typical 250 μLreaction contained 50 mM HEPES pH 7.5, 40 mM KCl, 10 mM $MgCl_2$, 0.3 mM NADH, 3.5 mM phophoenolpyruvate, 0.00125 units PK/LDH, 1% DMSO (v/v), antibiotic kinase, antibiotic substrate and nucleotide. The reaction was allowed to incubate for 5 minutes at room temperature in the absence of nucleotide, and then subsequently initiated with nucleotide and monitored for 5 minutes at 340 nm.

Initial rates were determined by utilizing the linear portion of the progress curve and analyzed by nonlinear least squares fitting of eq. 1,

$$v = V_{max}S/(K_M + S) \quad (1)$$

or eq. 2 for substrate inhibited reactions,

$$v = V_{max}S/(K_M + S + S^2/K_i) \quad (2)$$

Kinase inhibitor screening conditions. The assay conditions described above were scaled-down 100 μL to accommodate 384-well plate screening; the nucleotide

concentration was held at a concentration ~ K_m, antibiotic concentration was kept at 2-10 times K_m and the amount of enzyme added was determined empirically such that the reaction was in the linear range for 10 minutes at the fixed drug and nucleotide concentration (Table 4-2). A Z'-score (Zhang et al., 1999) was determined for each of the screening conditions, with high and low controls, as determined by reactions performed in the presence and absence of enzyme respectively, are compared statistically by eq. 3,

$$Z' = 1 - |(3\sigma_{High} + 3\sigma_{Low})/(\mu_{High} - \mu_{Low})| \qquad (3)$$

A Z'-score greater than a value of 0.5 was considered acceptable for screening purposes. A summary of the screening conditions is found in Table 4-2. The screen was conducted in duplicate at two concentrations (10 and 50 μM) of kinase inhibitor from the Screen-Well ™ Kinase Inhibitor library version 2.1 (Enzo Life Sciences/BIOMOL). Hits were assessed by residual activity which is calculated by eq. 4, where v is the velocity of the reaction.

$$\% \text{ Residual Activity} = (v - \mu v_{Low})/(\mu v_{High} - \mu v_{Low})*100 \qquad (4)$$

TABLE 4-2: SCREENING CONDITIONS OF AKS

Enzyme	[Enzyme] (μM)	Nucleotide	[Nucleotide] (μM)	Drug	[Drug] (μM)
APH(2")-Ia	1.06	GTP	5	Gentamicin	200
APH(2")-IIa	0.57	ATP	150	Kanamycin A	200
APH(2")-IIIa	0.29	GTP	25	Kanamycin A	200
APH(2")-IVa	0.34	ATP	200	Kanamycin A	200
APH(3')-Ia	0.19	GTP	100	Kanamycin A	200
APH(3')-IIa	0.34	ATP	50	Kanamycin A	200
APH(3')-IIIa	0.16	ATP	10	Neomycin B	200
APH(3')-Va	0.03	ATP	25	Neomycin B	200
APH(3")-Ia	0.03	ATP	300	Streptomycin	500
APH(4)-Ia	0.05	ATP	40	Hygromycin B	200
APH(6)-Ia	0.90	ATP	50	Streptomycin	200
APH(9)-Ia	0.06	ATP	12.5	Spectinomycin	200
MPHa	0.20	GTP	25	Erythromycin	200
MPHb	1.16	GTP	25	Azithromycin	200

Inhibition Kinetics. A secondary analysis was conducted on hits by assessing the IC_{50} of each compound against each enzyme (data not shown). If the IC_{50} showed dose-response against the activity of the enzyme, a K_i against ATP was conducted in triplicate. The K_i data were fit to one of four models and best fit assessed by Chi^2 values and F-test comparisons in Graffit 4.0.21 (Erithacus Software).

Competitive Inhibition:

$$v = V_{max}S/(K_m*(1 + I/K_i) + S) \quad (5)$$

Mixed Inhibition:

$$v = V_{max}S/(K_m(1+I/K_i) + S(1+I/K_i')) \quad (6)$$

Non-Competitive Inhibition:

$$v = (V_{max}S/(1 + I/K_i))/(K_m+S) \quad (7)$$

Uncompetitive Inhibition:

$$v = (V_{max}S)/(K_m+(S(1+I/K_i))) \quad (8)$$

RESULTS

Phylogeny of AKs. Previous phylogenetic comparisons between AKs were made using neighbour joining trees (Fong et al., 2010; Shaw et al., 1993; Wright and Thompson, 1999) with pair-wise alignment programs such as CLUSTALW (Thompson et al., 1994). These comparisons can be very useful when taking a cursory look at these enzymes to compare their relatedness to one another, but lack the ability to predict evolutionary distance between two members in this family. In order to infer inhibitor susceptibility based on relatedness, we required a more robust analysis of relatedness between AKs, and therefore have constructed a statistically relevant tree of 34 bona fide AKs (Figure 4-1) based upon the alignment in Appendix 2. The antibiotic kinase activity of each selected enzyme has been validated by either *in vivo* and/or *in vitro* activity. The topology of this tree is consistent with functional analysis of these enzymes, in that enzymes with the same regiospecificity have a tendency to group together in the same clade inferring common ancestry during speciation. The majority of probabilities at the nodes are very high (>0.97) with the exception of two points where the APH(3')-II enzymes and APH(4)-I enzymes branch with probabilities of 0.76 and 0.78 respectively. There were also areas where the tree was not fully resolved, namely among the APH(2") enzymes, which produced a polytomy at their node that lacks a probability marked with a star. There are two other polytomies present on this model, one at the node of all APH(3') and APH(3") enzymes and one among the APH(3')-V enzymes, these two nodes have associated probabilities but the order of speciation is unknown.

Michaelis-Menten kinetics of AKs. Of the 34 known AKs from the PKL family, fourteen were selected based on known or predicted diversity of antibiotic and nucleotide substrate specificity, and clinical relevance. All fourteen AKs were overexpressed, purified and quantitatively analyzed for substrate specificity and nucleotide selectivity using a coupled continuous steady state kinetic assay (Appendix 3). A striking trait among some AKs is their ability to utilize GTP in addition to ATP. This activity has only been previously described for the APH(2") subclass of enzymes (Toth et al., 2009), APH(4)-Ia (Stogios et al., 2011), and the MPHs (Shakya and Wright, 2010). This more extensive survey of AKs reveals that this phenomenon is present in a number of AKs, suggesting that these enzymes have a significant level of plasticity towards nucleotide usage.

Another interesting trait among these AKs is their variability in catalytic turnover of antibiotic. Generally it can be noted that enzymes of pathogenic origin with a broad substrate spectrum, tend to have lower k_{cat} values (ie. APH(2"), APH(3') and MPH(2') enzymes) as compared to enzymes from antibiotic producing organisms or enzymes with a narrower substrate spectrum (ie. APH(3')-Va, APH(3")-Ia and APH(9)-Ia). It is unknown whether there is an evolutionary advantage based on antibiotic exposure or if this is an epiphenomenon.

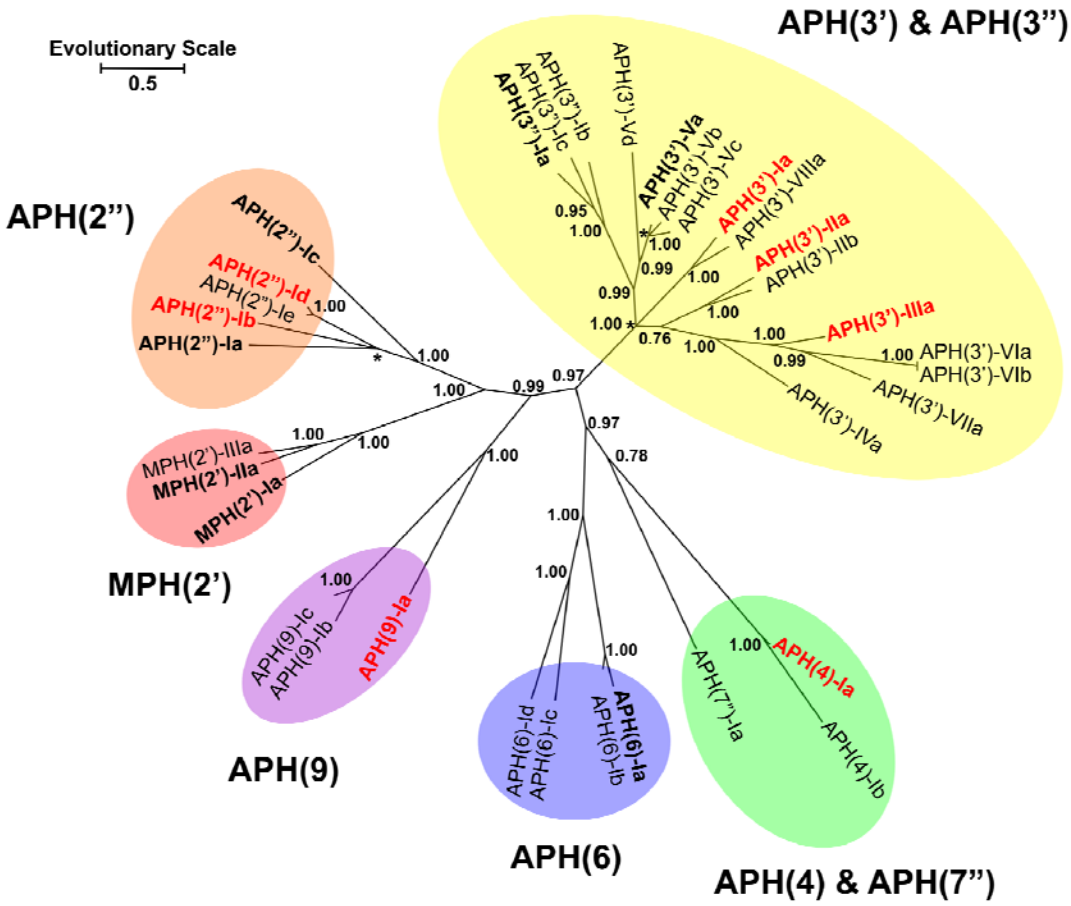

Figure 4-1: Phylogenetic tree of antibiotic kinases. A phylogenetic analysis of 34 bona fide AKs which have been grouped into six major groups: APH(2") – red, APH(3') and APH(3") – yellow, APH(4) and APH(7") – green, APH(6) – blue, APH(9) – purple and MPH(2') – red. Enzymes listed in bold were screened against the Screen-Well™ library, and of those in red represent enzymes with structural data. The evolutionary distances are to scale as stated. A star (*) represents a branch point where a polytomy was observed.

Screening protein kinase inhibitors as inhibitors of AKs. The fourteen AKs were screened against the Screen-Well™ protein kinase inhibitor library, a chemically diverse and well characterized compound collection in order to uncover and assess chemo-selectivity between AKs. The primary screen confirmed our prediction and experience (Daigle et al., 1997) that protein kinase inhibitors would serve as privileged scaffolds for AK inhibitors. We simultaneously conducted the screens at two inhibitor concentrations, (10 and 50 μM) enabling us to rapidly assess dose response for inhibitor-AK pairs (Figure 4-2). The primary screen identified compounds with promiscuous inhibitory action against AKs such as the natural product flavonoids apigenin and quercetin, the anthraquinone damnacanthal and adenosine mimic 5-iodotubericidin, along with narrow specificity compounds such as the tri-substituted imidazole MAP kinase inhibitor SB-203580 that only affects APH(3')-Va and the isoquinoline sulfonamides H8 and H9 that only inhibit APH(3')-IIIa.

Similarly, we found that some enzymes were especially amenable to inhibition, such as APH(2")-IIa from *E. coli*, APH(3')-Ia from *A. baumanii*, APH(3')-Va from the neomycin producer *S. fradiae*, APH(3")-Ia from the streptomycin producer *S. griseus*, APH(4)-Ia from *E. coli* and APH(9)-Ia from *L. pneumophila*. As demonstrated, inhibitor sensitivity/insensitivity was not restricted to a particular class with the exception of the MPHs, which in particular were especially insensitive to most of the inhibitors in this library.

The primary screening data were used to identify candidate compounds for further study based on the following criteria: representative chemical scaffolds, specificity/promiscuity of the inhibitors, and compound potency. Using this diverse selection criteria, 18 inhibitors were selected for follow up studies: apigenin, quercetin, genistein, LY294002, Tyrphostin 25, Tyrphostin 47, Tyrphostin AG1478 (AG1478), GW5074, indirubin-3'-monooxime, Ro-31-8220, olomoucine, PP1, KN-93, SB-202190, BML-259, LFM A13, SP600125 and ZM449829 (Figure 4-3).

Chemical genetic profiling of AKs. The 18 short listed compounds were reexamined using full dose dependency to determine IC_{50} values (not shown). Compound-enzyme pairs that showed tractable behavior for reversible inhibition (dose dependence, slope factor ~1) were further analyzed by determination of the K_i versus ATP to provide a robust and quantitative measure of inhibitor affinity for the enzyme (Appendix 4). We elected to only perform the K_i determination versus ATP since the compounds were largely designed as competitive inhibitors for the ATP binding pocket. Probing this site should prove more useful when comparing enzymes as compared to the antibiotic binding pocket where small changes in sequence can have significant impact on antibiotic selectivity, making this site too sensitive for chemical genetic studies. Indeed the vast majority of compounds were competitive with ATP with the exception of non-competitive behaviour noted for GW5074 vs. MPH(2')-Ia and MPH(2')-IIa, Ro-31-8220 vs. APH(2")-IIIa and APH(3')-Ia, and ZM449829 vs. APH(4)-Ia and APH(9)-Ia.

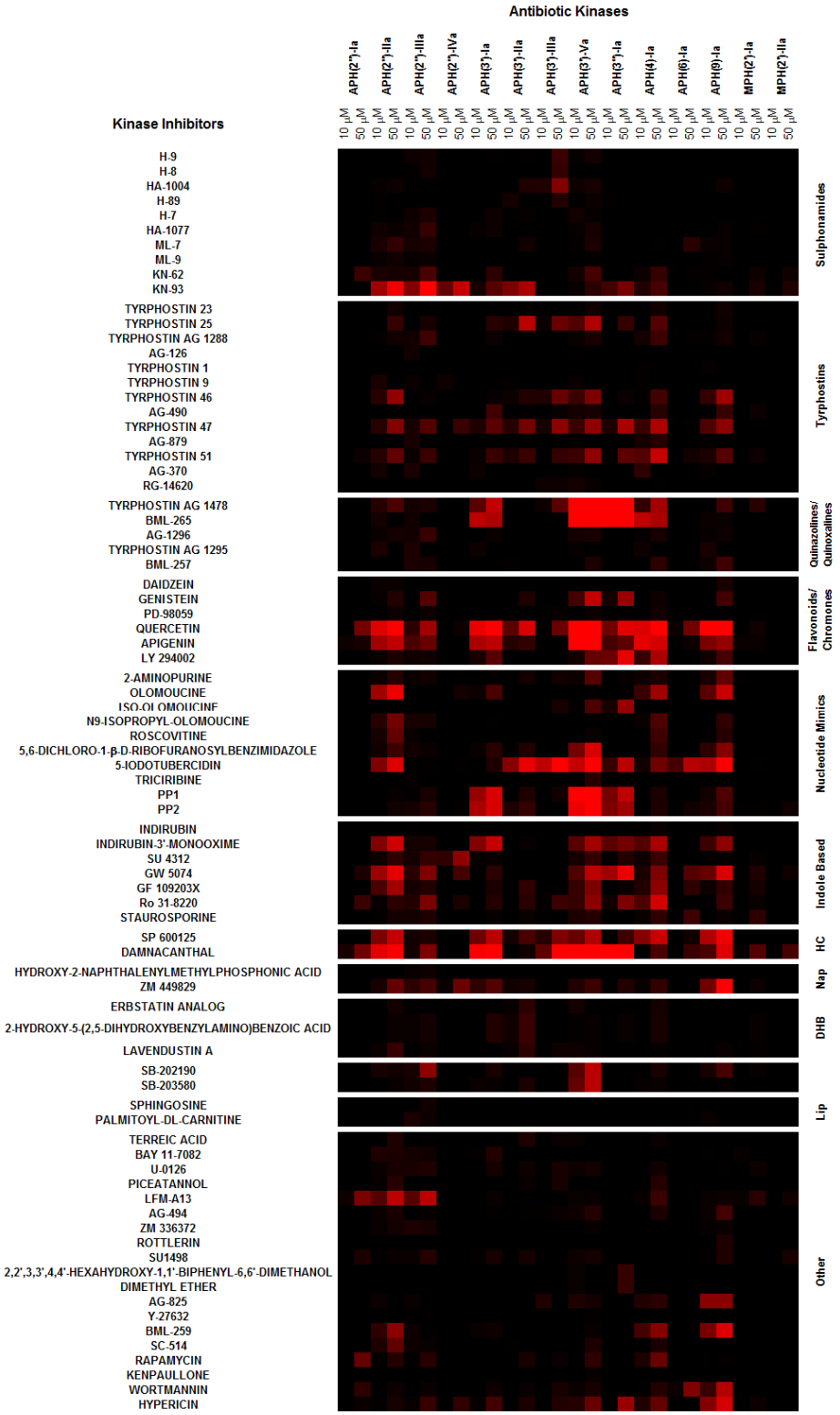

Figure 4-2: Heat plot of primary screening data. A 2-D array of the fourteen AKs against the 80 kinase inhibitors tested from the Screen-Well™ kinase inhibitor library. The average of the residual activities, at both 10 and 50 µM, were plotted and assigned a color based on the potency of the inhibitor. Red denotes complete inhibition and Black is a lack of inhibition. The compounds have been ordered based on relatedness by chemical substructure.

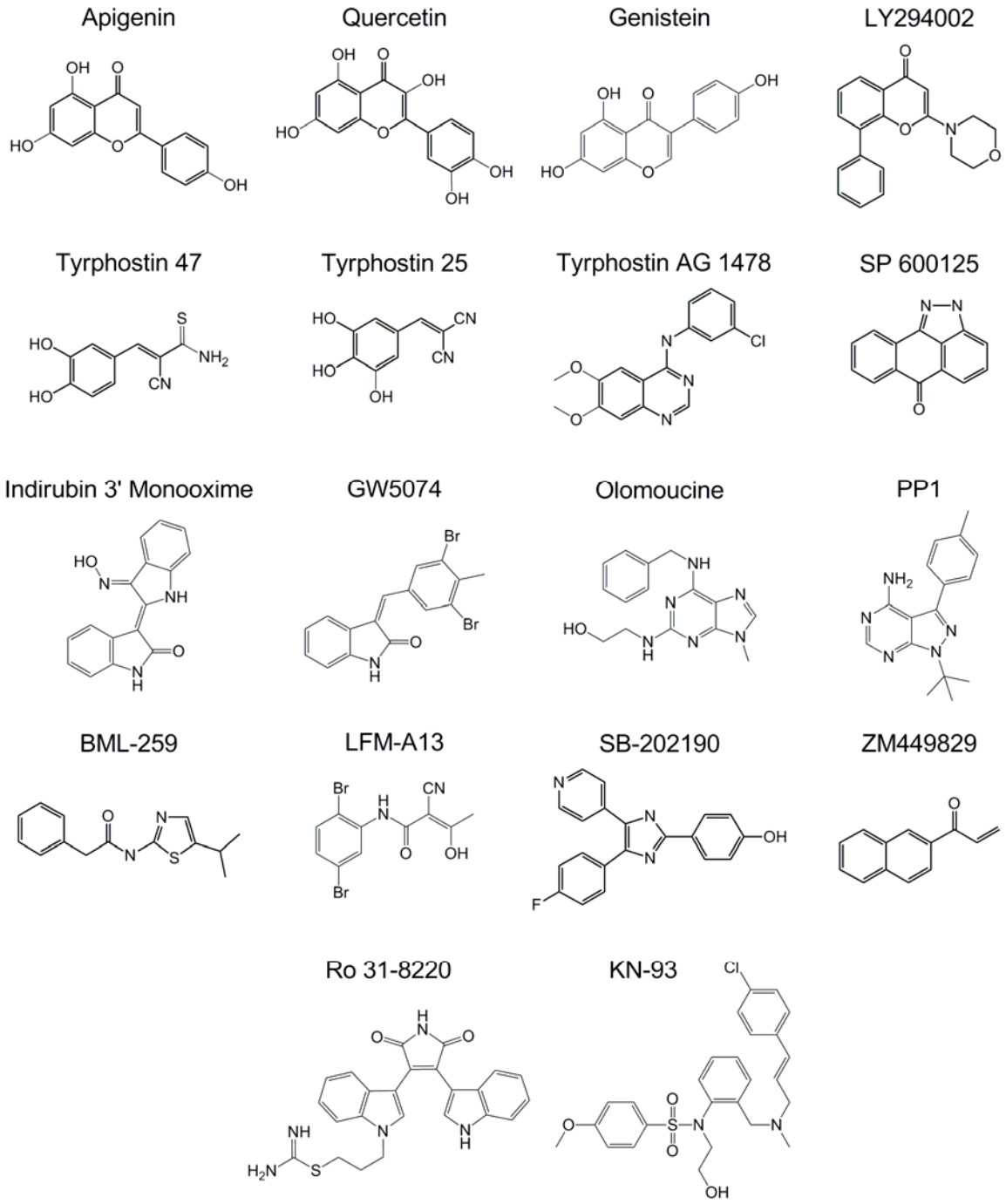

Figure 4-3: Summary of the structures of the 18 selected compounds.

Molecular phylogeny of kinase inhibitors. In a reciprocal analysis, the inhibitory data were correlated to the phylogenetic data by mapping the potency of each compound against each enzyme's respective branch on the phylogenetic tree (Figure 4-4). This cross-analysis revealed several interesting insights into the behavior of the inhibitor-enzyme interactions.

The most striking of the interactions were those that clustered on to specific clades of the tree. Although no single compound showed an absolute clade preference, several compounds were close such as the highly specific Bruton's tyrosine kinase inhibitor LFM-A13 (Mahajan et al., 1999), which showed specificity towards the APH(2") and MPH enzymes. LFM-A13 deviated by additionally inhibiting APH(4)-Ia, which is not surprising since a recent structural analysis of APH(4)-Ia reveals that it shares a high-level of homology with APH(2")-IIa in the nucleotide binding region (Stogios et al., 2011). The isoquinoline sulfonamide KN-93 is also able to weakly inhibit two of the four APH(2") enzymes and both MPH enzymes tested, in addition to APH(3')-Ia and APH(3')-IIa.

Some additional sub-clade specific interactions occurred with PP1 and AG1478 with APH(3')-Ia, APH(3')-Va and APH(3")-Ia, all with low micromolar/high nanomolar affinity. Although these compounds did not inhibit all of the APH(3') enzymes and hit compounds outside of this large family, APH(4)-Ia for AG1478 and APH(9)-Ia for PP1, these compounds may offer an understanding of how these enzymes behave within this sub-clade. The PP1 compounds were all further explored with a structure activity relationship study to determine essential chemical moieties for inhibitory action.

Several compounds were selected from the same compound class to assess potency and structure-activity relationship potential. The first pair selected was Tyrphostin 25 and Tyrphostin 47. Both compounds contain the same benzylidenemalonitrile core; however, Tyrphostin 47 shows a higher level of promiscuity as compared to Tyrphostin 25; specifically, in its ability to inhibit several APH(2") enzymes. This change in specificity could be attributed to lack of the C2-OH or the presence of a thioamide in place of the nitrile group in Tyrphostin 47. In addition to this varied enzyme specificity, K_i analyses support that these compounds are ATP competitive in AKs, which contrasts with their activity against protein tyrosine kinase (PTK) targets, where they have been shown to be competitive with the non-ATP substrate by mimicking the target tyrosine residue (Gazit et al., 1989).

Four flavonoid molecules were also surveyed: the flavone apigenin, the flavonol quercetin, the isoflavone genistein, and the flavan-like chromone LY294002. Genistein showed the least amount of potency and promiscuity, followed by LY294002. However, both apigenin and quercetin showed a high level of potency against several of the targets, with quercetin showing the most promiscuity by targeting 12 of the 14 enzymes tested and apigenin only inhibited five. The principal difference between these two molecules is that quercetin has two hydroxyl groups as compared to apigenin; the C3' position of

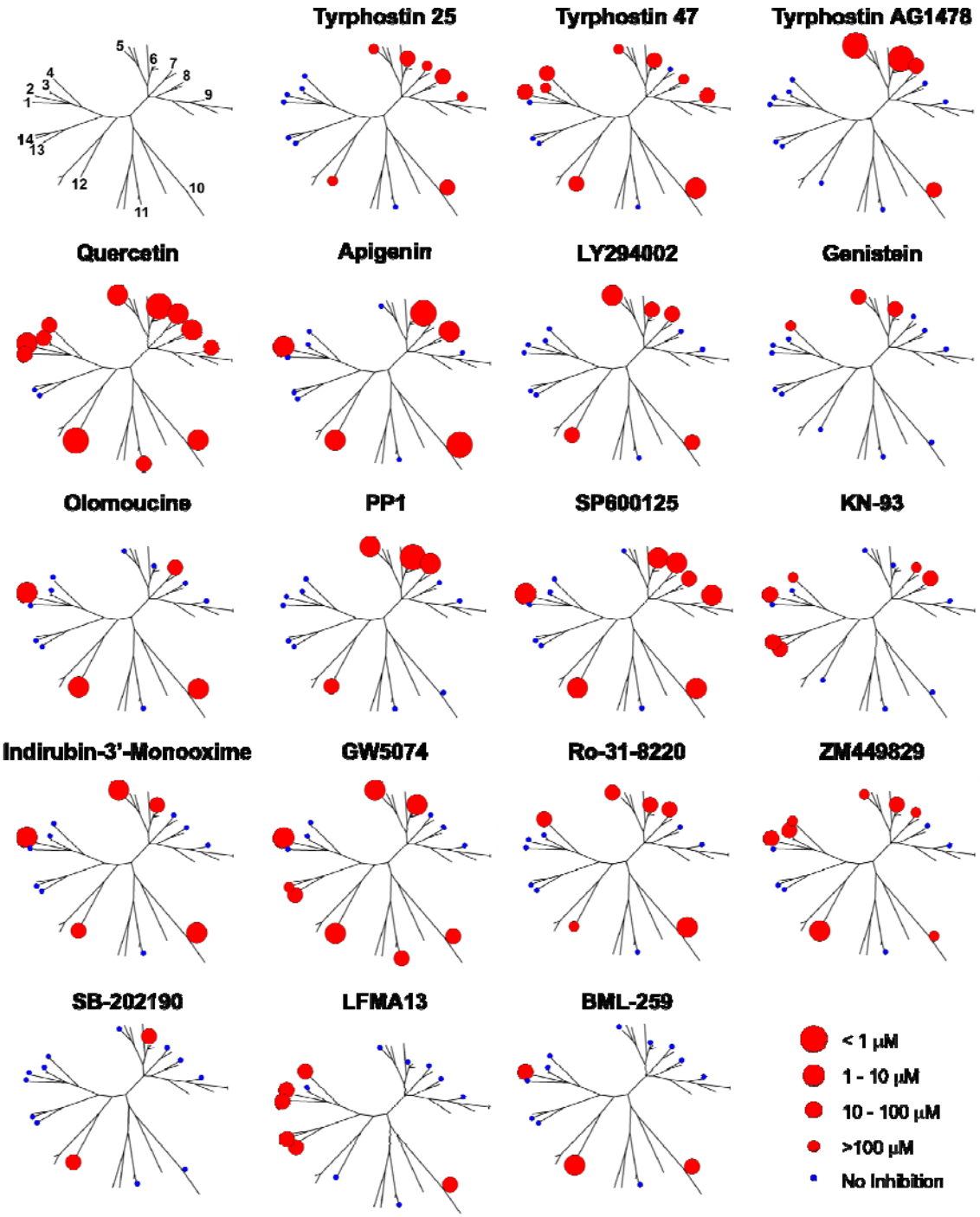

Figure 4-4: Specificity profiles of kinase inhibitors vs. AKs. The K_i of each compound was plotted against each enzyme on the phylogenetic tree. The K_is are graphically represented with a red circle to represent potency, the larger the circle, the lower the associated K_i value, a small blue circle denotes no inhibition. Complete quantitative data can be seen in Appendix 4. Tree legend – 1) APH(2")-Ia, 2) APH(2")-IIa, 3) APH(2")-IVa, 4) APH(2")-IIIa, 5) APH(3")-Ia, 6) APH(3')-Va,7) APH(3')-Ia, 8) APH(3')-IIa, 9) APH(3')-IIIa, 10) APH(4)-Ia, 11) APH(6)-Ia, 12) APH(9)-Ia, 13) MPH(2')-Ia and 14) MPH(2')-IIa.

the C ring and the C3 position of the B ring. The interactions of these molecules were further studied with respect to the structural information received with APH(2")-IVa bound to quercetin (see below).

The remaining molecules showed no particular clade specificity. However, what can be noted is that SP600125, indirubin-3'-monooxime, olomoucine and BML-259 all target APH(2")-IIa, APH(4)-Ia and APH(9)-Ia, a relationship that is obscured by phylogeny. These three enzymes also demonstrated hypersensitivity against the library of inhibitors; this relationship could be due in part to active site promiscuity rather than specific chemical interactions with the aforementioned probes. In addition GW5074 and SP600125 are chemically distinct compounds that show mid to low micromolar affinity for a number of AKs scattered across the entire tree. SP600125 in particular appears have potent activity against all of the APH(3') enzymes.

To focus our efforts to dissect these interactions, we targeted inhibitor-AK interactions where we could gain some structural knowledge of their binding.

Structure of APH(2")-IVa quercetin-kanamycin-bound form. To further investigate the action of these inhibitors versus the AKs, collaboration with Dr. Alexei Savchenko's group was initiated in order to probe the structural biology of these interactions. Based upon a personal communication from Dr. Peter Stogios, a member of Dr. Savchenko's lab, they were successful in solving the structure of APH(2")-IVa in the apo form and with both kanamycin and the flavonol quercetin bound. The apo structure of APH(2'')-IVa most closely resembled the structure of the apo form of this enzyme solved by another group (Toth et al., 2010), with the same space group, very similar unit cell parameters and a root-mean-squared deviation of 0.7 Å over 281 matching Cα atoms.

They were successful in soaking quercetin into crystals of the APH(2'')-IVa-kanamycin complex. Quercetin molecules were built into positive electron density in the nucleotide binding site of both chains in the asymmetric unit, with a third quercetin found between the two chains along the non-crystallographic symmetry axis (Figure 4-5a). The inhibitor interacts with the hinge region of the enzyme, mimicking some interactions and the shape similarity between ATP and APH enzymes. Quercetin forms a number of hydrogen bond contacts, including four to the backbone atoms of the hinge region where ATP binds. ATP itself is only expected to form two bonds in this region. There are additional H-bonds from the C7-OH of quercetin to both of the side chains from Lys-46 and Asp-217, residues involved in coordination of the α and β phosphates of ATP and Mg^{2+} respectively. A final H-bond is made to an ordered water molecule that in turn hydrogen bonds to Glu-60, a residue with a role in positioning Lys-46 to support ATP binding (Figure 4-5b). There are also a number of van der Waals interactions provided by Ile-44, Leu-204 and Ile-216 residues which could also provide hydrophobic interactions with the adenine ring of ATP.

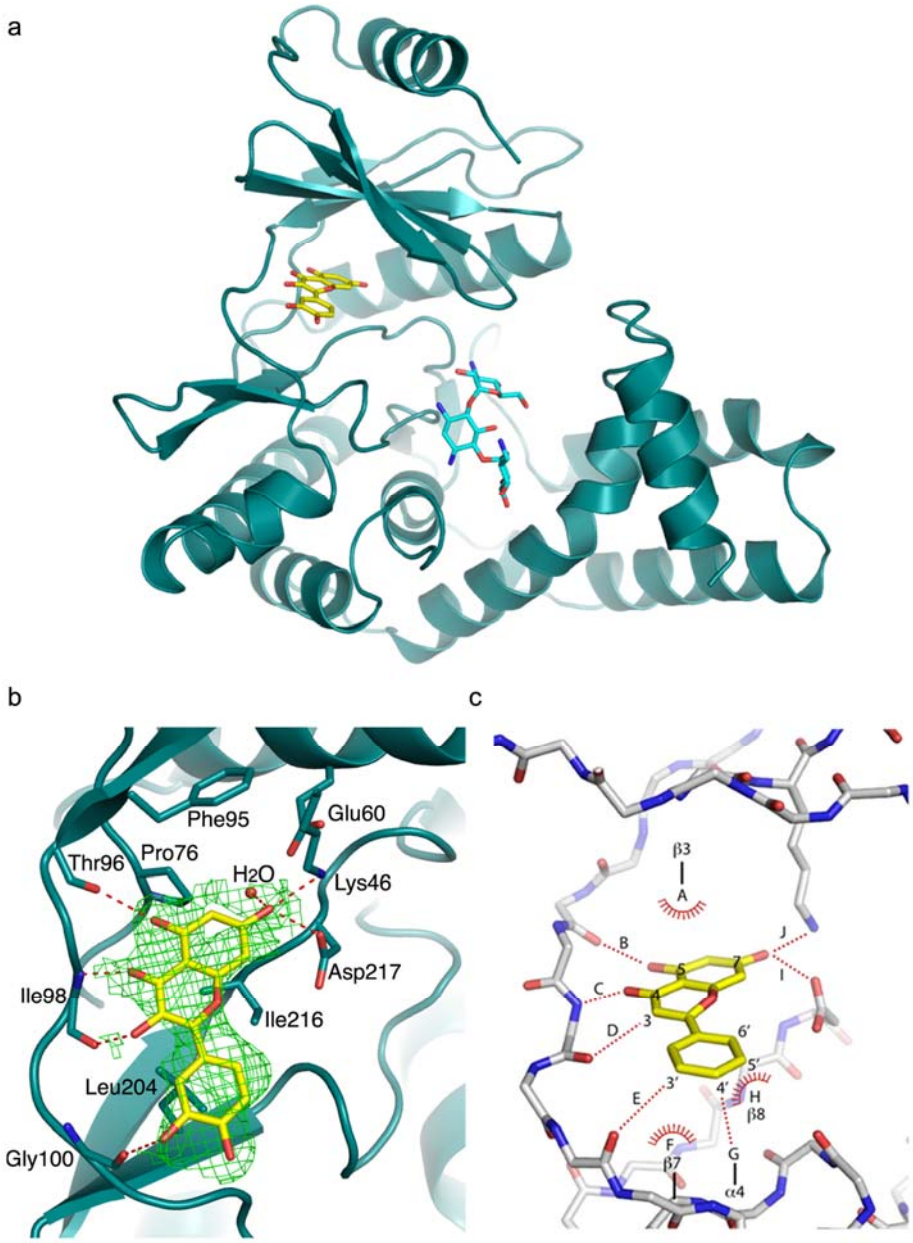

Figure 4-5: Structural analysis of the APH(2")-IVa-kanamycin-quercetin complex. (a) Structure of the APH(2'')-IVa-kanamycin-quercetin complex. (b) Quercetin molecules bound to chain A of APH(2'')-IVa, showing the electron density of the quercetin molecule (green). Side chains forming interactions with the inhibitor are labeled and hydrogen bonds are indicated with dashed red lines. (c) Key interactions between AKs and flavonoids. A generic flavonoid is shown in yellow with numbering in the APH(2'')-IVa quercetin binding site is shown. Interaction sites where the distance between the flavonoid and APH enzyme are within 4 Å are labeled with letters A through J, with H-bonds indicated by dashed red lines and van der Waals interactions indicated by red fans. Secondary structure elements that contribute residues to interactions are labeled as necessary. (Figure courtesy of Dr. P. Stogios)

Structure-activity relationship of flavonoids with APH(2")-IVa. To further elucidate the action of flavonoid binding with APH(2")-IVa, a structure activity relationship analysis was conducted to identify the determinants of flavonoid binding to APH(2")-IVa. Several types of flavonoid molecules were surveyed including: flavans ((+)-catechin, (±)-naringenin), flavones (apigenin, baicalein, luteolin), flavonols (3-hydroxyflavone, kaempferol, quercetin, morin and myricetin) and the isoflavone genistein (Figure 4-5c, Table 4-3).

TABLE 4-3: STRUCTURE ACTIVITY RELATIONSHIP OF FLAVONOID COMPOUNDS

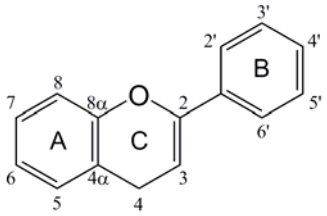

Compound	Position on Flavonoid												K_i
	2	3	4	5	6	7	8	2'	3'	4'	5'	6'	(μM)
Flavans													
(+)-Catechin	H	H, H	H, H	OH	H	OH	H	H	OH	OH	H	H	N.I.
(±)-Naringenin	H	H, H	H, H	OH	H	OH	H	H	H	OH	H	H	N.I.
Flavones													
Baicalein	-	H	O	OH	OH	OH	H	H	H	H	H	H	N.I.
Apigenin	-	H	O	OH	H	OH	H	H	H	OH	H	H	N.I.
Luteolin	-	H	O	OH	H	OH	H	H	OH	OH	H	H	81.3 ± 4.9
Isoflavone													
Genistein	H	*	O	OH	H	OH	H	H	H	OH	H	H	N.I.
Flavonols													
3-Hydroxyflavone	-	OH	O	H	H	H	H	H	H	H	H	H	N.I.
Kaempferol	-	OH	O	OH	H	OH	H	H	H	OH	H	H	108 ± 18
Morin	-	OH	O	OH	H	OH	H	OH	H	OH	H	H	N.I.
Quercetin	-	OH	O	OH	H	OH	H	H	OH	OH	H	H	25.1 ± 3.7
Myricetin	-	OH	O	OH	H	OH	H	H	OH	OH	OH	H	38.6 ± 2.9

N.I. – No Inhibition at highest concentration tested (100 μM)
* B ring is bound at the C3 in isoflavone molecules

The most prominent activity against APH(2")-IVa was seen with the flavones and flavonols. Quercetin and myricetin have similar inhibition kinetics against APH(2")-IVa. Myricetin differs from quercetin only in the addition of a hydroxyl on C5'; this moiety would be exposed to the ribose-binding pocket of the nucleotide binding site, an open space in this structure and would lead to no adverse affects. Luteolin was the only flavone to show a positive interaction with APH(2")-IVa; analogous to quercetin, this flavone only lacks a hydroxyl on C3. The removal of this group causes a loss in interaction D, which reduces the K_i 3-fold. The flavonol kaempferol lacks a hydroxyl moiety missing on C3', compared to quercetin, resulting in a loss in interaction E and a 4-

fold decrease in K_i. The impact of the loss of both interaction D and E is illustrated by apigenin, which shows no activity against APH(2")-IVa. Morin, on the other hand, is a structural isomer of quercetin and would be expected to have similar binding kinetics to that of kaempferol. However, the redistribution of the hydroxyl moiety from C3' to C2' results in a complete loss in activity and it is possible that the C2' hydroxyl produces a steric hindrance with the Cγ1 group of Ile216, which is within 3.4 Å of this group. Additionally, the flavone baicalein also had no interaction with APH(2")-IVa, which is consistent with the fact that it lacks the essential contacts D and E. In addition to this, baicalein has a hydroxyl moiety on C6, which could produce a steric clash with the Phe95 from β3 (refer to Figure 4-5c).

The lack of activity of apigenin versus APH(2")-IVa was somewhat surprising, since the closest structural relative of this enzyme, APH(2")-IIa, showed a high level of sensitivity to apigenin in molecular phylogenetic analysis. To resolve this discrepancy, a superposition of the quercetin-bound APH(2")-IVa and the structure of APH(2")-IIa was conducted. The superposition suggested that the differential activity of apigenin was due to the presence of Arg92 in APH(2")-IIa which could be capable of forming interaction "G" with the C4'-OH of apigenin, this is in contrast to the Pro102 in APH(2")-IVa which would not form this interaction. This suggests that the lack of interactions D and E could be compensated by the presence of interaction G with the C4'-OH.

Of the remaining compounds studied, none of the flavans (catechin and naringenin) showed any activity against APH(2")-IVa, which may reflect that the carbonyl on C4 is essential to flavonoid binding, a loss in interaction C, or that the chiral center at C2 creates an unfavorable conformation of the flavonoid disallowing binding in the hinge region. 3-hydroxyflavone contains the 4-carbonyl oxygen but lacks the C5 and C7 hydroxyls, suggesting one or both of these hydroxyl groups are critical for inhibition. The isoflavone genistein also showed no interaction against APH(2")-IVa, this is clearly due to the positioning of ring B at C3 versus C2 as seen in quercetin. This movement of the ring is predicted to sterically interfere with the hinge region of the enzyme destabilizing its interaction.

Interrogating pyrazalo-pyrimidines as selective inhibitors of AKs using a structure-activity relationship (SAR). During the screen, two pyrazalo-pyrimidines (PPs), PP1 and PP2, were determined to be semi-selective inhibitors of APH(3')-Ia, APH(3')-Va, APH(3")-Ia and APH(9)-Ia. PP1 and PP2 were originally found to be highly potent inhibitors of the Src family of non-receptor tyrosine kinases, suggesting that this scaffold lacks promiscuity against most eukaryotic protein kinases. The Src-family kinases (SFKs) are important in cancer biology due to their proto-oncogene capacity to progress apoptosis, proliferation, cell adhesion, cell migration, angiogenesis and metastasis of solid tumours. There are nine types of SFKs known, c-Src, Yes, Fyn, Lyn, Lck, Hck, Fgr, Blk and Yrk, making them a relatively small class of protein kinases (Kim et al., 2009). A recent survey of 3800 compounds against a panel 172 kinases confirmed that PP1 and PP2 have nanomolar affinity against most of the SFKs and have micromolar

affinity against some of the other RTKs like RET, BTK and EPHA2 (Metz et al., 2011). With the knowledge of this high selectivity against SFKs, we designed novel inhibitors of AKs based on the PP1 and PP2 scaffold to reduce fidelity against SFKs and increase binding for the selected AK targets.

Crystal structures of PP1 and PP2 in complex with Hck, Lyn and Lck have been solved and all reveal the same highlights: the main purine moiety binds in same plane as adenosine, the *t*-butyl group occupies the same space as the ribose sugar and the *para*-substituted phenyl moiety extends into a unique hydrophobic pocket found in SFKs (Schindler et al., 1999; Williams et al., 2009; Zhu et al., 1999) (Figure 4-6a-c). Our collaborators, Dr. Peter Stogios and Dr. Alexei Savchenko, have solved the structure of APH(3')-Ia in complex with ATP (personal communication) where they found a small hydrophobic pocket which could accommodate the *para*-substituted phenyl moiety and modeled PP1 into this space which follows PP1 binding as seen in Hck, Lck and Lyn (Figure 4-6d). Using this strictly as a model and not drawing too many inferences from it, we pursued novel compounds based on these PP scaffolds in an effort to increase their specificity for AK targets. In collaboration with Dr. Fred Capretta and Nick Todorovic, we were supplied 23 novel PP compounds (Appendix 5) to determine theSAR of these compounds. The PP compounds were tested against the four aforementioned AKs with a preliminary IC_{50} analysis. From these data, thirteen compounds were selected based on chemical diversity and inhibitory action and further analyzed via K_i determinations. The data were organized to show progressive substitutions at the R_1 and R_2 groups using four themes: butyl isomers, hydrocarbon substitutions, chloro-phenyl isomers and substituted phenyl groups (Table 4-4).

All four sets of compounds revealed a number of similarities and differences in affinity. Two sets of compounds were designed with modification at the N1 atom, there were the butyl isomers and hydrocarbon chain substitutions. Starting with the butyl isomers, APH(3')-Ia showed a 5-fold higher affinity for the tert-butyl isomer (PP2) over the linear butyl form (compound **11**), whereas, APH(9)-Ia showed the opposite trend of a 9-fold higher affinity for the butyl form (**11**) over the tert-butyl (PP2). Both APH(3')-Va and APH(3")-Ia showed negligible preferences with all of the K_i values falling within a single order of magnitude. Non-substitution at N1 (**14**) had a negative effect on all of the AKs tested, APH(3')-Ia, APH(3")-Va and APH(9)-Ia, showed a preference for methyl variant (**13**). However, both APH(3')-Va and APH(9)-Ia were able to accept up to a hexyl group at N1 (**12**) as compared to APH(3')-Ia and APH(3")-Ia showed considerably lower susceptibility to longer carbon chain substitutions (**11** & **12**).

The next two sets of compounds looked at the effect of phenyl group substitution at C3 by first looking at chloro-phenyl isomers and other substituted moieties. APH(3')-Ia, APH(3')-Va and APH(3")-Ia all showed the highest affinity for the *para*-chloro form (**10**), with APH(3')-Ia showing an almost equal affinity for the *meta*-chloro form (**16**) and APH(9)-Ia showed the highest affinity for the *meta*-chloro (**16**). The different phenyl

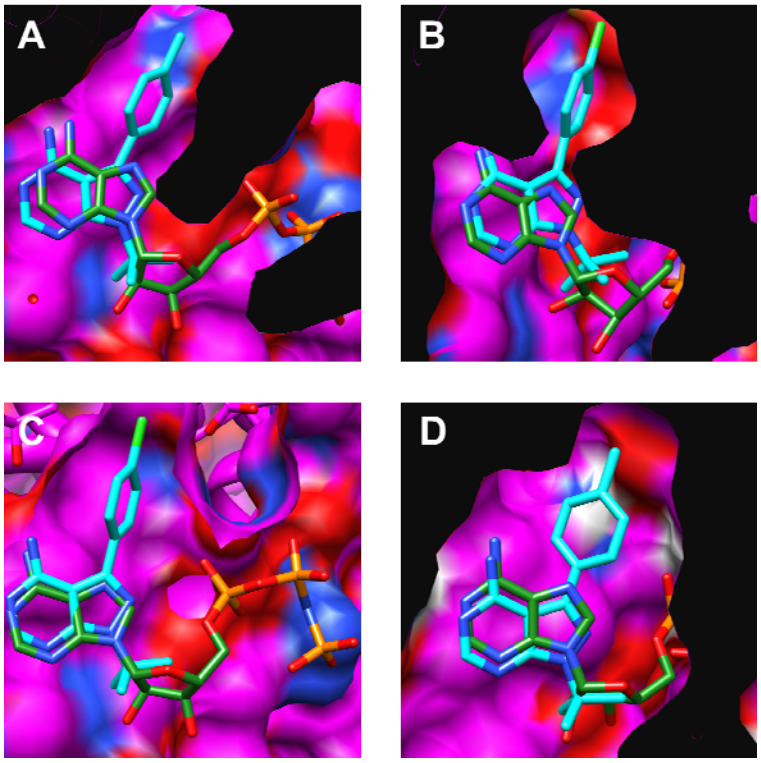

Figure 4-6: Comparison of PP1/PP2 bound crystal structures. Here a selected panel of Src kinases have been shown with PP1/PP2 bound compared to the model of APH(3')-Ia bound to PP1. a) Hck bound to PP1 (PDB# 1QCF) superimposed with the Hck bound to AMPPNP (PDB# 1AD5), b) Lck bound to PP2 (PDB# 1QPE) superimposed with the Lck bound to AMPPNP (PDB# 1QPC), c) Lyn bound to PP2 (PDB# 2ZV9) superimposed with the Lyn bound to AMPPNP (PDB# 2ZV8) and d) Structure of APH(3')-Ia with ATP bound (2.29 Å) superimposed with a model of APH(3')-Ia with PP1 bound in the active site with optimized energy minimization using the CNS software (Brunger et al., 1998). Structure superpositions were conducted using the UCSF Chimera software (Pettersen et al., 2004). Images were rendered with Chimera and show the enzyme surface features one with a cross-section of the binding site with surfaces capped in black.

substituted moieties did not reveal anything striking as would be expected with the variety of substitutions tested. APH(3')-Ia and APH(3")-Ia both had the same affinity for almost of phenyl substitutions tested varying in between 1-2 fold difference in K_i; APH(9)-Ia maintained its lower affinity for the *para*-substituted group showing its highest affinity for the unsubstituted phenyl group (**5**); and APH(3')-Va showed the highest affinity for the 3,4-dichlorophenyl group (**18**).

TABLE 4-4: KI DATA OF PYRAZOLO-PYRIMIDINES

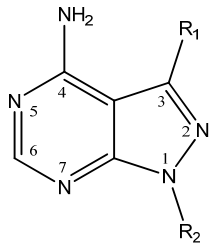

Compound	R_1	R_2	K_i (μM)			
			APH(3')-Ia	APH(3')-Va	APH(3")-Ia	APH(9)-Ia
Butyl Isomers						
PP2	*para*-Cl	*tert*-butyl	6.23 ± 0.45	1.15 ± 0.09	3.82 ± 0.20	57.8 ± 3.4
10	*para* -Cl	*sec*-butyl	22.0 ± 1.0	0.84 ± 0.05	5.31 ± 0.34	12.0 ± 0.7
11	*para* -Cl	butyl	33.7 ± 5.2	0.95 ± 0.04	7.04 ± 0.46	6.56 ± 0.21
Linear Hydrocarbon Substitutions						
14	*para* -Cl	hydrogen	24.6 ± 2.3	4.06 ± 0.20	25.0 ± 2.9	3.25 ± 0.13
13	*para* -Cl	methyl	8.81 ± 0.94	1.56 ± 0.07	4.48 ± 0.43	1.69 ± 0.09
11	*para* -Cl	butyl	33.7 ± 5.2	0.95 ± 0.04	7.04 ± 0.46	6.56 ± 0.21
12	*para* -Cl	hexyl	93.2 ± 20.0	2.35 ± 0.09	25.9 ± 1.4	3.43 ± 0.15
Chloro-phenyl Isomers						
10	*para* -Cl	*sec*-butyl	22.0 ± 1.0	0.84 ± 0.05	5.31 ± 0.34	12.0 ± 0.7
16	*meta*-Cl	*sec*-butyl	22.7 ± 2.1	1.25 ± 0.05	14.8 ± 2.2	3.74 ± 0.71
17	*ortho*-Cl	*sec*-butyl	43.5 ± 3.6	3.2 ± 0.30	16.4 ± 1.0	26.3 ± 1.8
Substituted Phenyl Groups						
5	phenyl	*sec*-butyl	25.5 ± 3.1	1.59 ± 0.03	15.4 ± 1.5	3.46 ± 0.13
7	*para* -Me	*sec*-butyl	20.7 ± 0.9	0.96 ± 0.03	7.65 ± 0.30	16.4 ± 1.2
19	*para* -F	*sec*-butyl	21.6 ± 1.6	2.04 ± 0.10	12.0 ± 0.7	8.78 ± 0.79
10	*para* -Cl	*sec*-butyl	22.0 ± 1.0	0.84 ± 0.05	5.31 ± 0.34	12.0 ± 0.7
20	*para* -Br	*sec*-butyl	48.9 ± 6.6	2.46 ± 0.13	7.15 ± 0.29	44.1 ± 2.1
21	*para* -OMe	*sec*-butyl	24.2 ± 2.1	2.52 ± 0.12	8.16 ± 0.51	15.9 ± 0.8
18	3,4-dichloro	*sec*-butyl	48.4 ± 6.3	0.50 ± 0.03	13.4 ± 1.7	16.4 ± 0.7

Overall, APH(3')-Ia, APH(3')-Va and APH(3")-Ia share similar trends with a preference for a bulkier branched substituent at N1 and *para*-substituted phenyl group at C3, and APH(9)-Ia opposes this with a preference for a linear substituent at N1 and either a ortho or non-substituted phenyl group at C3. This clustering of data is in accordance with the phylogenetic data showing APH(3')-Ia, APH(3')-Va and APH(3")-Ia belonging to a single family with common origin as compared to APH(9)-Ia which shows a more distant relationship to the previous three enzymes.

DISCUSSION

The global spread of antibiotic resistance has created an urgent need for novel antimicrobial therapies. Using the hypothesis that novel chemical scaffolds as antimicrobial compounds have been exhausted (Payne et al., 2007), we look at new strategies to combat microorganisms, such as targeting the resistance mechanisms. Here we focus on the study of AKs to understand their potential as targets for future therapies. The phylogeny of AKs has revealed that these somewhat divergent sequences are tightly related by several signature sequences which have been previously reported (Kannan et al., 2007; Scheeff and Bourne, 2005). The phylogenetic tree presented here validates the hypothesis that AK enzymes with similar regio and substrate specificities are indeed related and have divergent sequences due to radiation of species and evolutionary selection.

We have additionally compared these AKs using a small molecule-kinase interaction map using a traditional robust kinase assay to determine the dissociation constant for each interaction as compared to their genetic phylogeny. Using a common and robust activity assay not only confirms binding of the compound, it validates inhibition allowing us to report the value K_i instead K_d. Using the molecular phylogeny of these AKs, we can better understand the mechanism of action of these enzymes by first realizing their susceptibilities to various compounds and correlating these interactions to specific residues and motifs when compared to structural data.

Flavonoids as inhibitors of antibiotic resistance. The therapeutic potential of flavonoids is very high. Flavonoids are ubiquitous in nature and have been sourced from a number of plants, trees, fruits and vegetables. They have been found to be the active agent in many traditional medicines which has led several researchers to focus on their action. Recent literature boasts the use of flavonoids for their anti-oxidative effects (Woodman and Chan, 2004), ability to curb hypertension (Perez-Vizcaino et al., 2009), anticancer (Teillet et al., 2008) and antimicrobial action (Cushnie and Lamb, 2005). This wide range of effects would suggest that flavonoids are promiscuous in their action and could pose a threat as toxic agents (Galati and O'Brien, 2004). Although they are indeed promiscuous and their overuse and abuse could lead to undesired side effects, their therapeutic potential is large and should not be dismissed.

The antimicrobial effects of flavonoids have been well documented and reviewed (Cushnie and Lamb, 2005; Ozcelik et al., 2011). Two of the flavonoids used in this study, apigenin and quercetin, have been shown to inhibit the growth of methicillin-resistant *Staphylococcus aureus* (Sato et al., 2000) and inhibit bacterial growth by targeting DNA gyrase (Plaper et al., 2003), respectively.

Here we documented the use of flavonoids as inhibitors of AKs and have additionally solved the crystal structure of APH(2")-IVa bound to both kanamycin and the flavonol quercetin. We were able to resolve several key contacts required for

quercetin binding to the APH(2")-IVa active site and related them to inhibitory action of other flavonoid molecules. Although the indispensability of interactions D and E in APH(2")-IVa was determined, it was found that apigenin was an inhibitor for the closely related APH(2")-IIa, but not for APH(2")-IVa since it lacked the D and E contacts. A structural comparison revealed that APH(2")-IIa may form a novel contact G between the C4'-OH and Arg-92 which could override the necessity of contacts D and E. These findings validate that quercetin is a true inhibitor of AKs and the inhibition observed by quercetin is not the result of the formation of non-specific aggregates as demonstrated by other studies (McGovern and Shoichet, 2003).

Although we have not demonstrated an *in vivo* application of a flavonoid – aminoglycoside (FL-AG) therapy, there have been several studies previously conducted which have demonstrated their synergistic action together. One study has focused in on the synergy of the flavonoid baicalein and gentamicin in vancomycin-resistant *Enterococci* (VRE) (Chang et al., 2007). Approximately 69-71% of *E. faecalis* and *E. faecium* strains have been shown to have high-level aminoglycoside resistance and 40% of VRE strains (Linden, 2007), this resistance can be mediated via AKs. This study in particular demonstrated the ability of baicalein to lower gentamicin resistance 8-30 fold in four different strains of VRE *in vitro*. Although our preliminary studies did not show baicalein to directly inhibit any of the APHs in this study, this observation offers an example of FL-AG synergy in a resistant host. Animal models have also demonstrated the reduction in nephrotoxicity caused by gentamicin when co-administered with the flavonol quercetin due to its antioxidant properties, displaying another beneficial property of a FL-AG co-therapy (Abdel-Raheem et al., 2009). Quercetin already is being used as a nutraceutical and can be taken in doses as high 500-1000 mg/day with no observable toxic side effects (Bischoff, 2008). These observations FL-AG therapy provide support for a possible clinical application.

Kinase inhibitors that target phylogeny. The most compelling inhibitor-enzyme interactions were those that supported phylogeny, as seen with LFM A13, KN-93, PP1 and AG1478. All four of these molecules have been described as being highly specific against their intended ePK targets, however here we show that they can additionally target specific clades of AKs with high nanomolar to micromolar affinity.

We have further explored the effects of 14 PP compounds in addition to PP1 to elucidate the action of these molecules in the hopes of finding an AK selective variant of these molecules. It has been made evident that the chemical space we probed did not significantly impair or improve the action of these molecules. However, the compounds did reveal an important phylogenetic relationship. We observed that compounds that had a potent effect on closely related APH(3')-Ia, APH(3')-Va and APH(3")-Ia tended to have an opposite effect on the distantly related APH(9)-Ia, another AK that was susceptible to the action of PP1. Specifically, APH(9)-Ia preferred substitution at the N1 group with longer unbranched hydrocarbon chains versus smaller branched chains and no

substitution on the phenyl moiety, which is the exact opposite of what was observed for the APH(3') sub-clade.

Since, the completion of this preliminary work, our collaborators were successful in solving PP1 bound to APH(3')-Ia. This structure conflicted with the original model we had proposed (Figure 4-7). The fully resolved structure reveals that PP1 does not share the exact same binding mode as ATP; instead the molecule has a flipped orientation within the active site with the *t*-butyl moiety occupying the hydrophobic pocket and the phenyl moiety occupying the ribose-binding pocket. This would explain why *t*-butyl substitution was preferred by APH(3')-Ia and not the more linear hydrocarbon chains since they were constrained to the smaller hydrophobic pocket. Using this new structural data, a second set of compounds can be produced around this more definitive structure of PP1 bound to the APH(3')-Ia active site. In addition to the construction of new molecules, we need to counter screen them against a panel of Src kinases to establish the loss of activity against the original eukaryotic targets.

Conclusions. These comparative and collaborative studies help us understand the true relationship between these somewhat loosely related AKs. The end goal is to develop new molecules to target AKs; however, by looking at existing kinase inhibitor scaffolds, we are afforded the opportunity to re-purpose these compounds as adjuvants of antibiotics in a resistant host. Understanding the interaction of these molecules against a comprehensive collection of AKs increases the chance of discovering a broad-spectrum therapy, or the coveted mono-therapy against all AKs.

We conclude that in general, this kinase screen predicts similar chemical genetic profiles to those that are predicted based on molecular phylogeny. Therefore, inhibitor screening can be a valuable orthogonal tool when investigating new AKs and predicting behavior from sequence analysis.

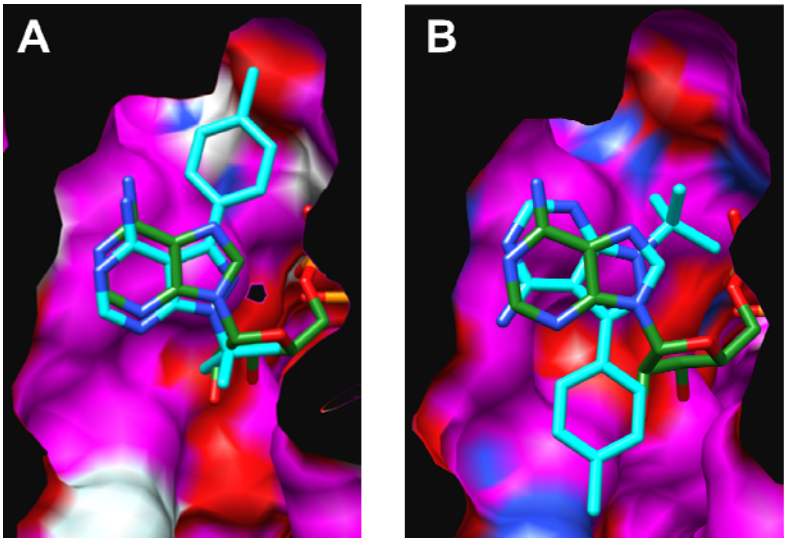

Figure 4-7: Comparison of the model and structure of APH(3')-Ia bound to PP1. a) Structure of APH(3')-Ia with ATP (2.29 Å) bound superimposed with a model of APH(3')-Ia with PP1 bound in the active site with optimized energy minimization using the CNS software (Brunger et al., 1998). b) Solved structure of APH(3')-Ia bound to PP1 and kanamycin (1.84 Å), superimposed with the solved structure of APH(3')-Ia bound to ATP (2.29 Å). Superpositions were conducted using the UCSF Chimera software (Pettersen et al., 2004). Images were rendered with Chimera and show the enzyme surface features one with a cross-section of the binding site with surfaces capped in black.

REFERENCES

Abdel-Raheem, I.T., Abdel-Ghany, A.A., and Mohamed, G.A. (2009). Protective effect of quercetin against gentamicin-induced nephrotoxicity in rats. Biol Pharm Bull *32*, 61-67.

Akova, M., Yang, Y., and Livermore, D.M. (1990). Interactions of tazobactam and clavulanate with inducibly- and constitutively-expressed Class I beta-lactamases. J Antimicrob Chemother *25*, 199-208.

Altekar, G., Dwarkadas, S., Huelsenbeck, J.P., and Ronquist, F. (2004). Parallel Metropolis coupled Markov chain Monte Carlo for Bayesian phylogenetic inference. Bioinformatics *20*, 407-415.

Baltz, R.H. (2006). Marcel Faber Roundtable: is our antibiotic pipeline unproductive because of starvation, constipation or lack of inspiration? J Ind Microbiol Biotechnol *33*, 507-513.

Bischoff, S.C. (2008). Quercetin: potentials in the prevention and therapy of disease. Curr Opin Clin Nutr Metab Care *11*, 733-740.

Boehr, D.D., Lane, W.S., and Wright, G.D. (2001). Active site labeling of the gentamicin resistance enzyme AAC(6')-APH(2") by the lipid kinase inhibitor wortmannin. Chem Biol *8*, 791-800.

Brunger, A.T., Adams, P.D., Clore, G.M., DeLano, W.L., Gros, P., Grosse-Kunstleve, R.W., Jiang, J.S., Kuszewski, J., Nilges, M., Pannu, N.S., *et al.* (1998). Crystallography & NMR system: A new software suite for macromolecular structure determination. Acta Crystallogr D Biol Crystallogr *54*, 905-921.

Chang, P.C., Li, H.Y., Tang, H.J., Liu, J.W., Wang, J.J., and Chuang, Y.C. (2007). In vitro synergy of baicalein and gentamicin against vancomycin-resistant Enterococcus. J Microbiol Immunol Infect *40*, 56-61.

Chow, J.W., Zervos, M.J., Lerner, S.A., Thal, L.A., Donabedian, S.M., Jaworski, D.D., Tsai, S., Shaw, K.J., and Clewell, D.B. (1997). A novel gentamicin resistance gene in Enterococcus. Antimicrob Agents Chemother *41*, 511-514.

Cushnie, T.P., and Lamb, A.J. (2005). Antimicrobial activity of flavonoids. Int J Antimicrob Agents *26*, 343-356.

D'Costa, V.M., McGrann, K.M., Hughes, D.W., and Wright, G.D. (2006). Sampling the antibiotic resistome. Science *311*, 374-377.

Daigle, D.M., McKay, G.A., and Wright, G.D. (1997). Inhibition of aminoglycoside antibiotic resistance enzymes by protein kinase inhibitors. J Biol Chem *272*, 24755-24758.

Distler, J., Ebert, A., Mansouri, K., Pissowotzki, K., Stockmann, M., and Piepersberg, W. (1987). Gene cluster for streptomycin biosynthesis in Streptomyces griseus:

nucleotide sequence of three genes and analysis of transcriptional activity. Nucleic Acids Res *15*, 8041-8056.

Eddy, S.R. (2008). A probabilistic model of local sequence alignment that simplifies statistical significance estimation. PLoS Comput Biol *4*, e1000069.

Edgar, R.C. (2004). MUSCLE: multiple sequence alignment with high accuracy and high throughput. Nucleic Acids Res *32*, 1792-1797.

Fabian, M.A., Biggs, W.H., 3rd, Treiber, D.K., Atteridge, C.E., Azimioara, M.D., Benedetti, M.G., Carter, T.A., Ciceri, P., Edeen, P.T., Floyd, M., *et al.* (2005). A small molecule-kinase interaction map for clinical kinase inhibitors. Nat Biotechnol *23*, 329-336.

Fischbach, M.A., and Walsh, C.T. (2009). Antibiotics for emerging pathogens. Science *325*, 1089-1093.

Fong, D.H., Lemke, C.T., Hwang, J., Xiong, B., and Berghuis, A.M. (2010). Structure of the antibiotic resistance factor spectinomycin phosphotransferase from Legionella pneumophila. J Biol Chem *285*, 9545-9555.

Fournier, P.E., Vallenet, D., Barbe, V., Audic, S., Ogata, H., Poirel, L., Richet, H., Robert, C., Mangenot, S., Abergel, C., *et al.* (2006). Comparative genomics of multidrug resistance in Acinetobacter baumannii. PLoS Genet *2*, e7.

Galati, G., and O'Brien, P.J. (2004). Potential toxicity of flavonoids and other dietary phenolics: significance for their chemopreventive and anticancer properties. Free Radic Biol Med *37*, 287-303.

Gazit, A., Yaish, P., Gilon, C., and Levitzki, A. (1989). Tyrphostins I: synthesis and biological activity of protein tyrosine kinase inhibitors. J Med Chem *32*, 2344-2352.

Hon, W.C., McKay, G.A., Thompson, P.R., Sweet, R.M., Yang, D.S., Wright, G.D., and Berghuis, A.M. (1997). Structure of an enzyme required for aminoglycoside antibiotic resistance reveals homology to eukaryotic protein kinases. Cell *89*, 887-895.

Hugonnet, J.E., Tremblay, L.W., Boshoff, H.I., Barry, C.E., 3rd, and Blanchard, J.S. (2009). Meropenem-clavulanate is effective against extensively drug-resistant Mycobacterium tuberculosis. Science *323*, 1215-1218.

Kannan, N., Taylor, S.S., Zhai, Y., Venter, J.C., and Manning, G. (2007). Structural and functional diversity of the microbial kinome. PLoS Biol *5*, e17.

Kim, L.C., Song, L., and Haura, E.B. (2009). Src kinases as therapeutic targets for cancer. Nat Rev Clin Oncol *6*, 587-595.

Knight, Z.A., Lin, H., and Shokat, K.M. (2010). Targeting the cancer kinome through polypharmacology. Nat Rev Cancer *10*, 130-137.

Labia, R., Morand, A., Lelievre, V., Mattioni, D., and Kazmierczak, A. (1986). Sulbactam: biochemical factors involved in its synergy with ampicillin. Rev Infect Dis *8 Suppl 5*, S496-502.

Leigh, D.A., Bradnock, K., and Marriner, J.M. (1981). Augmentin (amoxycillin and clavulanic acid) therapy in complicated infections due to beta-lactamase producing bacteria. J Antimicrob Chemother *7*, 229-236.

Lemke, C.T., Hwang, J., Xiong, B., Cianciotto, N.P., and Berghuis, A.M. (2005). Crystallization and preliminary crystallographic analysis of an aminoglycoside kinase from Legionella pneumophila. Acta Crystallogr Sect F Struct Biol Cryst Commun *61*, 606-608.

Linden, P.K. (2007). Optimizing therapy for vancomycin-resistant enterococci (VRE). Semin Respir Crit Care Med *28*, 632-645.

Livermore, D.M., Mushtaq, S., Warner, M., Miossec, C., and Woodford, N. (2008). NXL104 combinations versus Enterobacteriaceae with CTX-M extended-spectrum beta-lactamases and carbapenemases. J Antimicrob Chemother *62*, 1053-1056.

Mahajan, S., Ghosh, S., Sudbeck, E.A., Zheng, Y., Downs, S., Hupke, M., and Uckun, F.M. (1999). Rational design and synthesis of a novel anti-leukemic agent targeting Bruton's tyrosine kinase (BTK), LFM-A13 [alpha-cyano-beta-hydroxy-beta-methyl-N-(2, 5-dibromophenyl)propenamide]. J Biol Chem *274*, 9587-9599.

McGovern, S.L., and Shoichet, B.K. (2003). Kinase inhibitors: not just for kinases anymore. J Med Chem *46*, 1478-1483.

McKay, G.A., Thompson, P.R., and Wright, G.D. (1994). Broad spectrum aminoglycoside phosphotransferase type III from Enterococcus: overexpression, purification, and substrate specificity. Biochemistry *33*, 6936-6944.

Metz, J.T., Johnson, E.F., Soni, N.B., Merta, P.J., Kifle, L., and Hajduk, P.J. (2011). Navigating the kinome. Nat Chem Biol.

Miller, J.R., Dunham, S., Mochalkin, I., Banotai, C., Bowman, M., Buist, S., Dunkle, B., Hanna, D., Harwood, H.J., Huband, M.D., *et al.* (2009). A class of selective antibacterials derived from a protein kinase inhibitor pharmacophore. Proc Natl Acad Sci U S A *106*, 1737-1742.

Mitani, Y., Meng, X., Kamagata, Y., and Tamura, T. (2005). Characterization of LtsA from Rhodococcus erythropolis, an enzyme with glutamine amidotransferase activity. J Bacteriol *187*, 2582-2591.

Nakashima, N., and Tamura, T. (2004). Isolation and characterization of a rolling-circle-type plasmid from Rhodococcus erythropolis and application of the plasmid to multiple-recombinant-protein expression. Appl Environ Microbiol *70*, 5557-5568.

Noguchi, N., Katayama, J., and O'Hara, K. (1996). Cloning and nucleotide sequence of the mphB gene for macrolide 2'-phosphotransferase II in Escherichia coli. FEMS Microbiol Lett *144*, 197-202.

Nurizzo, D., Shewry, S.C., Perlin, M.H., Brown, S.A., Dholakia, J.N., Fuchs, R.L., Deva, T., Baker, E.N., and Smith, C.A. (2003). The crystal structure of aminoglycoside-3'-phosphotransferase-IIa, an enzyme responsible for antibiotic resistance. J Mol Biol *327*, 491-506.

Ozcelik, B., Kartal, M., and Orhan, I. (2011). Cytotoxicity, antiviral and antimicrobial activities of alkaloids, flavonoids, and phenolic acids. Pharm Biol.

Payne, D.J., Gwynn, M.N., Holmes, D.J., and Pompliano, D.L. (2007). Drugs for bad bugs: confronting the challenges of antibacterial discovery. Nat Rev Drug Discov *6*, 29-40.

Perez-Vizcaino, F., Duarte, J., Jimenez, R., Santos-Buelga, C., and Osuna, A. (2009). Antihypertensive effects of the flavonoid quercetin. Pharmacol Rep *61*, 67-75.

Pettersen, E.F., Goddard, T.D., Huang, C.C., Couch, G.S., Greenblatt, D.M., Meng, E.C., and Ferrin, T.E. (2004). UCSF Chimera--a visualization system for exploratory research and analysis. J Comput Chem *25*, 1605-1612.

Plaper, A., Golob, M., Hafner, I., Oblak, M., Solmajer, T., and Jerala, R. (2003). Characterization of quercetin binding site on DNA gyrase. Biochem Biophys Res Commun *306*, 530-536.

Pon, N.G., and Bondar, R.J. (1967). A direct spectrophotometric assay for pyruvate kinase. Anal Biochem *19*, 272-279.

Ronquist, F., and Huelsenbeck, J.P. (2003). MrBayes 3: Bayesian phylogenetic inference under mixed models. Bioinformatics *19*, 1572-1574.

Sato, Y., Suzaki, S., Nishikawa, T., Kihara, M., Shibata, H., and Higuti, T. (2000). Phytochemical flavones isolated from Scutellaria barbata and antibacterial activity against methicillin-resistant Staphylococcus aureus. J Ethnopharmacol *72*, 483-488.

Scheeff, E.D., and Bourne, P.E. (2005). Structural evolution of the protein kinase-like superfamily. PLoS Comput Biol *1*, e49.

Schindler, T., Sicheri, F., Pico, A., Gazit, A., Levitzki, A., and Kuriyan, J. (1999). Crystal structure of Hck in complex with a Src family-selective tyrosine kinase inhibitor. Mol Cell *3*, 639-648.

Shakya, T., and Wright, G.D. (2010). Nucleotide selectivity of antibiotic kinases. Antimicrob Agents Chemother *54*, 1909-1913.

Shao, Z., Dick, W.A., and Behki, R.M. (1995). An improved Escherichia coli-Rhodococcus shuttle vector and plasmid transformation in Rhodococcus spp. using electroporation. Lett Appl Microbiol *21*, 261-266.

Shaw, K.J., Rather, P.N., Hare, R.S., and Miller, G.H. (1993). Molecular genetics of aminoglycoside resistance genes and familial relationships of the aminoglycoside-modifying enzymes. Microbiol Rev *57*, 138-163.

Siregar, J.J., Lerner, S.A., and Mobashery, S. (1994). Purification and characterization of aminoglycoside 3'-phosphotransferase type IIa and kinetic comparison with a new mutant enzyme. Antimicrob Agents Chemother *38*, 641-647.

Stogios, P.J., Shakya, T., Evdokimova, E., Savchenko, A., and Wright, G.D. (2011). Structure and function of APH(4)-Ia, a hygromycin B resistance enzyme. J Biol Chem *286*, 1966-1975.

Teillet, F., Boumendjel, A., Boutonnat, J., and Ronot, X. (2008). Flavonoids as RTK inhibitors and potential anticancer agents. Med Res Rev *28*, 715-745.

Thompson, C.J., and Gray, G.S. (1983). Nucleotide sequence of a streptomycete aminoglycoside phosphotransferase gene and its relationship to phosphotransferases encoded by resistance plasmids. Proc Natl Acad Sci U S A *80*, 5190-5194.

Thompson, J.D., Higgins, D.G., and Gibson, T.J. (1994). CLUSTAL W: improving the sensitivity of progressive multiple sequence alignment through sequence weighting, position-specific gap penalties and weight matrix choice. Nucleic Acids Res *22*, 4673-4680.

Toth, M., Chow, J.W., Mobashery, S., and Vakulenko, S.B. (2009). Source of phosphate in the enzymic reaction as a point of distinction among aminoglycoside 2"-phosphotransferases. J Biol Chem *284*, 6690-6696.

Toth, M., Frase, H., Antunes, N.T., Smith, C.A., and Vakulenko, S.B. (2010). Crystal structure and kinetic mechanism of aminoglycoside phosphotransferase-2"-IVa. Protein Sci *19*, 1565-1576.

Trower, M.K., and Clark, K.G. (1990). PCR cloning of a streptomycin phosphotransferase (aphE) gene from Streptomyces griseus ATCC 12475. Nucleic Acids Res *18*, 4615.

Tsai, S.F., Zervos, M.J., Clewell, D.B., Donabedian, S.M., Sahm, D.F., and Chow, J.W. (1998). A new high-level gentamicin resistance gene, aph(2")-Id, in Enterococcus spp. Antimicrob Agents Chemother *42*, 1229-1232.

Whelan, S., and Goldman, N. (2001). A general empirical model of protein evolution derived from multiple protein families using a maximum-likelihood approach. Mol Biol Evol *18*, 691-699.

Williams, N.K., Lucet, I.S., Klinken, S.P., Ingley, E., and Rossjohn, J. (2009). Crystal structures of the Lyn protein tyrosine kinase domain in its Apo- and inhibitor-bound state. J Biol Chem *284*, 284-291.

Woodman, O.L., and Chan, E. (2004). Vascular and anti-oxidant actions of flavonols and flavones. Clin Exp Pharmacol Physiol *31*, 786-790.

Wright, G.D., and Thompson, P.R. (1999). Aminoglycoside phosphotransferases: proteins, structure, and mechanism. Front Biosci *4*, D9-21.

Young, P.G., Walanj, R., Lakshmi, V., Byrnes, L.J., Metcalf, P., Baker, E.N., Vakulenko, S.B., and Smith, C.A. (2009). The crystal structures of substrate and nucleotide complexes of Enterococcus faecium aminoglycoside-2"-phosphotransferase-IIa [APH(2")-IIa] provide insights into substrate selectivity in the APH(2") subfamily. J Bacteriol *191*, 4133-4143.

Zhang, J., Yang, P.L., and Gray, N.S. (2009). Targeting cancer with small molecule kinase inhibitors. Nat Rev Cancer *9*, 28-39.

Zhang, J.H., Chung, T.D., and Oldenburg, K.R. (1999). A Simple Statistical Parameter for Use in Evaluation and Validation of High Throughput Screening Assays. J Biomol Screen *4*, 67-73.

Zhu, X., Kim, J.L., Newcomb, J.R., Rose, P.E., Stover, D.R., Toledo, L.M., Zhao, H., and Morgenstern, K.A. (1999). Structural analysis of the lymphocyte-specific kinase Lck in complex with non-selective and Src family selective kinase inhibitors. Structure *7*, 651-661.

CHAPTER FIVE
CONCLUSIONS AND CONTINUING STUDIES

The incidence of antibiotic resistant infections is on the rise, while the discovery of effective treatments is on a sharp decline. As we continue to search for measures to combat prevalent MDR-bacteria, such as MRSA, new more virulent strains are emerging that are posing an even larger threat, such as extended spectrum β-lactmases (ESBL) in *Enterobacteriaceae, K. pneumoniae* carbapenemase (KPC) producing bacteria, *C. difficile*, and MDR *A. baumannii.* To curb the proliferation of these 'superbugs', new methodologies are required to ward them off.

Citing the decline in novel antimicrobial agents, we decided to approach the problem of antibiotic resistance directly via finding inhibitors of resistance by *in vitro* screening of small molecules against purified enzyme targets that confer resistance in bacteria. Considering the scope of antibiotic resistance enzymes, we focused on the antibiotic kinases (AKs), causative agents in aminoglycoside and macrolide resistance. The AKs are attractive targets for several reasons: they inactivate clinically significant antibiotics; they are widespread among pathogenic bacteria; and they have a high structural homology to eukaryotic protein kinases (ePKs). This latter point is of significance because ePKs are being studied extensively as druggable targets, resulting in the creation of plethora of compounds that are directed towards ATP catalysis. With the prior knowledge of the susceptibility of AKs against protein kinase inhibitors, our goal was to exploit such compounds to see if they could be repurposed as inhibitors of resistance. Before these potential inhibitors could be evaluated however, it was necessary to conduct several rigorous biochemical, structural and phylogenetic studies in order to better understand the action of these enzymes.

ANTIBIOTIC KINASES: A DIVERSE ARRAY OF ENZYMES

The discovery of antibiotic kinases (AKs) was initiated by Umezawa and co-workers with the discovery of the first APH(3') enzyme from *E. coli* (Umezawa et al., 1967). Since then, AKs have been found in a number of hosts ranging from environmental antibiotic producers to clinically relevant pathogens. The dissemination and spread of these mechanisms has been attributed to horizontal gene transfer starting from the antibiotic producers and eventually ending up in pathogenic organisms via several unknown intermediate species (Benveniste and Davies, 1973). If antibiotic producers are the supposed source of AKs in clinical pathogens, this transfer must have occurred much before the antibiotic era, as suggested by the divergence in amino acid sequences. This proved to be a challenge when trying to determine the phylogenetic relationship between 34 AKs. Trying to use the sequences alone to create an alignment repeatedly failed to bring consensus regions into alignment. This required us to create an alignment using a unique strategy of using a preliminary alignment using the Pfam group of APHs as a template in order to bring all consensus regions into alignment, followed by several rounds of refinement to resolve the remaining regions.

Although all AKs share the same action of transferring a phosphate moiety to an antibiotic leading to inactivation, the high-level divergence of sequences is not surprising

when you look at AK families specifically. The first important realization is that there are eight different classes of APHs and one class of MPH based strictly on regioselectivity. Every known AK family thus far is only capable of adding a single phosphate moiety at a specific site. The notable exception is APH(3')-IIIa, which has been shown to phosphorylate both at the C3'-OH and the C5"-OH of 4,5-disubstituted AGs to varying degrees, most likely due to the proximity of the C5"-OH to the catalytic Asp residue (Thompson et al., 1996). Structural data of AKs suggest that regioselectivity is due of an extensive network of hydrogen bonds and interactions which fix the orientation of the target antibiotic. This would imply that every family of AK has a unique antibiotic binding site in order to accommodate regioselectivity.

In addition to regioselectivity, AKs within a family have varied antibiotic spectra. This is best demonstrated in the APH(2"), APH(3') and MPH(2') family of enzymes, all of which have a broad, yet varied, substrate spectra among their variants. These broad-spectrum resistance enzymes also exhibit a larger binding space for the antibiotic, as seen in APH(3')-IIIa, as compared to narrow spectrum AKs like APH(9)-Ia, which has a smaller antibiotic binding site. We have also demonstrated a level of plasticity in the nucleotide binding pocket of AKs, which shows a varied selectivity for ATP and GTP, as described in Chapter 2. Using a competition assay, which mimicked intracellular concentrations of ATP and GTP, we studied three representative enzymes: the ATP specific APH(3')-IIIa, the GTP specific MPH(2')-Ia, and the ambivalent APH(2")-IIa (Ib). When the remaining AKs were surveyed with Michaelis-Menten kinetics it was observed that nucleotide promiscuity existed in a number of AKs and was not restricted to specific families as had been previously suggested. Nucleotide promiscuity has been observed among a number of kinases, but rarely is GTP the preferred phosphate donor. GTP preference outside of the AKs has only been documented in protein kinase Cδ (Gschwendt et al., 1995), calcium/calmodulin-dependent protein kinase II (Bostrom et al., 2009), glycerate kinase (Liu et al., 2009), and phosphoenolpyruvate carboxykinase (Dunten et al., 2002; Scheen and Legrand, 2006). We still lack the ability to predict the motifs that govern nucleotide selectivity due to the lack of structural data of AKs with GTP-bound. It has been suggested that nucleotide promiscuity in AKs may be due in part to a larger nucleotide pocket which offers two separate binding modes for both ATP and GTP (Toth et al., 2010), however this does not explain nucleotide preference.

The most compelling feature of AKs is that even though they only maintain sequence identity in the few residues involved in nucleotide binding and catalysis, they all demonstrate the same overall fold; notably, this tertiary structure is also shared with the core kinase domain of eukaryotic protein kinases (Kannan et al., 2007; Scheeff and Bourne, 2005). To date, six different AK structures have been solved, all of which support these findings, including the structure of the hygromycin resistance determinant APH(4)-Ia, described in detail in Chapter 3.

APH(4)-Ia is a unique resistance enzyme which was first isolated from an environmental strain of *E. coli* (Gritz and Davies, 1983). The most striking feature of

APH(4)-Ia is that it is different from the only other known hygB resistance gene, APH(7")-Ia, found in the hygB producer *Streptomyces hygroscopicus*. Our phylogenetic survey suggests that these two enzymes branched off from a common progenitor (Figure 4-1), but branch lengths show the relationship as being quite distant.

The structure of APH(4)-Ia showed a high level of structural similarity N-terminal domain with other AKs, namely APH(2")-IIa. Whereas, variations were principally noted with the C-terminal lobe where hygromycin (hygB) binding occurs, this is because hygB has an atypical structure compared to the majority of AG antibiotics, which is highlighted by its pucker around its central sugar moiety, giving it a unique twisted conformation. The C-terminal lobe architecture compensates for the structure of hygB, creating a novel AG binding pocket that only accommodates hygB and no other AG antibiotic. HygB binding is also supported by thirteen hydrogen bonds via nine amino acid residues which additionally aid in its binding to the active site.

With structural and sequence diversity in mind, we determined the best approach to finding a unified inhibitor of AKs was to follow the similarities, which clearly lie within the ATP catalysis region. These finding supported our initial predictions that ePK inhibitors could logically be repurposed as potential inhibitors of AKs.

KINASE INHIBITORS AS CHEMICAL BIOLOGICAL PROBES OF AKS

We began our work with the precedence of AKs being susceptible to the action of kinase inhibitors (Daigle et al., 1997). To further this observation, in Chapter 4 we interrogated 80 well characterized kinase inhibitors against a panel of 14 AKs. From this we have been able to visualize a network of chemical-biological interactions as compared to phylogeny creating a molecular phylogeny of AKs. The activity of the compounds ranged from highly promiscuous to selective and from weak to potent. Some of the most surprising interactions were those that followed phylogeny, as demonstrated by LFM A13, KN-93, PP1 and Tyrphostin AG1478. This suggested that small molecules are able to exploit inherited elements within families of AKs, marking the first step in finding broadly applicable synergistic therapies against AKs. To further elucidate the action of some of these interactions, we conducted SAR and structural studies with the flavonoids pyrazolo-pyrimidines and flavonoids.

We probed the action of the pyrazolo-pyrimidines (PP) against a sub-clade of the APH(3')/APH(3") enzymes and the distantly related APH(9)-Ia. Using a model of APH(3')-Ia bound to PP1, which we designed based on other known structures of kinases bound to PP compounds, we hypothesized the orientation of PP1 in the APH(3')-Ia ATP binding site. This paved the way for a SAR analysis of four AKs that showed moderate to strong activity with PP1 and PP2. From this we found that the three closely related AKs showed a similar SAR as compared to the distantly related APH(9)-Ia. We also noted that we were not able to significantly improve or impair inhibition with any of the newly derived PP compounds, which brought into question the validity of the model we had been using. This was confirmed when our collaborators solved the structure of

APH(3')-Ia bound to PP1, which revealed that the hypothesized orientation of PP1 was incorrect and it was in fact inverted as compared to the model.

The flavonol quercetin appeared to have the most robust and promiscuous action observed compared to the other compounds studied. In addition to its activity, we were able to obtain a structure of quercetin bound to APH(2")-IVa. Using these data coupled with the SAR, we have been able to determine critical contacts between the flavonoids and the APH(2")-IVa ATP binding site. It was clear from this analysis as to why apigenin was not a suitable inhibitor for APH(2")-IVa, however apigenin was able to inhibit the closely related APH(2")-IIa. A superposition of these structures revealed that an arginine residue in APH(2")-IIa has the propensity to form a compensatory interaction with apigenin that is lacking in APH(2")-IVa; this extra interaction could also explain why quercetin has a 15-fold higher binding affinity to APH(2")-IIa. The studies done with flavonoids as antimicrobial agents offer some promise towards the future application of these nutraceuticals as synergistic therapies against antibiotic resistant pathogens.

ONGOING STUDIES

As comprehensive as these AK studies were, a number of questions remain to be addressed. The first is to assess the bioactivity of the proven inhibitors in a bacterial host. There is precedence for a number of these compounds already having antibacterial activity on their own, such as the flavonoids (Cushnie and Lamb, 2005) and quinazolines (Bedi et al., 2004; Boyapati et al., 2010; Marino et al., 2011; Rodrigues and Renshaw, 2010). However, the majority of the compounds in our screening library have only been assessed for bioactivity in eukaryotic cell lines. Ideally, these tests should be conducted in a model organism expressing a single AK resistance determinant with a controlled level of expression, such that activity specifically against resistance mechanisms can be judged in addition to antimicrobial action. Such a library of strains needs to be constructed to carry out this work.

We have also had the good fortune of working with collaborators who have been proactive in producing inhibitor-bound structures of AKs. Considering the large number of positive inhibitor-AK interactions, these efforts need to continue in order to gain valuable insights on key active site residues that confer inhibitor susceptibility and to ascertain the similarity/difference in binding modes of common inhibitors in multiple AKs. As previously discussed, these types of data were pivotal in deciphering the action of flavonoids in APH(2")-IVa, which also led to our hypothesis of the action of flavonoids against APH(2")-IIa. Also, with structural data of APH(3')-Ia with PP1, we can move forward and rationally design inhibitors that can have an improved effect against the panel of selected AKs.

The ultimate achievement of this work would be to demonstrate the robustness of the chemical interaction map against uncharacterized AKs and to determine if they follow the same trends as their phylogenetically related AKs. This would provide a novel method by which to classify AKs based on their inhibitor susceptibility. The current

sample set has proven to be too small to attempt to make any broad statements with regards to molecular phylogeny. To make use of this technique, we need to interrogate all known AKs (34 in total) with our 80 kinase inhibitors, in order to fully validate molecular phylogeny as a tool for classifying putative and uncharacterized AKs.

CONCLUDING REMARKS

As discussed throughout this work, the problem of antibiotic resistance requires immediate attention with a focus on alternative therapies rather than relying upon the discovery of novel antibiotics. We have approached this issue by observing the action of AKs and asking if possible synergistic therapies could be developed against this class of resistance enzymes. Using a multi-disciplinary approach consisting of phylogeny, enzymology, chemistry and structural biology as tools to decipher the connections among AKs, we have identified several unique traits among AKs (i.e. nucleotide preferences and structural motifs). These studies culminated in the identification of a number of inhibitors that have the potential to be exploited in the development of synergistic therapies. This work provides invaluable insight towards this seldom realized method of antimicrobial therapy and provides the basis for the future development of novel synergistic treatments.

REFERENCES

Bedi, P.M., Kumar, V., and Mahajan, M.P. (2004). Synthesis and biological activity of novel antibacterial quinazolines. Bioorg Med Chem Lett *14*, 5211-5213.

Benveniste, R., and Davies, J. (1973). Aminoglycoside antibiotic-inactivating enzymes in actinomycetes similar to those present in clinical isolates of antibiotic-resistant bacteria. Proc Natl Acad Sci U S A *70*, 2276-2280.

Bostrom, S.L., Dore, J., and Griffith, L.C. (2009). CaMKII uses GTP as a phosphate donor for both substrate and autophosphorylation. Biochem Biophys Res Commun *390*, 1154-1159.

Boyapati, S., Kulandaivelu, U., Sangu, S., and Vanga, M.R. (2010). Synthesis, antimicrobial evaluation, and docking studies of novel 4-substituted quinazoline derivatives as DNA-gyrase inhibitors. Arch Pharm (Weinheim) *343*, 570-576.

Cushnie, T.P., and Lamb, A.J. (2005). Antimicrobial activity of flavonoids. Int J Antimicrob Agents *26*, 343-356.

Daigle, D.M., McKay, G.A., and Wright, G.D. (1997). Inhibition of aminoglycoside antibiotic resistance enzymes by protein kinase inhibitors. J Biol Chem *272*, 24755-24758.

Dunten, P., Belunis, C., Crowther, R., Hollfelder, K., Kammlott, U., Levin, W., Michel, H., Ramsey, G.B., Swain, A., Weber, D., *et al.* (2002). Crystal structure of human cytosolic phosphoenolpyruvate carboxykinase reveals a new GTP-binding site. J Mol Biol *316*, 257-264.

Gritz, L., and Davies, J. (1983). Plasmid-encoded hygromycin B resistance: the sequence of hygromycin B phosphotransferase gene and its expression in Escherichia coli and Saccharomyces cerevisiae. Gene *25*, 179-188.

Gschwendt, M., Kittstein, W., Kielbassa, K., and Marks, F. (1995). Protein kinase C delta accepts GTP for autophosphorylation. Biochem Biophys Res Commun *206*, 614-620.

Kannan, N., Taylor, S.S., Zhai, Y., Venter, J.C., and Manning, G. (2007). Structural and functional diversity of the microbial kinome. PLoS Biol *5*, e17.

Liu, B., Wu, L., Liu, T., Hong, Y., Shen, Y., and Ni, J. (2009). A MOFRL family glycerate kinase from the thermophilic crenarchaeon, Sulfolobus tokodaii, with unique enzymatic properties. Biotechnol Lett *31*, 1937-1941.

Marino, J.L., Moore, V.M., Rumbold, A.R., and Davies, M.J. (2011). Fertility treatments and the young women who use them: an Australian cohort study. Hum Reprod *26*, 473-479.

Rodrigues, C.S., and Renshaw, K.D. (2010). Associations of coping processes with posttraumatic stress disorder symptoms in national guard/reserve service members deployed during the OEF-OIF era. J Anxiety Disord *24*, 694-699.

Scheeff, E.D., and Bourne, P.E. (2005). Structural evolution of the protein kinase-like superfamily. PLoS Comput Biol *1*, e49.

Scheen, A.J., and Legrand, D. (2006). Aspirin and clopidogrel resistance in patients with diabetes mellitus. Eur Heart J *27*, 2900; author reply 2900-2901.

Thompson, P.R., Hughes, D.W., and Wright, G.D. (1996). Regiospecificity of aminoglycoside phosphotransferase from Enterococci and Staphylococci (APH(3')-IIIa). Biochemistry *35*, 8686-8695.

Toth, M., Frase, H., Antunes, N.T., Smith, C.A., and Vakulenko, S.B. (2010). Crystal structure and kinetic mechanism of aminoglycoside phosphotransferase-2"-IVa. Protein Sci *19*, 1565-1576.

Umezawa, H., Okanishi, M., Kondo, S., Hamana, K., Utahara, R., Maeda, K., and Mitsuhashi, S. (1967). Phosphorylative inactivation of aminoglycosidic antibiotics by Escherichia coli carrying R factor. Science *157*, 1559-1561.

APPENDICES

APPENDIX 1: Oligonucleotide Primers for Gene Amplification and Site Mutations

Primer name	Direction	Sequence (5' to 3')*
Chapter 2 Primers		
mphA (mph(2')-I)	Forward	CGCGAATTC**CATATG**ACCGTAGTCACGACCGCCGA
mphA (mph(2')-I)	Reverse	CCC**AAGCTT**GGATCCTTGCCGATCCGGAAGAGAAAGGTA
aph(2")-Ib(IIa)	Forward	GGGG**ACAAGTTTGTACAAAAAAGCAGCCTTC**ATGGTTAACTTGGACG CTGAG
aph(2")-Ib(IIa)	Reverse	GGGG**ACCACTTTGTACAAGAAAGCTGGGTC**CTAAAATATAAACATCT CTGCTTGTG
Chapter 3 Primers		
aph(4)-Ia ΔNdeI	Forward	CATGGCGTGATTTCAT**C**TGCGCGATTGCTGATCCC
aph(4)-Ia ΔNdeI	Reverse	GGGATCAGCAATCGCGCA**G**ATGAAATCACGCCATG
aph(4)-Ia	Forward	GGGGATC**CATATG**AAAAAGCCTGAACTCACCGCGACG
aph(4)-Ia	Reverse	GGGGATCC**AAGCTT**CTATTCCTTTGCCCTCGGACGAGTG
aph(4)-Ia R49A	Forward	CGTGGATATGTCCTG**GC**GGTAAATAGCTGCGCC
aph(4)-Ia R49A	Reverse	GGCGCAGCTATTTACC**GC**CAGGACATATCCACG
aph(4)-Ia Q101A	Forward	CAGGGTGTCACGTTG**GC**AGACCTGCCTGAAACC
aph(4)-Ia Q101A	Reverse	GGTTTCAGGCAGGTCT**GC**CAACGTGACACCCTG
aph(4)-Ia D126A	Forward	GCGATCGCTGCGGCCG**C**TCTTAGCCAGACGAGC
aph(4)-Ia D126A	Reverse	GCTCGTCTGGCTAAGA**G**CGGCCGCAGCGATCGC
aph(4)-Ia D198A	Forward	CTCGTGCACGCGG**C**TTTCGGCTCCAACAATG
aph(4)-Ia D198A	Reverse	CATTGTTGGAGCCGAAA**G**CCGCGTGCACGAG
aph(4)-Ia S201A	Forward	CACGCGGATTTCGGC**G**CCAACAATGTCCTGACG
aph(4)-Ia S201A	Reverse	CGTCAGGACATTGTTGG**C**GCCGAAATCCGCGTG
aph(4)-Ia N203A	Forward	GATTTCGGCTCCAAC**GC**TGTCCTGACGGACAATGGCC
aph(4)-Ia N203A	Reverse	GGCCATTGTCCGTCAGGACA**GC**GTTGGAGCCGAAATC
aph(4)-Ia D216A	Forward	CATAACAGCGGTCATTG**C**CTGGAGCGAGGCGATG
aph(4)-Ia D216A	Reverse	CATCGCCTCGCTCCAG**G**CAATGACCGCTGTTATG
aph(4)-Ia N231A	Forward	CCCAATACGAGGTCGCC**GC**CATCTTCTTCTGGAGGCCG
aph(4)-Ia N231A	Reverse	CGGCCTCCAGAAGAAGATGG**CG**GCGACCTCGTATTGGG
aph(4)-Ia W238L	Forward	CTTCTTCTGGAGGCCG**CT**GTTGGCTTGTATGGAG
aph(4)-Ia W238L	Reverse	CTCCATACAAGCCAAC**AG**CGGCCTCCAGAAGAAG
aph(4)-Ia Q273A	Forward	GCTCCGCATTGGTCTTGAC**GC**ACTCTATCAGAGCTTGG
aph(4)-Ia Q273A	Reverse	CCAAGCTCTGATAGAGT**GC**GTCAAGACCAATGCGGAGC
aph(4)-Ia D285A	Forward	GACGGCAATTTCGATG**C**TGCAGCTTGGGCGCAG
aph(4)-Ia D285A	Reverse	CTGCGCCCAAGCTGCA**G**CATCGAAATTGCCGTC
Chapter 4 Primers		
aph(2")-IIIa	Forward	GGGGATC**CATATG**AAACAAAATAAACTTCACTATACCACAATGATAA TG
aph(2")-IIIa	Reverse	GGGGATCC**AAGCTT**TTAAGCACTGTTCGCACCAAAATTGTTG
aph(2")-IVa	Forward	GGGGATC**CATATG**ACAACTTATACTTTCGACCAGGTAGAAGAGG
aph(2")-IVa	Reverse	GGGGATCC**AAGCTT**CTATTTAATTTTAATGCTTCTGATTTCATTTAA TCCC
aph(3')-Ia	Forward	GGGGATC**CATATG**AGCCATATTCAACGGGAAACGTC
aph(3')-Ia	Reverse	GGGGATCC**GGATCC**TTAGAAAAACTCATCGAGCATCAAATGAAAC
aph(3')-IIa	Forward	GGGGATC**CATATG**ATTGAACAAGATGGATTGCACGC
aph(3')-IIa	Reverse	GGGGATCC**AAGCTT**TCAGAAGAACTCGTCAAGAAGGCGATAG

Primer name	Direction	Sequence (5' to 3')*
Chapter 4 Primers cont...		
aph(3')-Va	Forward	GGGGACAAGTTTGTACAAAAAAGCAGGCTTCCATATGGACGAC AGCACGTTGCGCC
aph(3')-Va	Reverse	GGGGACCACTTTGTACAAGAAAGCTGGGTCAAGCTTTCAGAAG AACTCGTCGAGAAGCTGGTAGAAGGC
aph(3")-Ia	Forward	GGGAATTCCATATGAGTGATCACCCCGGGCCGG
aph(3")-Ia	Reverse	GGGAATTCAAGCTTCTAGCCCCAGGTGAGCGGATCGAG
aph(6)-Ia	Forward	GGGGATCCATATGAGTTCGTCGGACCACATCCAC
aph(6)-Ia	Reverse	GGGGATCCAAGCTTTCAGGGCTTCGCCAGCGCTTCG
mphB (mph(2')-II)	Forward	GGGGATCCATATGAGTAAAGATATTAAACAAGTAATCGAGATAGC
mphB (mph(2')-II)	Reverse	GGGGATCCCTCGAGTTACGAACCTTGTACTTCCAATGCTTCC

* Regions that are bold, underlined and blue are the clone sites used, and regions in bold and red are the specific site mutations

List of clone sites used:

BamHI – GGATCC
EcoRI – GAATTC
HindIII – AAGCTT
XhoI – CTCGAG
attB1 – ACAAGTTTGTACAAAAAAGCAGCCTTC
attB2 – ACCACTTTGTACAAGAAAGCTGGGT

APPENDIX 2: Alignment of AKs

Complete identity – red, high identity/similarity – orange; low identity/similarity – yellow. Key kinase domains are outlined in bold below each alignment with key residues highlighted in red.

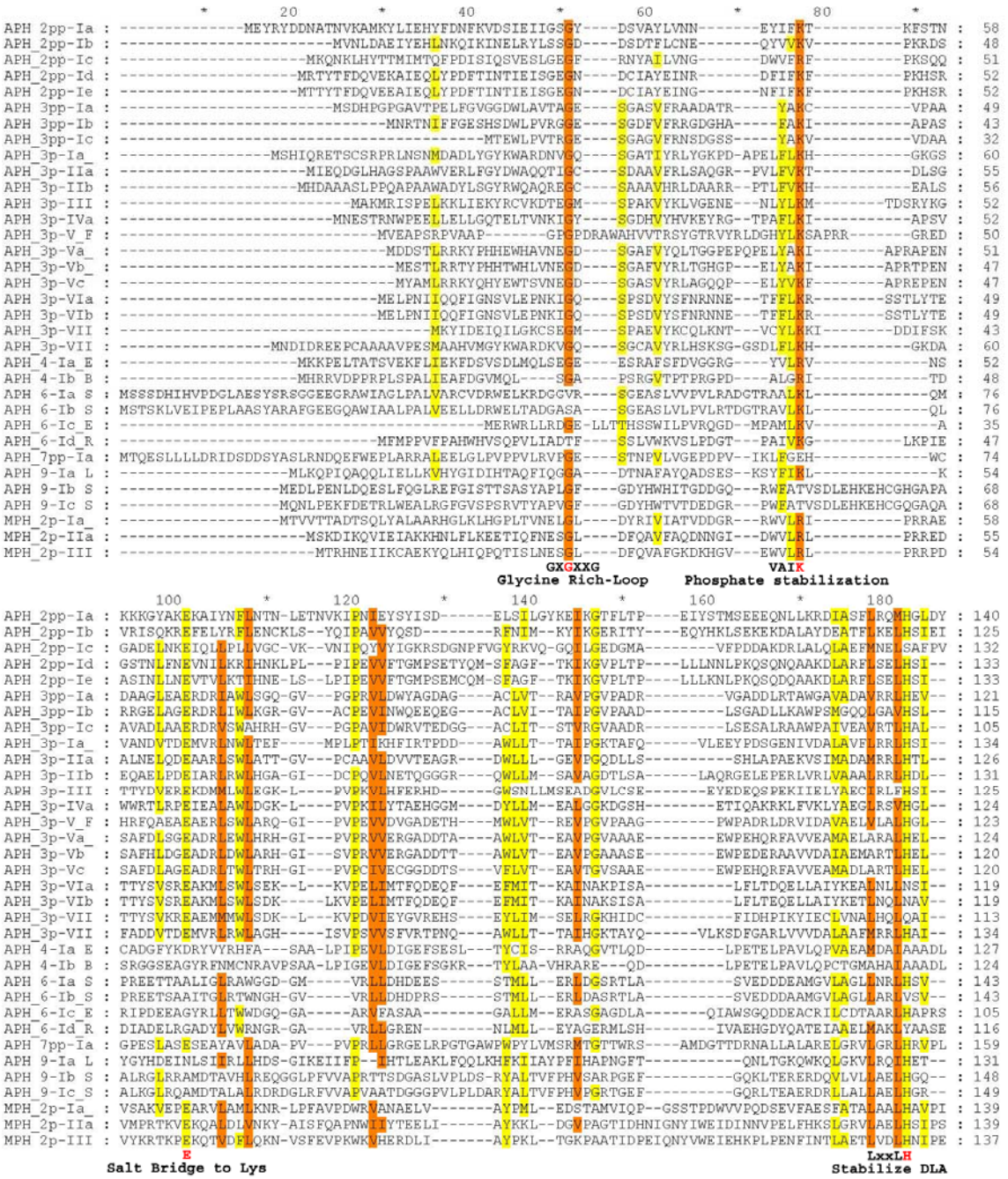

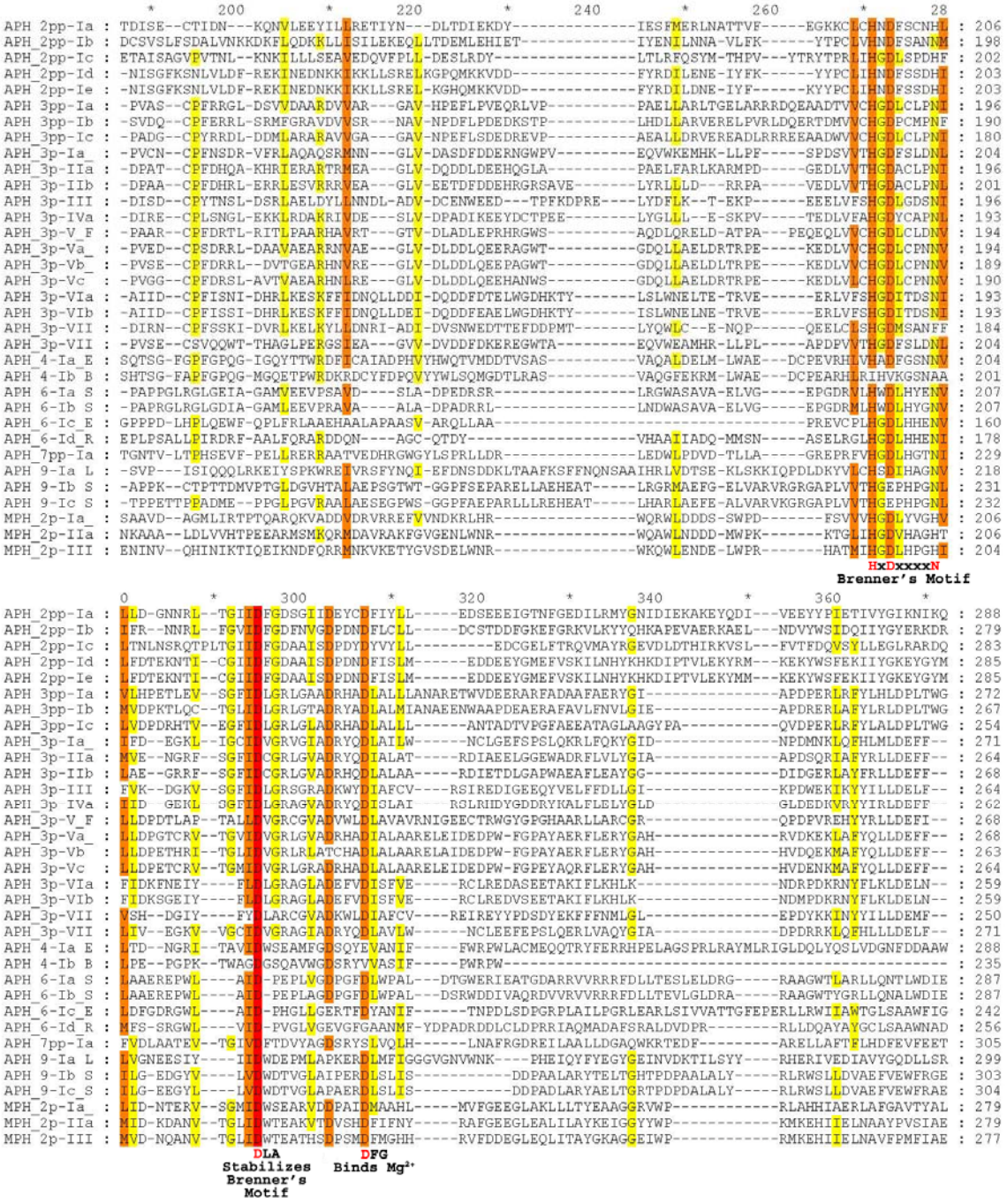
HxDxxxxN
Brenner's Motif
DLA
Stabilizes
Brenner's
Motif
DFG
Binds Mg2+

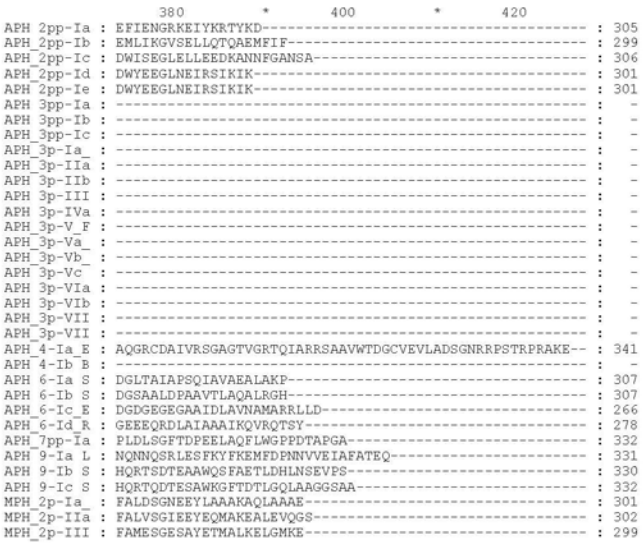
380 * 400 * 420
APH_2pp-Ia : EFIENGRKEIYKRTYKD---------- : 305
APH_2pp-Ib : EMLIKGVSELLQTQAEMFIF---------- : 299
APH_2pp-Ic : DWISEGLELLEEDKANNFGANSA---------- : 306
APH_2pp-Id : DWYEEGLNEIRSIKIK---------- : 301
APH_2pp-Ie : DWYEEGLNEIRSIKIK---------- : 301
APH_3pp-Ia : ---------- : -
APH_3pp-Ib : ---------- : -
APH_3pp-Ic : ---------- : -
APH_3p-Ia_ : ---------- : -
APH_3p-IIa : ---------- : -
APH_3p-IIb : ---------- : -
APH_3p-III : ---------- : -
APH_3p-IVa : ---------- : -
APH_3p-V_F : ---------- : -
APH_3p-Va_ : ---------- : -
APH_3p-Vb_ : ---------- : -
APH_3p-Vc_ : ---------- : -
APH_3p-VIa : ---------- : -
APH_3p-VIb : ---------- : -
APH_3p-VII : ---------- : -
APH_3p-VII : ---------- : -
APH_4-Ia_E : AQGRCDAIVRSGAGTVGRTQIARRSAAVWTDGCVEVLADSGNRRPSTRPRAKE-- : 341
APH_4-Ib_B : ---------- : -
APH_6-Ia_S : DGLTAIAPSQIAVAEALAKP---------- : 307
APH_6-Ib_S : DGSAALDPAAVTLAQALRGH---------- : 307
APH_6-Ic_E : DGDGEGEGAAIDLAVNAMARRLLD---------- : 266
APH_6-Id_R : GEEEQRDLAIAAAAIKQVRQTSY---------- : 278
APH_7pp-Ia : PLDLSGFTDPEELAQFLWGPPDTAPGA---------- : 332
APH_9-Ia_L : NQNNQSRLESFKYFKEMFDPNNVVEIAFATEQ---------- : 331
APH_9-Ib_S : HQRTSDTEAAWQSFAETLDHLNSEVPS---------- : 330
APH_9-Ic_S : HQRTQDTESAWKGFTDTLGQLAAGGSAA---------- : 332
MPH_2p-Ia_ : FALDSGNEEYLAAAKAQLAAAE---------- : 301
MPH_2p-IIa : FALVSGIEEYEQMAKEALEVQGS---------- : 302
MPH_2p-III : FAMESGESAYETMALKELGMKE---------- : 299

APPENDIX 3: Complete K_m Data for all AKs

Substrate	Saturating Substrate	[2nd Subs.] (μM)	K_m (μM)	K_i (μM)	k_{cat} (sec^{-1})	k_{cat}/K_m ($sec^{-1}*M^{-1}$)
APH(2")-Ia						
Amikacin	GTP	200	31.5 ± 4.8		0.07	2.2E+03
Gentamicin C	GTP	200	12.2 ± 2.0		0.33	2.7E+04
Kanamycin A	GTP	200	2.9 ± 1.6	382 ± 268	0.04	1.3E+04
Sisomicin	GTP	200	28.3 ± 7.5		0.60	2.1E+04
Tobramycin	GTP	200	85 ± 61		0.02	2.4E+02
ATP	Gentamicin C	200	67.6 ± 24.3		0.06	8.4E+02
GTP	Gentamicin C	200	16.8 ± 0.6		0.13	1.8E+04
APH(2")-IIa						
Gentamicin C	ATP	1000	15.6 ± 0.9		0.38	2.5E+04
Kanamycin A	ATP	1000	17.0 ± 2.0		0.21	1.3E+04
Netilmicin	ATP	1000	24.3 ± 2.3		0.24	1.0E+04
Tobramycin	ATP	1000	11.7 ± 3.3		0.45	3.9E+04
ATP	Kanamycin	200	152 ± 13		0.32	2.1E+03
GTP	Kanamycin	200	18 ± 1.9		0.10	5.4E+03
APH(2")-IIIa						
Gentamicin C	GTP	200	15.9 ± 3.9		0.47	3.0E+04
Kanamycin A	GTP	200	23.1 ± 3.1		0.50	2.2E+04
Tobramycin	GTP	200	21.8 ± 7.4		0.49	2.2E+04
ATP	Kanamycin A	200	43.6 ± 9.9		0.03	6.7E+02
GTP	Kanamycin A	200	59.5 ± 4.0		0.49	8.3E+03
APH(2")-IVa						
Gentamicin C	ATP	1000	11.3 ± 4.1		0.15	4.2E+04
Kanamycin A	ATP	1000	11.1 ± 1.3		0.27	2.4E+04
Netilimicin	ATP	1000	7.9 ± 1.9		0.45	5.7E+04
Tobramycin	ATP	1000	22.3 ± 4.8		0.45	2.0E+04
ATP	Kanamycin	200	127 ± 6		0.55	4.3E+03
GTP	Kanamycin	200	195 ± 19		0.54	2.8E+03
APH(3')-Ia						
Kanamycin A	GTP	500	24.1 ± 5.3		0.58	2.4E+04
Lividomycin A	GTP	500	59.5 ± 15.7		1.10	1.9E+04
Neamine	GTP	500	70.5 ± 17.5		1.15	2.6E+04
Neomycin B	GTP	500	34.4 ± 6.4		0.75	2.2E+04
Paromomycin	GTP	500	68.4 ± 12.9		1.12	1.6E+04
Ribostamycin	GTP	500	19.1 ± 5.9		0.46	2.4E+04
ATP	Kanamycin	200	5.4 ± 0.5		0.09	1.7E+04
GTP	Kanamycin	200	127 ± 15		0.75	5.9E+03

Substrate	Saturating Substrate	[2nd Subs.] (μM)	K_m (μM)	K_i (μM)	k_{cat} (sec^{-1})	k_{cat}/K_m ($sec^{-1}*M^{-1}$)
APH(3')-IIa						
Amikacin	ATP	400	245 ± 161		0.67	2.7E+03
Butirosin	ATP	400	14.5 ± 5.1		1.05	7.2E+04
Kanamycin A	ATP	400	8.9 ± 2.0		0.53	6.0E+04
Neamine	ATP	400	4.9 ± 1.1		0.46	2.4E+04
Neomycin B	ATP	400	8.6 ± 3.8		0.65	7.6E+04
Paromomycin	ATP	400	3.2 ± 1.4		0.45	1.4E+05
Ribostamycin	ATP	400	10 ± 3.0		0.70	7.0E+04
ATP	Kanamycin	200	61.4 ± 6.9		0.51	8.3E+03
GTP	Kanamycin	200	455 ± 88		0.12	2.6E+02
APH(3')-IIIa						
Amikacin	ATP	400	10.3 ± 2.3		0.20	1.9E+04
Butirosin	ATP	400	4.6 ± 2.0		0.19	4.0E+04
Kanamycin A	ATP	400	6.8 ± 1.3	247 ± 63	0.38	5.5E+04
Lividomycin A	ATP	400	17.9 ± 6.2		0.53	2.9E+04
Neamine	ATP	400	13.4 ± 3.2		0.55	2.6E+04
Neomycin B	ATP	400	10.7 ± 2.9		0.70	6.6E+04
Paromomycin	ATP	400	20.3 ± 6.3		0.79	3.9E+04
Ribostamycin	ATP	400	0.43 ± 0.3		0.20	4.6E+05
ATP	Neomycin	200	10.6 ± 1.4		1.60	1.5E+05
APH(3')-Va						
Butirosin	ATP	200	257 ± 51		0.08	3.2E+02
Kanamycin A	ATP	200	22.0 ± 2.0		0.41	1.9E+04
Neomycin B	ATP	200	2.6 ± 0.5		4.80	1.8E+06
Paromomycin	ATP	200	6.2 ± 1.6		2.10	3.4E+06
Ribostamycin	ATP	200	4.6 ± 1.8		1.10	2.4E+06
ATP	Neomycin	200	21.5 ± 4.2		0.38	1.2E+04
APH(3'')-Ia						
Streptomycin	ATP	1000	313 ± 48	653 ± 244	5.28	1.2E+04
ATP	Streptomycin	1000	288 ± 52		3.60	1.2E+04
GTP	Streptomycin	1000	589 ± 62		2.08	3.5E+03
APH(4)-Ia						
Hygromycin B	ATP	1000	4.4 ± 1.7		0.81	1.8E+05
ATP	Hygromycin B	200	40.5 ± 7.1		1.44	3.6E+04
GTP	Hygromycin B	200	1320 ± 289		3.36	2.5E+03

Substrate	Saturating Substrate	[2nd Subs.] (μM)	K_m (μM)	K_i (μM)	k_{cat} (sec^{-1})	k_{cat}/K_m ($sec^{-1}*M^{-1}$)
APH(6)-Ia						
Streptomycin	ATP	1000	9.0 ± 0.7		0.48	5.4E+04
ATP	Streptomycin	200	28.0 ± 2.3		0.39	1.4E+04
APH(9)-Ia						
Spectinomycin	ATP	200	18.7 ± 4.9	232 ± 128	15.97	8.5E+05
ATP	Spectinomycin	200	12.4 ± 1.9		10.21	8.2E+05
MPHa						
Azithromycin	GTP	200	27.7 ± 3.4		0.29	1.1E+04
Clarythromycin	GTP	200	45.9 ± 7.4		0.31	6.8E+03
Erythromycin	GTP	200	37.2 ± 5.6		0.28	7.5E+03
Spiramycin	GTP	200	478 ± 55		0.20	4.2E+02
Tylosin	GTP	200	131 ± 45		0.17	1.3E+03
Telithromycin	GTP	200	7.4 ± 1.5	622 ± 196	0.15	2.1E+04
ATP	Erythromycin	200	1890 ± 310		0.02	1.1E+01
GTP	Erythromycin	200	59.2 ± 4.7		0.64	1.1E+04
MPHb						
Azithromycin	GTP	200	9.4 ± 0.8		0.28	3.0E+04
Clarythromycin	GTP	200	10.5 ± 4.2		0.09	8.4E+03
Erythromycin	GTP	200	4.1 ± 0.9		0.05	1.2E+04
Spiramycin	GTP	200	1.6 ± 0.7		0.03	1.7E+04
Tylosin	GTP	200	2.7 ± 0.8		0.04	1.4E+04
Telithromycin	GTP	200	15.2 ± 4.7		0.60	4.0E+04
GTP	Azithromycin	200	9.4 ± 0.7		0.19	2.0E+04

APPENDIX 4: K_i data of Kinase Inhibitors vs. AKs

Enzyme	APH(2")-Ia	APH(2")-IIa	APH(2")-IIIa	APH(2")-IVa	APH(3')-Ia	APH(3')-IIa	APH(3')-IIIa
Apigenin	-	3.7 ± 0.5	-	-	5.3 ± 0.3	-	-
Quercetin	24.6 ± 0.9	1.5 ± 0.1	23.5 ± 1.4	25.1 ± 3.7	1.0 ± 0.1	8.1 ± 0.5	23.7 ± 0.7
Genistein	-	-	109 ± 6	-	-	-	-
LY294002	-	-	-	-	79.0 ± 8.0	-	-
Tyrphostin 25	-	-	-	-	275 ± 37	28.2 ± 3.5	102 ± 13
Tyrphostin 47	-	50.3 ± 8.0	59.3 ± 5.6	170 ± 14	-	122 ± 13	77.8 ± 7.9
Tyrphostin AG1478	-	-	-	-	15.6 ± 1.0	-	-
GW5074	-	2.1 ± 0.3	-	-	-	-	-
Indirubin-3'-Monooxime	-	8.1 ± 1.5	-	-	-	-	-
Ro-31-8220	-	-	41.8 ± 3.1*	-	97.5 ± 12.6*	-	-
LFMA13	56.7 ± 1.6	16.6 ± 1.8	21.9 ± 1.7	-	-	-	-
PP1	-	-	-	-	3.8 ± 0.4	-	-
SP600125	-	5.4 ± 1.3	-	-	7.2 ± 0.7	28.6 ± 7.6	6.6 ± 1.0
BML-259	-	30.3 ± 3.9	-	-	-	-	-
KN-93	-	59.5 ± 16.2	196 ± 13	-	183 ± 36	95.6 ± 15.2	-
Olomoucine	-	3.6 ± 0.5	-	-	49.2 ± 2.2	-	-
SB-202190	-	-	-	-	-	-	-
ZM449829	-	29.6 ± 5.8	120 ± 13	25.8 ± 0.8	300 ± 47	-	-

Enzyme	APH(3')-Va	APH(3")-Ia	APH(4)-Ia	APH(6)-Ia	APH(9)-Ia	MPH(2')-Ia	MPH(2')-IIa
Apigenin	0.18 ± 0.01	-	0.86 ± 0.03	-	5.9 ± 0.2	-	-
Quercetin	0.07 ± 0.005	8.4 ± 0.6	1.2 ± 0.1	15.0 ± 0.6	0.56 ± 0.03	-	-
Genistein	21.3 ± 1.5	17.8 ± 0.9	-	-	-	-	-
LY294002	68.5 ± 6.7	2.4 ± 0.1	14.7 ± 0.4	-	64.1 ± 2.2	-	-
Tyrphostin 25	16.5 ± 0.8	110 ± 6	49.0 ± 2.3	-	231 ± 19	-	-
Tyrphostin 47	59.4 ± 1.4	128 ± 6	8.9 ± 0.4	-	23.5 ± 2.3	-	-
Tyrphostin AG1478	0.82 ± 0.07	0.73 ± 0.05	14.1 ± 0.8	-	-	-	-
GW5074	9.7 ± 0.3	4.5 ± 0.4	11.2 ± 0.9	20.6 ± 1.3	4.5 ± 0.2	190 ± 16*	80.4 ± 5.0*
Indirubin-3'-Monooxime	11.4 ± 1.2	8.3 ± 0.8	5.9 ± 1.2	-	22.9 ± 2.7	-	-
Ro-31-8220	27.4 ± 1.8	66.7 ± 11.7	7.1 ± 0.1	-	130 ± 7	-	-
LFMA13	-	-	94.3 ± 7.7	-	-	68.4 ± 4.4	93.5 ± 5.0
PP1	0.47 ± 0.03	5.2 ± 0.5	-	-	36 ± 3	-	-
SP600125	4.7 ± 0.3	-	3.8 ± 0.2	-	1.6 ± 0.1	-	-
BML-259	-	-	32.1 ± 1.2	-	7.6 ± 0.3	-	-
KN-93	-	-	-	-	-	40.3 ± 4.0	41.7 ± 2.8
Olomoucine	-	-	9.6 ± 0.5	-	9.7 ± 0.3	-	-
SB-202190	10.2 ± 0.8	-	-	-	87.0 ± 8.2	-	-
ZM449829	88.4 ± 8.5	109 ± 10	289 ± 13*	-	8.8 ± 0.7*	-	-

* Enzyme-inhibitor interactions that showed a non-competitive inhibition trend

APPENDIX 5: List of PP Compounds

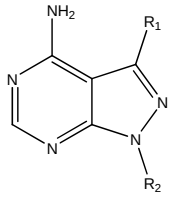

Compound	R_1	R_2
pyrazolo[3,4-d]pyrimidine	H	H
1	H	*sec*-butyl
2	H	Hexyl
3	I	*sec*-butyl
4	Phenyl	*tert*-butyl
5	Phenyl	*sec*-butyl
6	Phenyl	butyl
PP1	*para*-CH_3	*tert*-butyl
7	*para*-CH_3	*sec*-butyl
8	*para*-CH_3	butyl
9	*para*-CH_3	H
PP2	*para*-Cl	*tert*-butyl
10	*para*-Cl	*sec*-butyl
11	*para*-Cl	butyl
12	*para*-Cl	hexyl
13	*para*-Cl	methyl
14	*para*-Cl	H
15	*para*-Cl	4-(4-methyl-1H-1,2,3-triazol-1-yl)butan-1-ol
16	*meta*-Cl	*sec*-butyl
17	*ortho*-Cl	*sec*-butyl
18	3,4-dichloro-phenyl	*sec*-butyl
19	*para*-F	*sec*-butyl
20	*para*-Br	*sec*-butyl
21	*para*-OMe	*sec*-butyl
22	5-indole	*sec*-butyl
23	5-benzo[d][1,3]dioxole	*sec*-butyl